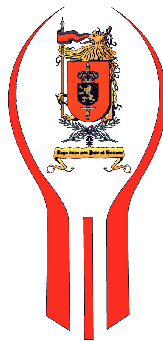# UNIVERSIDAD CARLOS III DE MADRID

ESCUELA POLITÉCNICA SUPERIOR

INGENIERÍA INDUSTRIAL

PROYECTO FINAL DE CARRERA

Study of the effect of admixtures on the early hydration of self-compacting mortars: comparison of experimental methods.

Realizado en la Real Academia Militar Belga

AUTORA: Nuria ORTIZ TABOADA

TUTORA: M. Asunción BAUTISTA ARIJA

Leganés, Octubre 2012

TÍTULO: *Study of the effect of admixtures on the early hydration of self-compacting mortars: comparison of experimental methods..*

AUTORA: *Nuria ORTIZ TABOADA*

TUTORA: *M. Asunción BAUTISTA ARIJA*

La defensa del presente Proyecto Fin de Carrera se realizó el día 22 de Octubre de 2012; siendo calificada por el siguiente tribunal:

PRESIDENTE: *Francisco J. VELASCO LÓPEZ*

SECRETARIO *Carlos RODRÍGUEZ VILLANUEVA*

VOCAL *Silvia SANTALLA ARRIBAS*

Habiendo obtenido la siguiente calificación:

CALIFICACIÓN:

Presidente **Secretario** **Vocal**

"Thiotimoline! First mentioned in 1948, according to legend, by Azimuth or, possibly, Asymptote, who may, very likely, never have existed. There is no record of the original article supposed to have been written by him; merely vague references to it, none earlier than the twenty-first century.

Serious study began with Almirante, who either discovered thiotimoline, or re-discovered it, if the Azimuth/Asymptote tale is accepted. Almirante worked out the theory of hypersteric hindrance and showed that the molecule of thiotimoline is so distorted that one bond is forced into extension through the temporal dimension into the past; and another into the future.

Because of the future-extension, thiotimoline can interact with an event that has not yet taken place. It can, for instance, to use the classic example, dissolve in water approximately one second before the water is added."

Isaac Asimov - Thiotimoline to the stars.

Resumen

Introducción y objetivos

El *fraguado* es el proceso de rigidización y endurecimiento de una mezcla, en este caso de agua y cemento. Dentro del fraguado se debe diferenciar entre el tiempo inicial de fraguado que se refiere a la primera rigidización, donde se pierde la plasticidad y trabajabilidad de la mezcla, mientras que el fraguado final se refiere a una rigidez significativa, cuando la mezcla es un material sólido rígido. El fraguado es un factor fundamental en investigación y construcción, ya que determinará hasta cuándo se puede realizar el colado y la compactación (inicio) y cuándo se puede retirar el encofrado (fin).

En un entorno de investigación, el fraguado se ha estudiado tradicionalmente con ensayos de penetración como la *aguja Vicat*. Sin embargo, estos ensayos pueden requerir un alto índice de mano de obra y tener una alta dependencia del técnico que los realiza; también hay que tener presente que no dan ninguna información sobre las reacciones o cambios microestructurales de la mezcla. Por lo tanto, es imperativo para los investigadores relacionar los resultados obtenidos en los ensayos estandarizados con otros ensayos que proporcionen mayor información sobre el proceso de fraguado.

El objetivo de este proyecto fin de carrera es desarrollar y ejecutar un programa experimental paramétrico para distintas composiciones de mortero, que permita realizar una comparativa entre distintos métodos experimentales (*ensayo de resistencia a la penetración, ensayo semiadiabático, ensayo aguja Vicat, ensayo de la velocidad de la onda-p*) buscando una correlación entre los mismos. Para ello se compararán los puntos característicos de hidratación y los tiempos de fraguado.

Procedimiento experimental

Métodos de ensayo

Ensayos de aguja Vicat

Este ensayo se ha realizado según la norma UNE 196-3 (*Métodos de ensayo de cementos. Parte 3: Determinación del tiempo de fraguado y de la estabilidad de volumen*). El tiempo de fraguado se determina observando la penetración de una aguja de 300 g y diámetro de 1 mm en una pasta de cemento hasta que la distancia entre la aguja y la placa base es (6 ± 3) mm. Además existe una norma americana, ASTM 187 (Consistencia Normal del cemento hidráulico), para la realización de este ensayo, la cual define el tiempo de inicio de fraguado como el tiempo en el cual la distancia entre la aguja y la placa base es de 15 mm. Ambos valores sirven como puntos convenientes de comparación entre muestras.

Es importante recalcar que el ensayo de la aguja Vicat se lleva a cabo en pasta de cemento, no en mortero como en el resto de los ensayos. Por tanto, se determinó una pasta con una equivalencia en trabajabilidad. Sin embargo, la trabajabilidad de la pasta de cemento es drásticamente distinta y después de una serie de pruebas se le dio prioridad al ensayo de asiento.

Ensayos de resistencia a la penetración

Este ensayo para la determinación del fraguado de la mezcla por la resistencia a la penetración está estandarizado por la norma ASTM C403 (*Método de ensayo. Determinación del tiempo de fraguado de mezclas de hormigón por resistencia a la penetración*). Una muestra con dimensiones 140 mm (alto) x 150 mm (ancho) x 150 mm (largo) que admite 6 penetraciones en un ensayo. El mortero es penetrado 25 mm en 10 s. La resistencia a la penetración ejercida por el mortero se calcula dividiendo la fuerza por el área de la sección de la aguja. Se define el inicio de fraguado a una resistencia de 3,4 MPa. Tuthill y Cordon demostraron que a partir de esta resistencia a la penetración no se podía plastificar el

hormigón por vibración. También definieron que a 27,6 MPa se puede considerar que el hormigón ha fraguado completamente, en este punto tiene una resistencia a compresión de 0,6 MPa y puede soportar cierta carga.

Aunque la norma establece una altura de 140 mm de las muestras, debido a limitaciones del laboratorio, se usaron muestras de 80 mm de alto. Se realizó un experimento para comparar cualitativamente el efecto que esto supondría en los resultados. Se concluyó que las muestras de 80 mm muestran mayor resistencia a la penetración, resultando en tiempos de fraguado menores, del orden de unos 20 min.

Los dos ensayos anteriores (aguja Vicat y resistencia a la penetración) son ensayos intrusivos puesto que se basan en la penetración de la muestra. Estos ensayos por lo tanto se basan en la resistencia a cizalladura y compresión de la muestra [1]. Los otros dos ensayos (velocidad de la onda-p y calorimetría semi-adiabática) no son ensayos intrusivos. Sin embargo, las muestras no se pueden utilizar para varios ensayos debido a que son ensayos continuos en mortero fresco.

Ensayos de ultrasonidos: velocidad de la onda-p

Los ultrasonidos son ondas con una frecuencia por encima de los 20 kHz. Las ondas-p son ultrasonidos que se transmiten por el medio a través de compresiones y dilataciones en la dirección de propagación. Su velocidad de propagación por el medio está relacionada con las propiedades mecánicas del material.

Los cambios de la microestructura del mortero fresco durante el fraguado conllevan cambios en las propiedades elásticas del mismo. Estos cambios a su vez afectan a la velocidad de propagación de la onda-p.

Investigaciones anteriores proponen puntos característicos como indicadores del fraguado:

1. Tiempo en el que la velocidad de la onda-p alcanza el valor de 1500 m/s, velocidad que corresponde a la del agua) [2–4].

2. Tiempo del punto de inflexión [2, 5–7] (punto de transición en la velocidad de la

onda-p) en la velocidad de la onda-p. En estos ensayos se encuentran 2 puntos de inflexión de los que se consideran:

- *a*) Tiempo del máximo gradiente.

- *b*) Tiempo del primer punto de inflexión.

- *c*) Tiempo del segundo punto de inflexión.

3. Tiempo en el que la velocidad de la onda-p alcanza el valor de 2975 m/s, velocidad calculada por Alexander Herb [8] como estimación para fin de fraguado.

4. Tiempo en el que la velocidad de la onda-p alcanza 2/3 de la velocidad final del ensayo.

5. Tiempo en el que el gradiente de la velocidad de la onda-p alcanza el 20 % del máximo gradiente, propuesto por Robeyst [9] como indicador de fin de fraguado.

Ensayos de calorimetría semi-adiabática

Este ensayo está estandarizado en la norma EN 196-9 *(Métodos de ensayo de cementos, parte 9: determinación del calor de hidratación. Método semi adiabático)*. Los procesos químicos en el mortero generan una evolución del calor de hidratación. Para este ensayo se monitoriza la temperatura de una muestra en un contenedor semi adiabático. Las pérdidas de calor se compensan por comparación con un calorímetro de referencia. Siguiendo el procedimiento indicado en la norma, se calcula el calor de hidratación y el flujo de calor de la muestra.

En este ensayo se permite que la temperatura de la muestra aumente libremente. Este aumento de temperatura que afecta a la velocidad de las reacciones genera el "efecto de entrecruzamiento". Para compensar este efecto se ajusta la escala del tiempo con el método de la madurez. Éste método determina la edad equivalente a la cual se obtendría cierto grado de hidratación en condiciones isotermas [10].

La curva de flujo de calor normalmente muestra un descenso inicial que acaba en un mínimo relativo (qmin) seguido de un máximo (qmax) para volver a decrecer. Sandberg y Liberman [11] proponen el tiempo de mínimo y máximo flujo de calor como indicadores

del fraguado. Zingg [12] propuso el tiempo de mínimo flujo más 0,25 J/gh para mezclas con policarboxilatos. Debido a que los resultados experimentales muestran irregularidades y a que la etapa de inducción es alargada por el superplastificador, los criterios para el tiempo de inicio de fraguado no se consideraron aplicables para este ensayo, en el que se propusieron los siguientes criterios:

1. Tiempo de qmin+0,2△q

2. Tiempo de qmin+1,5 J/gh

3. Tiempo de qmax

Materiales

Para este programa experimental se utilizó mortero o pasta de cemento, dependiendo de los requerimientos del ensayo. Los materiales utilizados son los siguientes:

- Cemento Holcim CEMI 52.5N (ver anexo A)

- Agua

- Arena normalizada según EN 196-1.

- Cenizas volantes clase C.

- Superplastificador de tercera generación desarrollado por la universidad de Lovaina.

- Acelerador nitrato de calcio tetrahidratado $((Ca(NO_3)_2 \cdot 4H_2O))$

La notación de cada mezcla se relaciona con su composición de la siguiente manera:

$$\mathbf{S}-SP_{m\%CEM} * 100-\mathbf{F}-C/P * 100-\mathbf{A}-A_{m\%CEM} * 100-\mathbf{R}-R_{m\%CEM} * 100 \qquad (1)$$

Donde:

$SP_{m\%CEM}$: Porcentaje de superplastificador en función de la masa de cemento.

C/P: Ratio cemento a material cementante.

$A_{m\%CEM}$: Porcentaje de acelerador en función de la masa de cemento.

$R_{m\%CEM}$: Porcentaje de retardante en función de la masa de cemento.

Para la pasta de cemento la notación utilizada será la de su mortero correspondiente. La diferencia en su composición es que no tiene arena y el ratio W/C es 0,33.

Se han ensayado 10 composiciones diferentes y sus correspondientes pastas de cemento equivalentes. Estas composiciones se dividen en 2 series: serie de superplastificador y serie de acelerador. La serie del superplastificador consta de 6 morteros con diferentes cantidades de superplastificador: 0,00 %mCEM (porcentaje de la masa de cemento), 0,5 %mCEM, 0,75 %mCEM, 1,00 %mCEM, 1,25 %mCEM y 1,50 %mCEM, con un ratio C/S de 0,33, W/C de 0,45 y C/P 0,72, excepto la composición sin superplastificador, que tiene un C/P de 1. La serie del acelerador usa mortero con 1 %mCEM de superplastificador, C/S de 0,33, W/C de 0,45 y C/P de 0,72 y una cantidad de acelerador de 0,00 %mCEM, 0,40 %mCEM, 1,00 %mCEM, 2,00 %mCEM y 3,00 %mCEM. Las cantidades detalladas se encuentran en el cuadro 1.

Cuadro 1: *Proporciones de las composiciones*

	Cemento $\pm0{,}1$ [g]	Arena ±5 [g]	Agua $\pm0{,}1$ [g]	CV $\pm0{,}1$ [g]	SP $\pm0{,}001$ [g]	Ac $\pm0{,}001$ [g]
Serie de superplastificador						
S-00-F-100-A-000-R-000				0,0	0,000	
S-50-F-72-A-000-R-000					2,250	
S-75-F-72-A-000-R-000					3,375	
S-100-F-72-A-000-R-000	450,0	1350	202,5	175,0	4,500	0
S-125-F-72-A-000-R-000					5,625	
S-150-F-72-A-000-R-000					6,750	
Serie de acelerador						
S-100-F-72-A-000-R-000						0,000
S-100-F-72-A-40-R-0						1,800
S-100-F-72-A-100-R-0						4,500
S-100-F-72-A-200-R-0	450,0	1350	202,5	175,0	4,500	9,000
S-100-F-72-A-300-R-0						13,500

Resultados y análisis

Para evitar reiteraciones no se muestran en éste resumen las gráficas, que se pueden encontrar en los capítulos 4 y 5, así como en los anexos.

Resultados experimentales de la serie del superplastificador

Los ensayos de resistencia a la penetración y aguja Vicat (figuras 4.21 y 4.17) muestran un retardo con el incremento de la cantidad de superplastificador. Esto es una característica de los superplastificadores, que retardan la evolución de la resistencia mecánica. Esto implica que el inicio y fin de fraguado tienen lugar más tarde, y la duración del fraguado también aumenta.

En las curvas de transmisión de la onda-p (figura 4.1) se puede observar que la velocidad después de unas horas es mayor para mezclas con mayor cantidad de superplastificador, lo que podría ser debido a que el superplastificador hace la muestra menos porosa, por tanto se obtiene una muestra más densa y una microestructura más consistente. Mirando las curvas del gradiente de velocidad de la onda-p (figura 4.2) observamos 2 máximos: el primer máximo baja su intensidad al aumentar la cantidad de superplastificador, mientras que el segundo se mantiene relativamente constante. Esto sugiere que el primer máximo está relacionado con el superplastificador mientras que el segundo con las cenizas volantes. La disminución en la intensidad del primer máximo puede deberse a que el efecto de repulsión del superplastificador ocasiona una hidratación más lenta a un ritmo menor. La evolución del flujo de calor con el tiempo corregido por el efecto de madurez (figura 4.10) muestra una disminución del máximo flujo de calor para cantidades altas de superplastificador, lo que apuntala la hipótesis de una hidratación más lenta.

Resultados experimentales de la serie del acelerador

Los ensayos de resistencia a la penetración y aguja Vicat (figuras 4.23 y 4.19) muestran que al aumentar la cantidad de acelerador el inicio del desarrollo de la resistencia mecánica sucede antes, aunque el ritmo en el que se desarrolla es menor. Sin embargo este acelera-

miento parece llegar a un límite, sobre todo para el fin del fraguado. Este comportamiento tiene sentido ya que el acelerador usado acelera el fraguado pero no el endurecimiento para altas cantidades.

En el ensayo de ultrasonidos se observa un cambio significativo en la forma de la curva de la velocidad de la onda-p (figura 4.5), el primer punto de inflexión es más pronunciado mientras que el segundo disminuye, mostrando un comportamiento más bilineal.

En el ensayo semi-adiabático (figura 4.14) vemos que para altas cantidades del super-plastificador aparece un aumento inicial, sugiriendo una cadena de reacciones modificada. Esta modificación claramente contribuye a un inicio de fraguado más temprano, en línea con la información aportada por el resto de los ensayos.

Correlaciones

Se han ensayado once composiciones diferentes en el desarrollo de este programa experimental. Para los ensayos de ultrasonidos y calorímetria se han propuesto varios puntos de referencia que se han comparado con los tiempos de inicio y fin de fraguado obtenidos por los ensayos normalizados. La mejor correlación posible es y=x (donde x es el ensayo normalizado), que indicaría que los 2 hitos están relacionados de la misma manera con la hidratación, y demostrando que el indicador es útil como resultado de referencia para determinar el fraguado. Sin embargo, el indicador propuesto podría tener una sensibilidad distinta al proceso de hidratación (m) o un desfase respecto a este (c) lo que resulta en un ajuste y=mx+c, este tipo de correlación es igualmente significativo.

Correlaciones con el inicio de fraguado

Al trazar los tiempos de inicio de fraguado de los métodos normalizados (ensayo de resistencia a la penetración y de aguja Vicat) se realiza una línea de ajuste por mínimos cuadrados (figura 5.4), que muestra una correlación entre los datos de y=1,01x+27,4 con un valor de R^2 de 0,983, corroborando lo que otros autores [13] ya han mencionado, que aunque los criterios difieran, sirven como puntos de comparación convenientes entre muestras. Es interesante recalcar que el ensayo de la aguja Vicat es menos conservador, ya que

da tiempos de inicio de fraguado mayores.

Entre el ensayo de la velocidad de la onda-p y los indicadores de inicio de fraguado obtenemos una buena correlación con la edad del mortero a la velocidad de 1500 m/s, obteniendo una R^2 de 0,972 con el ensayo de resistencia a la penetración para un ajuste de y=x (figura 5.5). Comparando este indicador con el inicio de fraguado obtenido en el ensayo de la aguja de Vicat (figura 5.6) es interesante recalcar que se ven 2 comportamientos diferenciados entre las series, pero serían necesarios más puntos para verificarlo. Aun así se obtiene una línea de ajuste de y=0,957x-23,3 con un R^2 de 0,967.

Para el ensayo semi-adiabático no se obtiene ninguna correlación perfecta, aunque el indicador de qmin+1,5 J/gh (figuras 5.8 y 5.9) da unas correlaciones aceptables. Es importante recalcar que este indicador no es verosímil para la mezclas con más de 2,00 %mCEM de acelerador por los motivos anteriormente indicados. Este indicador muestra una correlación más fuerte con el ensayo de la aguja Vicat, con el que obtenemos una R^2 de 0,902 para y=x. Para el ensayo de resistencia a la penetración obtenemos un ajuste de y=0,983x+31,8 con un R^2 de 0,911.

Correlaciones con el fin de fraguado

Para el tiempo de fin de fraguado sólo se dispone del ensayo de resistencia a la penetración. Aunque en el ensayo de la aguja Vicat está contemplada la determinación de este tiempo, no se disponía del material necesario.

Para los indicadores propuestos como fin de fraguado en el ensayo de la onda-p obtenemos buenas correlaciones excepto para el del tiempo en el que el gradiente de la velocidad de la onda-p alcanza el 20 % del máximo gradiente. El indicador que da mejores correlaciones es el del tiempo en el que la velocidad de la onda-p alcanza 2/3 de la velocidad a 2600 min (figura 5.11), obteniendo un ajuste de y=x+200 con un R^2 de 0,941.

Con el indicador propuesto para el ensayo semi-adiabático (tiempo de qmax) también se obtiene una correlación aceptable con un ajuste de y=1,04x+209 y un R^2 de 0,945 (figura

5.12).

En las correlaciones con el ensayo de resistencia a la penetración se observa un desfase de unos 200 min entre el tiempo de fin de fraguado y los indicadores propuestos. Este desfase podría ser debido a la elección de los indicadores o a la falta de adaptación de la madurez de los resultados del ensayo. Aunque el proceso seguido para la adquisición de datos ha sido el especificados en la norma ASTM C403, para realizar una comparación realista con las otras técnicas experimentales, se debería aplicar la adaptación por madurez para la serie temporal. Debido a las grandes diferencias en tamaño y peso, es lógico que las muestras más propensas a cambios de temperatura significativas sean las de los ensayos de resistencia a la penetración.

La adaptación de la serie temporal resultaría en una edad equivalente para la cual se obtendría un cierto grado de hidratación. Para el tiempo de inicio de fraguado, el aumento de temperatura es despreciable, por lo tanto los resultados obtenidos son válidos. Sin embargo para el fin de fraguado, debido a que en general no hay variaciones energéticas entre las composiciones ensayadas, esta adaptación podría ser equivalente a un desfase de 200 min.

Valores atípicos

En las correlaciones descritas se observan una serie de valores atípicos. Todos los ensayos excepto el de ultrasonidos muestran unos valores atípicos que se repiten en sus correlaciones.

El ensayo de resistencia a la penetración muestra un valor atípico para la mezcla con $0,50\,\%$mCEM, es importante recalcar que para esta cantidad de superplastificador no se encuentra ninguna mejora en la trabajabilidad de la mezcla con respecto a una mezcla sin superplastificador. Por tanto tiene sentido que si el superplastificador no lubrica la mezcla, el rozamiento entre los granos de arena pudiera generar unos valores de resistencia a la penetración mayores, lo que resultaría en tiempos de fraguado menores que para el resto de la serie.

El ensayo de la aguja Vicat muestra un valor atípico para la muestra con 0,75 %mCEM. Hay que recalcar que estos ensayos se hacían utilizando pasta de cemento en vez de mortero, la cual tiene una trabajabilidad y consistencia muy distintas a las del mortero. Es posible que estas muestras tuvieran un mayor contenido en aire, resultando en mayores penetraciones de la aguja Vicat. También es posible que este distinto comportamiento significara una resistencia al cizallamiento menor. Para verificar la razón de este comportamiento serían necesarios más ensayos.

Para el ensayo semi-adiabático los indicadores propuestos no son verosímiles para altas cantidades de acelerador. Como ya se ha comentado, para estas cantidades la cadena de reacción se ve severamente afectada y los indicadores pierden mucho de su significado, ya que el tipo de curva en la que están basados no es la obtenida.

Conclusiones y futuras líneas de trabajo

De los resultados obtenidos de los ensayos experimentales se puede llegar a las siguientes conclusiones primarias relacionadas con el tema central del trabajo:

- Se han hallado correlaciones directas entre los tiempos de fraguado estandarizados y puntos característicos de los ensayos de velocidad de la onda-p y calorimetría semi-adiabática. Estos resultados ilustran la importancia del significado de la curva de velocidad de la onda-p y el flujo de calor.

- No todos los indicadores propuestos han demostrado ser referencias apropiadas para el inicio y fin de fraguado. Del ensayo de la velocidad de la onda-p los indicadores de tiempo en el que la velocidad de la onda-p alcanza los valores: 1500 m/s, 2975 m/s y 2/3 de la velocidad final han demostrado ser indicadores significativos. Para el ensayo de calorimetría semi-adiabática qmin+1,5 J/gh y qmax son indicadores fiables para el inicio y fin de fraguado respectivamente.

Además, se pueden realizar una serie de conclusiones sobre los resultados experimentales:

- Altas cantidades de acelerador modifican la cadena de reacciones, lo cual afecta al

fraguado y la dureza, los indicadores de fraguado propuestos en este trabajo para el ensayo semi-adiabático no son válidos para estas mezclas.

- Las correlaciones para el fin de fraguado muestran un desfase de aproximadamente 200 min. Este desfase puede ser debido a la elección de los indicadores o a la falta de adaptación de madurez.

- Los ensayos que dependen directamente de la resistencia al cizallamiento y a la compresión de la mezcla (resistencia a la penetración y aguja Vicat) son más propensos a resultados atípicos para mezclas con bajas trabajabilidades.

- El superplastificador de policarboxilato usado en este programa experimental, hace que la hidratación ocurra más despacio y de manera más constante.

- El acelerador (nitrato de calcio) hace que la hidratación empiece antes y tiene un mayor impacto sobre la hidratación los primeros 1000 min, contrarrestando el efecto del superplastificador.

Para permitir el desarrollo de indicadores para el fraguado realmente genéricos, deberían llevarse a cabo los siguientes estudios:

- Ampliar el programa experimental con mezclas con distintos aditivos y otros cementos para determinar si las correlaciones obtenidas siguen siendo válidas.

- Repetición de los ensayos de resistencia a la penetración con medidas de temperatura para aplicar la adaptación de madurez.

- Investigación de indicadores útiles para valores extremos de los aditivos.

- Estudio completo para obtener composiciones equivalentes de pasta de cemento para los ensayos de la aguja Vicat.

- Debido a que se han detectado irregularidades en el empaquetamiento del cemento, se recomienda un estudio de la eficiencia de la preservación en vacío del cemento y su efecto en la hidratación de mortero fresco.

Symbols and Abbreviations

Symbols

c: Total thermal capacity of the calorimeter (J/K).

E_a: Activation energy (J/mol).

f: Frequency (Hz).

G: Shear modulus (Pa).

K: Bulk modulus (Pa).

m_{ad}:   Mass of addition contained in the mixture (g).

m_b: Mass of empty mortar box plus lid (g).

m_c: Mass of cement contained in the mixture (g).

m_{fa}:   Mass of fly ash contained in the mixture (g).

m_P: Total mass of powder contained in the mixture (g).

m_s: Mass of sand contained in the mixture (g).

m_w: Mass of water contained in the mixture (g).

Q: Heat of hydration (J/g).

Q_A: Heat accumulated in the calorimeter (J/g).

Q_B: Heat lost into the environment (J/g).

q: hydration heat flux (J/gh).

R: Universal gas constant (kJ/molK).

R^2:   Coefficient of determination.

t: Hydration time (h).

t_e: Equivalent age at reference temperature (h).

Δt_i: Elapsed time between the measurement of temperature at point in time, $t_{(i-1)}$, and the next measurement at point in time, $t_{(i)}$ (h).

v_P: P-wave velocity (m/s).

v_{phase}:   Phase velocity (m/s).

α: Coefficient of heat loss of the calorimeter (J/hK).

$\bar{\alpha}_i$:   Average coefficient of total heat loss of the calorimeter in the period of time, $\Delta t_{(i)}$ (J/hK).

γ: Acceleration factor.

θ_t: Temperature rise of the test sample at time t (K).

$\bar{\theta}_i$:   Average of the temperature rise of the test sample, between times $t_{(i)}$ and $t_{(i-1)}$ (K).

λ: Wavelength (m).

μ: Thermal capacity of the empty calorimeter (J/K).

ρ: Density ($\frac{kg}{m^3}$).

Abbreviations

AC series: Accelerator quantity variation series.

C/P: Cement-powder ratio.

C/S: Cement-Sand ratio

CEN: European Committee for Standardization.

IST: Initial setting time.

FST: Final setting time.

$m\%_{CEM}$:   Admixture quantity as a mass percentage of the cement.

OPC: Ordinary Portland Cement.

SCC: Self-compacting concrete.

SP: Superplasticizer.

SP series: Superplasticizer quantity variation series.

W/C: Water-cement ratio.

Contents

1. Objectives and Scopes of the Research Work

The stiffening and hardening behaviour of a mixture of water and cement is defined as "setting". Setting of concrete is a determinant factor for research and construction. Initial setting time (IST) is defined to be the point in time when the mixture stiffens to a degree where plasticity and workability are lost, thus it is important to contractors as placing and compaction must be performed before IST. Final setting time (FST) is when the mixture is a rigid and solid material, this is when formwork can be removed.

Setting of concrete was traditionally studied by penetration tests such as the Vicat needle. However, penetration tests can be labour intensive, dependent on the technician and do not give us any information on the hydration reactions or microstructural changes in the mixture. Therefore, it is imperative for researchers to correlate the results obtained from other test methods to the setting times.

The objective of this master thesis was to develop and execute a parametric experimental programme for different mortar compositions. By analysing the data of the different experimental methods (penetration test, semi-adiabatic test, Vicat test and continuous ultrasound transmission test), possible correlation factors between the hydration characteristics and IST and FST by these methods will be sought.

2. Introduction

Nowadays, concrete based on ordinary portland cement (OPC) is one of the most consumed materials . Its low price per ton, high availability, transportability, ability to fill forms of nearly any shape, setting and hardening at room temperature with little overall volume change, durability and price account for its widespread use.

The main mechanical characteristic for concrete is its high resistance to compressive stresses, however it does not have a good resistance to other kinds of stresses. For this reason, the concrete is normally reinforced with steel bars which will improve its mechanical characteristics.

From an environmental point of view concrete is also interesting as it requires 0.75 MJ/kg for its production and emits 0.10 kg of CO_2 per kg of concrete (compared to 10 MJ/kg and 0.41 kg of CO_2 for timber) [14]. However, the enormous volume of concrete produced results in 5-8% of global CO_2 emissions. The industrial manufacturing process is reaching its optimum and estimations say that only a 2% further saving could be achieved in this way, therefore the current approach is to decrease the CO_2 produced by the chemical reactions, which will in turn change the composition and therefore all its reactions and properties [15].

2.1. History

Cementing materials have been used throughout the history. Egyptians, Romans and Greeks already used these materials in their constructions. Egyptians used cementing materials obtained by burning gypsum, while Greeks and Romans used volcanic ash and turf, mixed with lime and sand, which produced mortar [16]. A mayor example of the

use of concrete by Romans can be found in Rome, the Pantheon, rebuilt in 126 AD has a coffered, concrete dome with a central opening, it is the world's largest unreinforced concrete dome.

Lime is known since ancient times, however it does not set under water. In 1756 John Smeaton discovered lime containing clay produced hydraulic cement. He used these properties to build Eddystone lighthouse. In 1796 James Parker patented Roman Cement (although it has nothing to do with the cement used by the Romans) made from calcareous clay from North Kent, which was burnt and then grounded to a powder. In 1824 Joseph Aspdin patents a hydraulic lime, which he named Portland Cement (the name is due to its resemblance to Portland building stone) which was produced using separate clay and lime-bearing materials. Portland cement was improved by Isaac-Charles Johnson in 1835, when by increasing the firing temperature he produced burnt clinker pieces which better cement after grinding, thus and starting to produce real modern Portland Cement [15, 17]

Self-compacting concrete (SCC) was developed in Japan in the late 1980's, this concrete is able to flow through and around heavily congested reinforcement, achieving full and uniform compaction without vibration. These properties compensated for a lack of skilled construction workers and was rapidly adopted [18, 19].

2.2. Basic Compositions

Cement paste is the mixture of cement and water with or without admixtures, this is the matrix material for concrete. When fine aggregate (particles with a diameter smaller than 5 mm) is added the resulting mixture is called mortar, it is more commonly used for small volume applications, or as a glue in masonry.

Concrete is composed of a mixture of cement, water, fine aggregate (sand), coarse aggregate (gravel or crushed rocks) and other additions (figure 2.1). The cement and water react, hardening and forming a binder for the non-reacting aggregate [18].
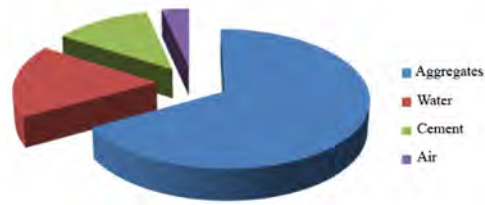
Figure 2.1: *Concrete composition. citeGheysens2006.*

Ratios

Mix ratios indicate the relationship between the components in a mixture. These ratios are established in the following way:

Cement-Sand Ratio   The cement-sand ratio is defined as:

$$C/S = \frac{m_c}{m_s} \tag{2.1}$$

C/S: Cement-Sand ratio

m_c: Mass of cement contained in the mixture (g)

m_s: Mass of sand contained in the mixture (g)

Water-Cement Ratio   The water-cement ratio is defined as:

$$W/C = \frac{m_w}{m_c} \tag{2.2}$$

W/C: Water-Cement ratio

m_w: Mass of water contained in the mixture (g)

Powder-Cement Ratio   The powder-cement ratio is defined as:

$$C/P = \frac{m_c}{m_P} \tag{2.3}$$

Where:

C/P: Powder-cement ratio

m_P: Total mass of powder contained in the mixture (g)

Admixture quantity as a mass of the cement percentage For admixtures the quantity of addition is generally described as a percentage of the cement mass:

$$m\%_{CEM} = \frac{m_{ad}}{100 \times m_c} \tag{2.4}$$

Where:

$m\%_{CEM}$: Admixture quantity as a mass percentage of the cement

m_{ad}: Mass of addition contained in the mixture (g)

2.2.1. Cement

As a hydraulic binder, cement is a finely ground inorganic material that mixes with water to form cement paste which undergoes hydration reactions. After cement paste hardens it maintains its resistance and stability even under water. It is made out of fine grain powder of a mixture of compounds (mostly calcareous materials such as clay and chalk) but its composition is homogeneous due to the manufacturing process [19].

The most commonly used cement nowadays is OPC, whose four main compounds can be seen in table 2.1. The manufacturing process basically consists of clay and chalk which are crushed separately to particle sizes of 75 μm or less and then mixed in certain proportions. The mixture can then either be mixed with water to form a slurry or dried to be transported as a powder. In the dry process, the powder is then put into the rotary kiln (an inclined steel cylinder lined with refractory bricks), the kiln is heated at its lower end to about 1500 °C. In the wet process, the slurry is fed into the higher end of the kiln, and is heated as it moves down due to the combined action of rotation and gravity. The dry process requires less energy than the wet process since the raw material does not need to be dried [16, 17].

The European Committee for Standardization (CEN) divides the family of common cements into 27 products, which are grouped into the following five main cement types:

- CEM I Portland cement

- CEM II Portland-composite cement

Table 2.1: *Basic composition of OPC*

Name	Composition	Short Notation	Mineral	Content [%]
Tricalcium silicate	$3CaO \cdot SiO_2$	C_3S	Alite	50
Dicalcium silicate	$2CaO \cdot SiO_2$	C_2S	Belite	25
Tricalcium aluminate	$3Cao \cdot Al_2O_3$	C_3A		10
Tetracalcium aluminoferrite	$4CaO \cdot Al_2O_3 \cdot Fe_2O_3$	C_4AF	Celite	10

- CEM III Blastfurnace cement

- CEM IV Pozzolanic cement

- CEM V Composite cement

EN 197-1 (Cement. Part 1: Composition, specifications and conformity criteria for common cements) also classifies cements according to their mechanical, physical, chemical and durability requirements. According to the mechanical requirements six different classes are established related to the standard and early strength. Three classes of standard strength are defined: class 32,5, class 42,5 and class 52,5. Two classes of early strength are defined for each class of standard strength: ordinary early strength, indicated by N, and high early strength, indicated by R.

CEM cements are identified by at least the notation of the cement type as specified by the CEN and the number and letter indicating the strength class.

2.2.2. Water

Water is one of the main constituents of concrete as it starts the hydration reaction and controls the spacing of the cement grains. The amount of water to be added must be strictly controlled. It has to be enough to produce the hydration reaction and to obtain the required workability (property of freshly mixed concrete which determines the ease and homogeneity with which it can be mixed, placed, consolidated and finished). However, too much water can produce some problems such as: property variations, segregation and/or micro-structure defects. Strength and nearly all other properties are influenced

by water to cement ratio (W/C).

Water assures cement hydration. Chemically, the amount of water necessary for the reactions is limited to around 25% of the mass of cement, however not all the water added will be able to react. On the other hand, an excess of water is necessary to assure workability of the mixture. As the amount of water is increased, the porosity will also increase, which will result in lower resistance. In general, a low W/C will give us a high resistance mixture but with low workability, while a high W/C will obtain a low resistance but high workability mixture [15, 17].

2.2.3. Aggregates

Aggregates are inert materials which conform the skeleton of the concrete. In essence, concrete is a mixture of aggregates binded together by the cement. In the hardened concrete, the coarse aggregates are generally the most resistant element. Thus the optimum is to use as much aggregate as possible with the largest possible aggregate size.

Aggregates form the bulk of the concrete volume, typically around 70-80% of the total volume. They have two main missions: to act as a filler and to give strength to the mixture. Classification can be done according to density, particle size, shape, source (natural or artificial) and their formation method. All particles with a diameter smaller than 5 mm are classified as fine aggregate, and all particles with a diameter bigger than 5 mm as coarse aggregate [19].

2.2.4. Additions

Additions are inert, pozzolanic or hydraulic minerals that are added to concrete to improve certain properties. If the addition is pozzolanic or hydraulic, its cementing properties are used in addition to or as a partial replacement of some of the cement, and are classified as supplementary cementing materials.

All kinds of additions will modify the behaviour of the mixture due to the filler effect.

Fillers interact chemically by acting as a nucleation site for hydrates. Physically they will interact by filling the intergranular space and increasing the space between the other particles, which will increase the compactness and densify the mixture.

Principal supplementary cementing materials are: fly ash, natural pozzolanas, ground granulated blast furnace slag, silica fume, metakaolin and limestone. The main compounds are quicklime (calcium oxide), silica (silicon dioxide) and alumina (aluminium oxide). As the amount of quicklime increases and silica decreases the hydraulic reactivity increases.

Although the main use of supplementary cementing materials comes from the decrease in price, they can also be used to improve a particular property through hydraulic and/or pozzolanic activity, such as resistance to alkali-aggregate reactivity. Careful consideration of the material to be used and the dosage must be made to assure the expected results are obtained.

As stated before, supplementary cementing materials can have hydraulic and/or pozzolanic activity. A hydraulic binder reacts chemically with water to form hydrates that have cementing properties. A pozzolan is a siliceous or aluminosiliceous material, by itself they have little or no cementitious value. However in a finely divided state and in the presence of moisture pozzolanas will chemically react with alkalis to form cementing compounds [15, 20, 21].

Fly Ash

Fly ash or pulverised fuel ash is a pozzolanic addition. It is made out mainly of silicate glass containing silica, alumina, iron, and calcium. Minor constituents are magnesium, sulphur, sodium, potassium and carbon. Crystalline compounds are present in small amounts. When ground or powdered coal is combusted, the residue produced is fly ash. However, only selected ashes have a suitable composition and particle range size for use in concrete. Figure 2.2 shows a micrograph of the particles, most of the particles are solid spheres, but some particles are hollow (cenospheres).
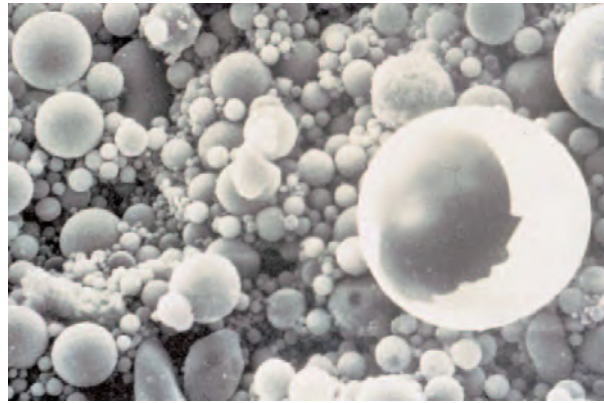
Figure 2.2: *Scanning electron microscope (SEM) micrograph of fly ash particles at 1000X [20].*

Fly ash is classified into two types:

- Class F- Fly ash with pozzolanic properties, generally low-calcium oxide (less than 10% CaO). It is usually a by-product from burning anthracite or bituminous coal.

- Class C-Fly ash with pozzolanic and hydraulic properties, generally high-calcium oxide (10%-32% CaO). It is usually a by product from burning sub-bituminous or lignite coal.

As shown in figure 2.3, class F and C- Fly ash have an increase of hydraulic activity as the amount of calcium oxide is increased. However, this hydraulic reactivity is still much lower than that of portland cement.
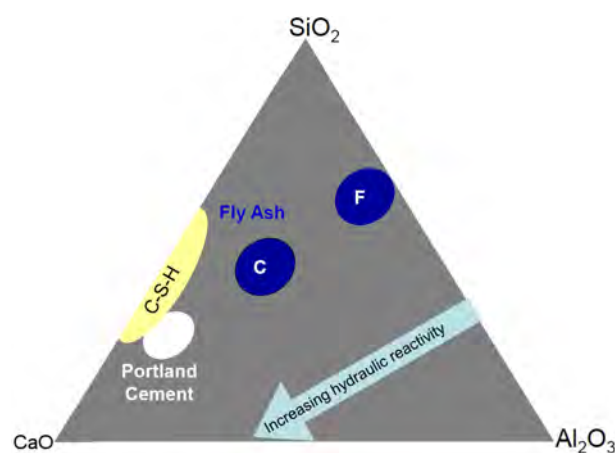
Figure 2.3: *Chemical composition of various fly ash as compared to OPC [15].*

When fly ash is added into concrete, the pozzolanic reaction occurs between the silica glass and the lime. This means fly ash can reduce the amount of cement (reducing the cost). As the heat produced by this reaction is lower than that of cement, the heat of hydration and therefore the temperature rise, are reduced. An increase in setting time will also be observed in comparison to an equivalent grade of OPC concrete. As described before, fly ash will also act as a filler, densifying the mixture. Other benefits from using fly ash in concrete include: low permeability, resistance to sulphate attack and prevention of the alkali-silica reaction.

However, fly ash concretes has slower hydration rates, meaning longer setting and hardening times and they are susceptible to dry out which can lead to premature end of hydration [19–21].

2.2.5. Admixtures

Admixtures are chemicals that can be added to cement, mortar or concrete to significantly change its fresh, early age or hardened state to economic or physical advantage. Modern concretes almost always posses additives, either in the mineral or chemical form. UNE-EN 934-2 defines admixture as an additive added during mixing of concrete in a quantity not above 5% mass of cement content, with the object of modifying the properties of the mixture in fresh and /or hardened state [19, 22].

A number additives can be used, including:

- Water reducers: reduce the water demand for a given workability

- Air entrainers: entrain air in the mixture, providing resistance to freezing and thawing action.

- Accelerators and retarders: control the setting time and strength gain rate.

- Special purposes: viscosity modifying agents, corrosion inhibitors, alkali-aggregate expansion inhibitors, shrinkage reducing admixtures...

The most important admixtures in the market are superpasticizers and accelerators.

Superplasticizers

Superplasticizers (SPs) are water reducing agents. Water reducers are classified into two broad categories:

1. Plasticizers, also called normal water reducers, reduce the amount of water by 5-10%.

2. SPs, also called high range water reducers, reduce the amount of water by 15-40%.

As figure 2.4 shows, there are three mayor uses for SPs on fresh and hardened concrete.

- I is reducing water in order to increase the strength, lowering the W/C ratio and increasing the strength and durability while maintaining the workability.

- II is reducing the quantity of water and cement obtaining a similar strength, durability and workability, saving cement.

- III is not changing the mix proportions, this will mean the workability is increased while the strength and durability will be similar.

However, the use of SPs will have a negative effect on setting time, hardness and air content [22].
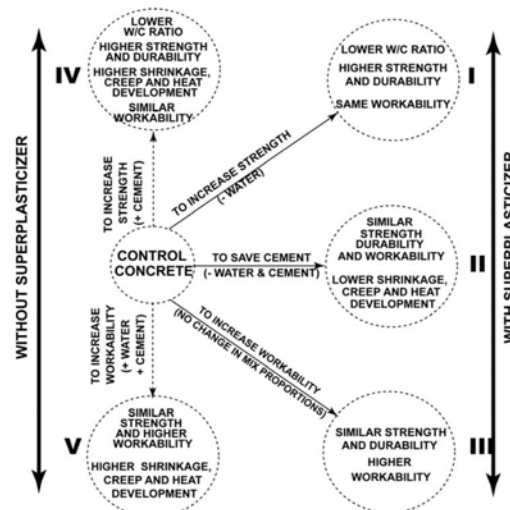
Figure 2.4: *SP effects on fresh and hardened concrete [22].*

There are four main types of SP: nodified lignosulphates (also called "1st generation"), sulphonated melamine formaldehyde condensates (also called "2nd generation"), sulphonated naphthalene formaldehyde condensates and polymers containing carboxylic acid

groups (also called "3rd generation"). Depending on the SP used, water reduction will vary greatly along with all the effects obtained [17, 21].

The amount of polycarboxylic ether superplasticizer required for a specific workability is much lower than that of sulphonated naphthalene formaldehyde condensates or nodified lignosulphates. Therefore, although the cost of PCE is much higher, the overall cost of a normal mixture would not be influenced by the choice of the SP except for sulphonated melamine formaldehyde condensates, which are much more expensive.

SPs reduce the amount of water required by lubrificating cement grains, which in turn liberates water that is trapped inside the flocks of cement (figure 2.5), and makes the mixture more workable by giving mobility to the cement grains. There are two main mechanisms involved depending on the type of SP: electrostatic repulsion and steric hindrance. In electrostatic repulsion, electrostatic attractive forces existing among cement particles are neutralised by the adsorption of anionic polymers, while dispersion is obtained by the electrical repulsion between the negatively charged groups on the other side of the chain. In steric hindrance, side carboxyl groups are adsorbed onto the cement particles, these particles are separated due to the obstruction between the graft chains. Steric hindrance is a more effective mechanism than electrostatic repulsion.
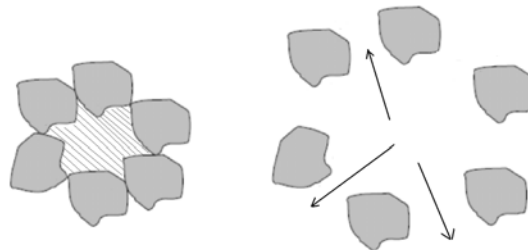
Figure 2.5: *Deflocculation of the cement flocks and liberation of water.*

The particle dispersion retards the hydration reaction. This dispersion also means a higher fluidity of the mixture, as there is less contact and less friction between solid particles in the mixture and more free water. With lower friction air bubbles are able to escape more easily, meaning a lower air content and higher density for these mixtures [17]. On the other hand, if too much SP is used side effects may include: segregation, bleed water

or a excessive retardation in the hydration process. There is also a limit to the increase in fluidity obtained, a saturation point will be reached and no more workability will be obtained.

Accelerators

Accelerating admixtures are divided in two main groups: set accelerators and strength accelerators. Set accelerators reduce setting time of the mixture while strength accelerators increase the rate of gain of early strength development.

Accelerators are very useful for low-temperature concreting, as they are used to reduce the risk of damage by freezing when the concrete is cast in cold weather and it allows the early removal of formwork. However, a technically better way of enhancing early strength at normal temperature is to use a high range SP. Accelerators can also be used along with SP where very early strength is required, specially at low temperatures.

Some widely used chemicals that accelerate the rate of hardening of concrete mixtures are: calcium chloride, other chlorides, triethanolamine, silicates, fluorides, alkali hydroxide, nitrites, nitrates, formates, bromides and thiocyanates. Calcium chloride has historically been widely used because it is the most effective and economical. Unfortunately, it also reduces passivation of embedded steel, increasing the risk of corrosion. Therefore it is not recommended for steel reinforced concrete. Chloride-free accelerators are typically based on salts of nitrate, nitrite, formate and thiocyanate [23].

2.3. Hydration of Ordinary Portland Cement

As water is added to OPC, a paste of cement and water forms, and instantly the hydration reaction starts. At IST the mixture starts to stiffen. However, the paste strength is still very low, hardening will only start after FST [15, 17, 18, 21].

For the hydration reaction to occur, the anhydrous phases need to be dissolved in water. These dissolved ions will then react to form the hydrates, which will precipitate due to

the saturation of the solution. It is important to point out that no solid state reactions occur, only the dissolved ions react [15]. A schematic representation of the reactions of the four main compounds of OPC can be seen on Figure 2.6, [15, 24].
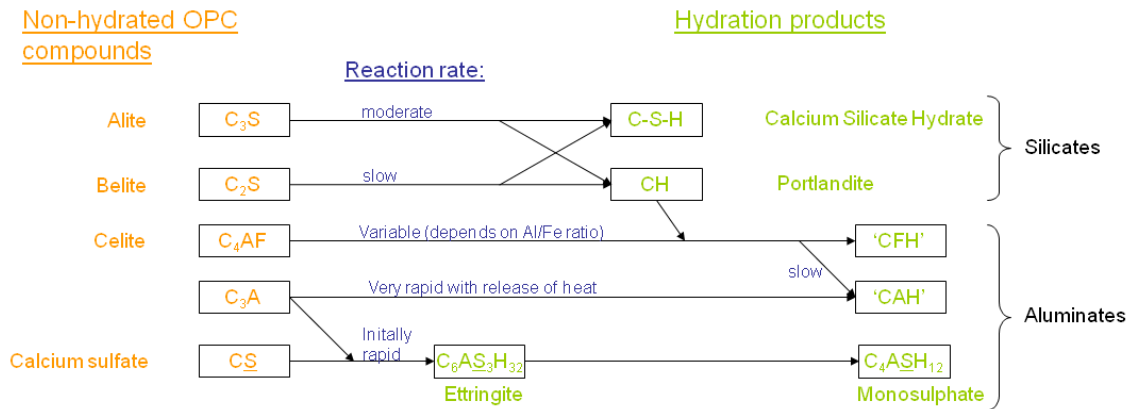

Figure 2.6: *Schematic representation of OPC hydration reactions. Adapted from [19]*

Hydration is a very complex process, researchers do not completely agree upon the microstructure forming. A simplified illustration of the hydration of OPC is shown in figure 2.7. After water is added to OPC grains, some C_3A reacts with calcium sulphate in solution. A protective layer of aluminate-rich gel forms on the surface and short ettringite rods nucleate on the gel. As shown in Figure 2.7 b) the initial rapid reaction slows down simply due to the build up of ions in solution which are unable to react due to the protective gel, leading to the dormant period where slow reaction of silicates and aluminates occurs.

After the dormant period rapid formation of C-S-H and portlandite starts. "Outer C-S-H" forms around the ettringite network. As shown in Figure 2.7 c) However, C-S-H is not in contact with the underlying grain, forming "hollow" shells known as Hadley grains [25]. Slow reaction of aluminates continue taking place.

After around 18 hours (figure 2.7.d), the speed of reaction of C-S-H and CH slows down due to lack of space the mixture starts cooling down. Secondary ettringite long rods form from sulphate absorbed in C-S-H. "Inner C-S-H" starts to form inside the shell from the continuing hydration of C_3S.

As the sulphate dissolved exhausts (figure 2.7.e), C_3A will react with any ettringite inside the shell to form monosulfate. At this stage the "inner C-S-H" reduces the separation between the grain an the hydrated shell.

After 2 weeks hydration, the gap between the "hydrating shell" and the grain is completely filled with CSH. The original and "outer CSH" becomes more fibrous as shown in Figure 2.7 [15, 21, 26].
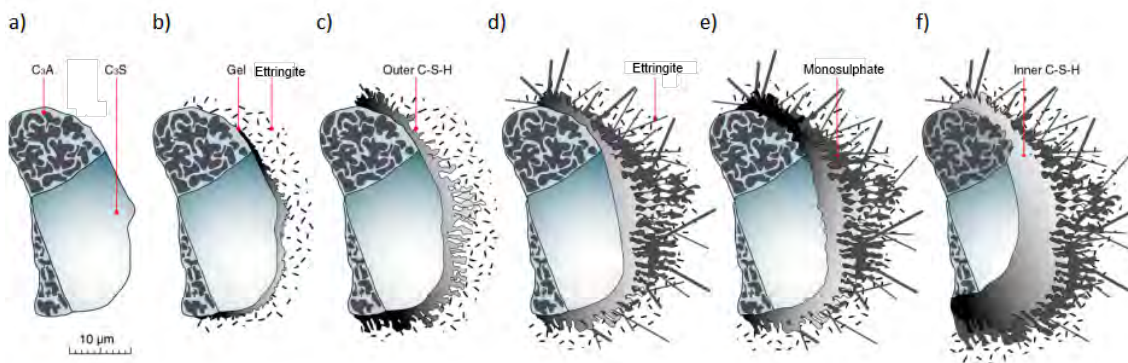

Figure 2.7: *Development of microstructure during the hydration of OPC [26].*

Hydration reactions are exothermic, thus heat is given off to the environment. This heat is called heat of hydration, figure 2.8 shows its typical variation. Heat of hydration can be described in five stages. Just after mixing there is a high but very narrow peak corresponding to the initial wetting reactions and the formation of the protective gel and ettringite. This quickly develops into the dormant period where the mixture is relatively inactive. After the dormant period, at a time corresponding roughly to the initial set [24], an acceleration occurs as the C-S-H is formed, the heat rate starts to increase rapidly and reaches a maximum peak. As the reactions gradually slow down the mixture starts cooling and a second smaller peak appears due to the formation of monosulphate. During the final stage it is possible that a further narrow peak occurs after one or two days [17].
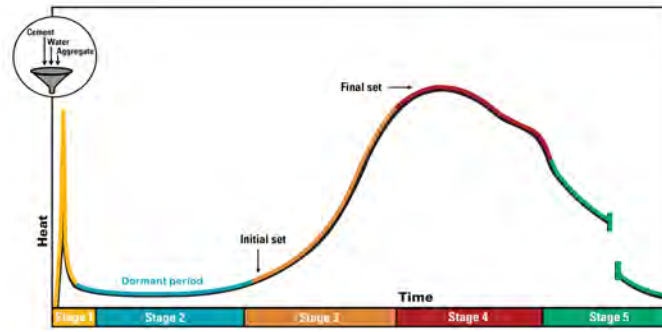
Figure 2.8: *Heat of hydration. Adapted from [24].*

2.3.1. Relationship between microstructure formation and macroproperties

As hydration reactions take place, cement grains are surrounded by a layer of hydration products that grows both in the inside and outside directions. As the grains of the hydrating cement expand, friction increases between the grains and workability is lost. Initial set is reached. Bonds are formed between the grains creating a continuity in the solid structure [19]. Considering this, hydration can be studied using the percolation theory, which is a mathematical model to describe the behaviour of connected particles.

Two concepts of the percolation theory are critical for the study of setting: percolation threshold and solid percolation probability. Percolation threshold (figure 2.9) is reached when a critical fraction of particles connected to each other, achieving the first long-range connectivity. Solid percolation probability is defined as the probability of a path of connected particles extends from one side of the sample to the other [9].
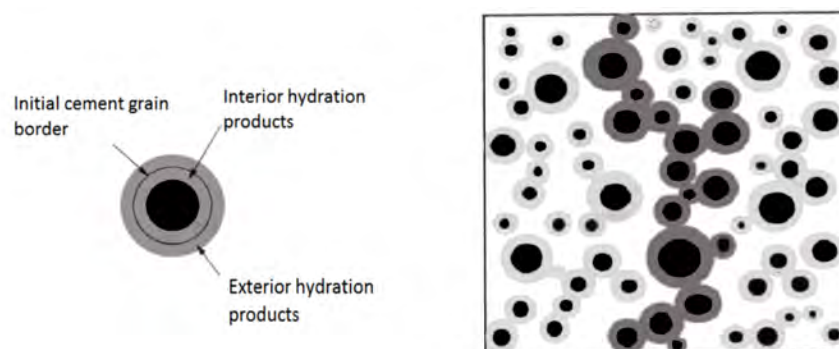
Figure 2.9: *Cement grain hydration and percolation threshold. Adapted from [19].*

After IST, as the hydration proceeds, more bonds are formed between particles, as this happens clusters form and the percolation threshold is reached. From then, the solid percolation probability increases rapidly and reaches a value of nearly 1 [9]. When this happens, the mixture changes from plastic to solid state. The elastic modulus, compresive resistance, Poison's coefficient.... develop [27]. Final set is reached.

2.4. Self-Compacting Concrete

Self-compacting concrete (SCC) is a kind of high performance concrete. Its composition allows a uniform compaction without vibration, only under the effect of gravity. It is different to high-workability concrete in that it is capable of flowing into heavily reinforcements while maintaining its integrity and homogeneity. There are three ways to obtain SCC properties:

- With viscosity agent and SP.

- High powder content and SP. This type of SCC mixtures normally contains secondary or tertiary binders. This is to reduce its price and because if only cement is used in this sort of mixtures higher temperatures would develop due to the high heat of hydration.

- The combination of the two previous compositions to obtain a less sensitive mixture to the variation of water content in a high powder content mixture [17, 19].

3. Experimental programme

In order to evaluate possible correlations between experimental techniques, a laboratory testing programme was undertaken. Details on the tests undertaken, materials used, mixture proportions and mixing procedure each mixture can be found in this chapter.

3.1. Experimental techniques

Four types of experiments were carried for this experimental programme: p-wave transmission test, Semi-adiabatic calorimetry, Vicat needle test and penetration resistance test. Semi-adiabatic calorimetry is used to determine the hydration heat generation and p-wave transmission test the evolution of the mechanical properties through hydration. On the other hand, penetration and Vicat tests are used to determine penetration resistance.

Detailed procedures used for this experimental programme can be consulted in annex B

3.1.1. Ultrasonic testing : p-wave transmission test.

Ultrasound waves are acoustical waves with a frequency higher than 20 kHz. These waves can be used for non-destructive testing methods with various uses in different fields (for example, used in the medical field for ultrasound scans or in the industrial field for distance determination).

Wave propagation

Ultrasounds are transmitted through a medium or interface in three main propagation waves:

1. P-waves (compressional)- propagate through the medium

2. S-waves (transverse)- propagate through the medium

3. Rayleigh waves (surface)- propagate through the interface
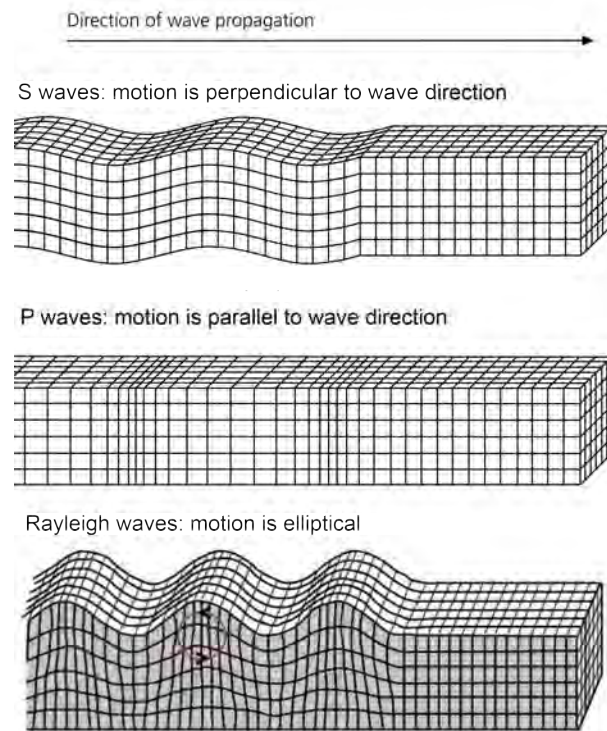
Figure 3.1: *Representation of wave propagations*

Figure 3.1 shows p-waves are compressions and rarefactions of matter in the direction of propagation. S-waves are the perpendicular movement of the matter in comparison to the direction of propagation. Rayleigh waves arise from the interaction of P and S waves with the interface, matter moves elliptically in the vertical plane and parallel to the direction of propagation to comply with the equilibrium.

In concrete, p-waves have the highest velocity and Rayleigh waves the lowest, the relative velocity compared to p-waves is 60 % and 55 % for S-waves and Rayleigh waves respectively. However, S-waves do not propagate through fluids. The equipment used in this series of experiments generated p-waves.

For periodic waves, its frequency f, in Hertz, is a characteristic property defined by:

$$f = \frac{v_{phase}}{\lambda}.$$
(3.1)

Where:

f: Frequency (Hz)

v_{phase}: Phase velocity (m/s)

λ: Wavelength (m)

For p-waves, velocity of propagation v_p, is related to the mechanical properties. For elastic, homogeneous, isotropic solids the p-wave velocity is given by:

$$v_P = \sqrt{\frac{K + \frac{3}{4}G}{\rho}} \tag{3.2}$$

Where:

v_P: p-wave velocity (m/s)

K: Bulk modulus (Pa)

G: Shear modulus (Pa)

ρ: Density ($\frac{kg}{m^3}$)

For liquids, shear modulus is negligible thus p-wave velocity is given by:

$$v_P = \sqrt{\frac{K}{\rho}} \tag{3.3}$$

p-wave velocity in concrete will therefore depend on the elastic properties as well as on the proportions of the constituent materials and the air entrapped in the specimen. Before percolation, concrete behaves as a suspension of aggregates and powder particles (cement and mineral additions), as hydration reactions take place and the microstructure develops, concrete behaves as a porous solid.

Changes in the microstructure of the specimen as hydration takes place will cause a rise of the p-wave velocity. Thus ultrasound transmission velocity can be used to study hydration. This experimental technique has the advantage in comparison to other techniques (such as penetration standardized resistance test) that it is non-destructive. Therefore changes in the microstructure can be followed on test specimens and the specimen can be monitored for an unlimited number of tests [3].

p-wave transmission test

p-wave velocity of a mortar specimen is monitored. Each specimen is placed in a silicon mould (70mm diameter and 60mm high) with an ultrasonic sender an receiver positioned diametrically opposite to each other. The transducer transmits a wave into the specimen and the receiving transducer receives the pulse. For this series of experiments the multi-channel "Ultrasonic Multiplex IP-8 tester" manufactured by UltraTest GmbH is used. This data acquisition system allows the recording of up to eight different channels, although only four where used simultaneously as shown in figure 3.2.
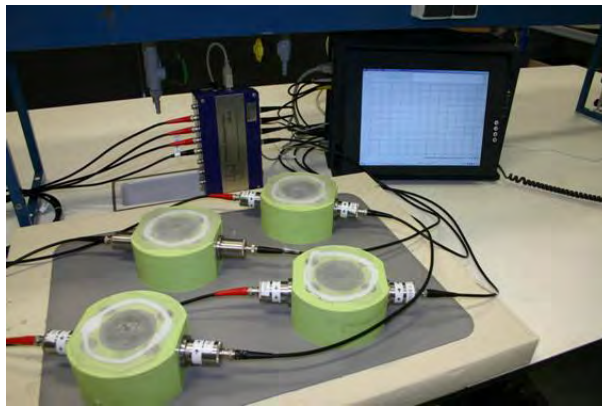
Figure 3.2: *p-wave transmission testing device in a 4 channel setup.*

The data acquisition is discrete. A compressional pulse is emitted every 60 s. p-wave velocity is calculated from the transmission time which is measured and the distance between the two transducers. p-wave velocity in function of time is obtained and its gradient curve can be determined. For these curves variability, local errors and the discrete nature of the data have to be taken into account. Velocity curve results are therefore smoothened, methods used are (Figure 3.3):

1. Polyfit: finds the coefficients of a polynomial p(x) of degree 10 to 60 that fits the data in a least squares sense [28].

2. Splines: uses a cubic spline interpolation to fit the data [28].

p-wave velocity and setting

Figure 3.5 shows the p-wave velocity curve divided in three steps. In step I, hydrates are beginning to form, p-waves are propagating through a suspension of these hydrates
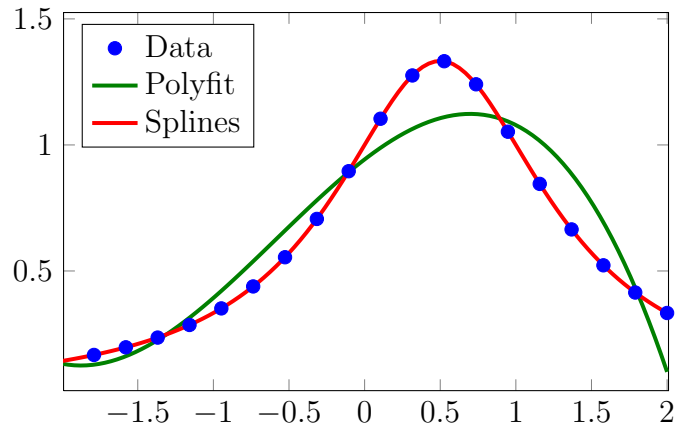
Figure 3.3: *Interpolation methods*

in water, in this step G is low and K is developing. As hydration continues, step II is reached when a sharp rise in p-wave velocity is achieved. Percolation threshold is reached in the early part of step II [4]. As the porous solid structure forms and more and more hydration products are formed p-wave velocity continues rising due to the rise of G. As the volume of pores decreases p-wave velocity stabilizes entering in step III.

Several authors have proposed different points that could correspond to IST and FST. For this work six characteristic points are used for comparison (figure 3.4).
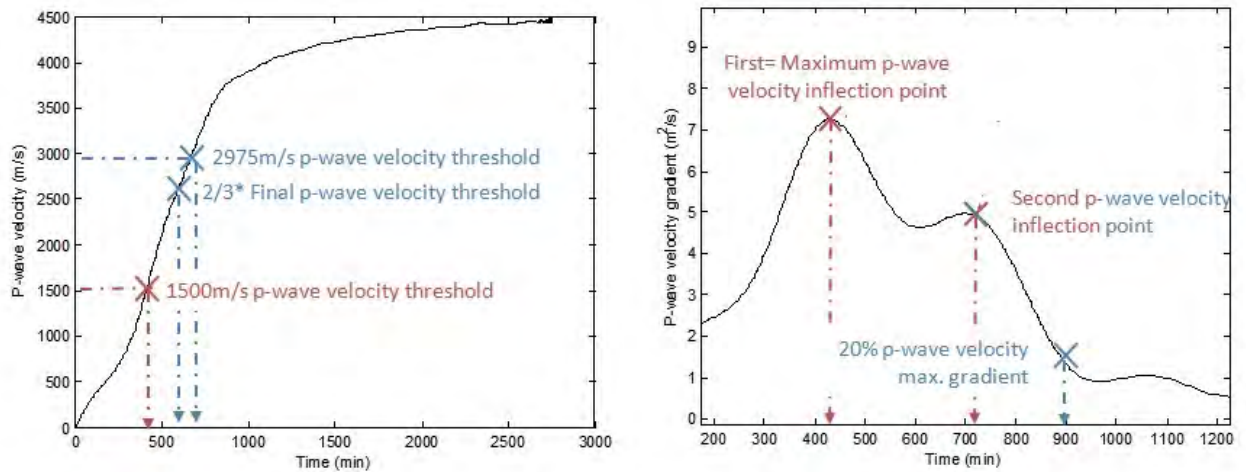
Figure 3.4: *IP-8 possible indicators for IST (red) and FST (blue).*

IST **possible indicators**   Previous research has proven good correlation between IST and time corresponding to:

- First inflection point, corresponding to the transition between step I and II of figure

3.5 [2, 5–7]

- 1500m/s threshold value, corresponding to pulse velocity in water [2–4].

The inflection point criteria had to be modified to accommodate it to the fact that there were at least two inflection points in the experimental curves obtained. Besides the 1500m/s threshold criteria four more points were considered as possible indicators for IST. With these modifications the characteristic mortar ages considered for IST are:

1. 1500m/s threshold.

2. First inflection point.

3. Second p-wave inflection point.

4. Maximum p-wave velocity gradient inflection point.

FST **possible indicators**   Previous researchers have proposed mortar ages corresponding to:

1. 2975m/s threshold proposed by Alexander Herb [8] as a good estimate for FST.

2. 20 % maximum p-wave velocity gradient, proposed by Robeyst [9].

   Besides these two points two further criteria has been studied:

3. Mortar age at second inflection point.

4. Mortar age corresponding to 2/3 of p-wave velocity at 2600 min.

Figure 3.4 exemplifies these eight points.

3.1.2.   Semi-adiabatic calorimetry

As described in section 2.3, hydration of OPC is an exothermic reaction. Temperature rise of the sample will depend upon the total heat generated, the heat flux generated and the thermal efficiency of the system. Heat generation depends on the cement properties, the environment temperature and the thermal characteristics of the system [30]. Studying temperature variations is interesting not only because it determines the degree
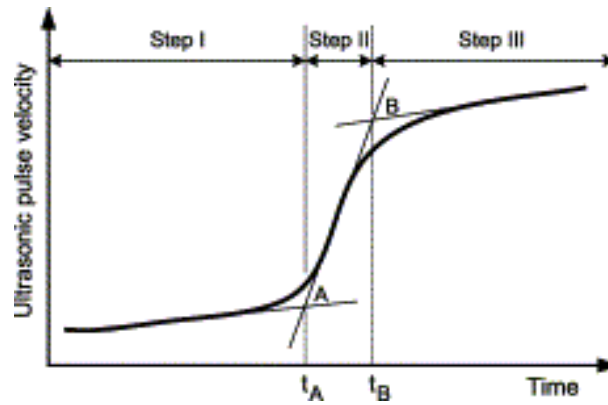
Figure 3.5: *Schematic representation of typical p-wave velocity [29].*

of hydration and thus the resistance, but also because temperature gradients may lead to early-age cracking and consequently reduce the serviceability of the material.

Different techniques can be used to measure the heat of hydration. These include:

- Heat of solution

- Isothermal calorimetry

- (Semi)-adiabatic calorimetry

Heat of solution The details of this method can be found in the standard EN 196-8 Methods of testing cement- Part 8: Heat of hydration-Solution method.

This method involves dissolving cement in an acidic mixture within a calorimeter and measuring the temperature rise, its main advantage being the measurements can be taken during long periods. It has fallen into disuse due to its limited relevance to concrete performance and high degree of operator skill required to obtain good results. It is important to note this method has not been proven reliable where supplementary cementing materials are used.

Isothermal calorimetry This method is not yet standardised. Samples are placed in a calorimeter which is maintained at constant temperature. As heat is released it is measured. It is important to note the sample will therefore be at a constant temperature.

(Semi)-adiabatic calorimetry This method consists in the introduction of a sample inside a calorimeter and measuring the temperature variation. In this method heat losses are allowed, and accounted for by comparison to a reference calorimeter containing a fully

hydrated mortar of equivalent thermal mass. It is classified in 2 categories, depending on the type of insulation:

- Langavant semi-adiabatic calorimeter which uses a dewar flask to insulate (figure 3.6). This method is normalised in the standard EN 196-8 (Methods of testing cement- Part 9: Heat of hydration-Semi adiabatic method).

- Adiabatic test which is totally isolated from the environment.

Figure 3.6: *Langavant semi-adiabatic calorimeters*

For this experimental programme Langavant semi-adiabatic calorimeter is used.

Heat of hydration calculation

Heat of hydration Q, can be calculated using the equation:

$$Q = \frac{c}{m_c}\theta_t + \frac{1}{m_c}\int_0^t \alpha \times \theta_t \, \mathrm{d}t. \tag{3.4}$$

Where:

Q: Heat of hydration (J/g)

m_c: Mass of cement contained in the test sample (g)

t: Hydration time (h)

c: Total thermal capacity of the calorimeter (J/K)

α: Coefficient of heat loss of the calorimeter (J/hK)

θ_t: Temperature rise of the test sample at time t (K)

This equation divides itself into two terms: the first term of the equation represents the heat accumulated in the calorimeter and the second term the heat lost into the environment.

$$Q = Q_A + Q_B \tag{3.5}$$

Where:

Q_A: Heat accumulated in the calorimeter (J/g)

Q_B: Heat lost into the environment (J/g)

Finally, the hydration heat flux is defined as follows:

$$q = \frac{\partial Q}{\partial t} \tag{3.6}$$

Where:

q: hydration heat flux (J/gh)

Heat accumulated in the calorimeter   As seen before, the heat accumulated is calculated using:

$$Q_A = \frac{c}{m_c}\theta_t \tag{3.7}$$

The total thermal capacity of the calorimeter depends upon the composition of the test sample and the properties of the calorimeter. Standard 196-9 states formula 3.8.

$$c = 0.8(m_c + m_s) + 3.8m_w + 0.50m_b + \mu \tag{3.8}$$

Where:

0.8:   Thermal capacity per unit of mass of cement plus sand (J/gK)

3.8:   Average thermal capacity per unit of mass of water (J/gK)

0.50:   Thermal capacity per unit of mass of the mortar box (J/gK)

μ: Thermal capacity of the empty calorimeter (J/K)

$$m_s: \quad \text{Mass of sand contained in the test sample (g)}$$

$$m_b: \quad \text{Mass of empty mortar box plus lid (g)}$$

However the standard does not consider the use of SCMs of admixtures. To include the effect of these additions the following formula was used:

$$c = 0.8(m_c + m_s + m_{fa}) + 3.8m_w + 0.50m_b + \mu \tag{3.9}$$

Where:

$$m_{fa}: \quad \text{Mass of fly ash contained in the test sample (g)}$$

Heat lost into the environment The heat lost into the environment, is defined as:

$$Q_B = \frac{1}{m_c} \int_0^t \alpha \times \theta_t \, \mathrm{d}t. \tag{3.10}$$

This expression can be simplified into:

$$Q_B = \frac{1}{m_c} \sum_{i=1}^n \bar{\alpha}_i \times \bar{\theta}_i \times \Delta t_i \tag{3.11}$$

Where:

$$\Delta t_i: \quad \text{Elapsed time between the measurement of temperature at point in time,}$$
$$t_{(i-1)}, \text{ and the next measurement at point in time, } t_{(i)} \text{ (h)}$$

$$\bar{\alpha}_i: \quad \text{Average coefficient of total heat loss of the calorimeter in the period of}$$
$$\text{time, } \Delta t_{(i)} \text{ (J/hK)}$$

$$\bar{\theta}_i: \quad \text{Average of the temperature rise of the test sample, between times } t_{(i)}$$
$$\text{and } t_{(i-1)} \text{ (K)}$$

The average coefficient of heat loss of the calorimeter is calculated by:

$$\bar{\alpha}_i = a + b \times \bar{\theta}_i \tag{3.12}$$

Where a and b are the calibration constants of the calorimeter.

Maturity method

As explained before, in semi-adiabatic calorimetry the temperature of the sample is allowed to rise freely. However, the rise in temperature affects the properties, this is known as the "crossover effect" (figure 3.7). The maturity method adapts the sample's properties to the combined effect of temperature and time [10].
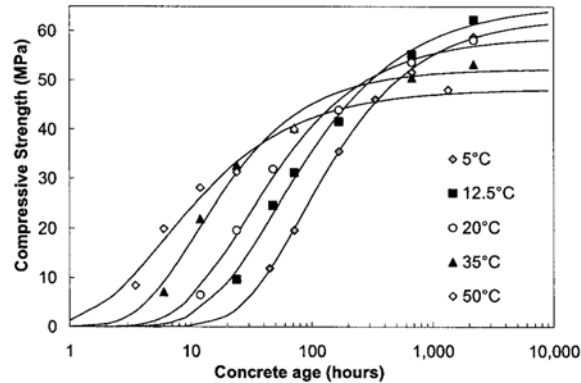
Figure 3.7: *Variation of compressive strength results for mortar curing at different temperatures [10]*

In 1977, Freiesleben, Hansen, and Pedersen proposed the use of a maturity function based on the Arrhenius equation. This equation accounts for the fact that as temperature increases, so does the rate of the hydration reaction. The acceleration factor for a reference temperature of $20°C$ is defined as follows:

$$\gamma(\theta) = e^{\frac{E_a}{R}\left(\frac{1}{293} - \frac{1}{273+\theta}\right)} \tag{3.13}$$

Where:

γ: Acceleration factor

E_a: Activation energy (J/mol). For OPC, assumed to be 33.5 kJ/mol.

R: Universal gas constant (kJ/molK)

Using the acceleration factor, an equivalent mortar age is calculated:

$$t_e = \sum_0^t \gamma(\theta)\Delta t \tag{3.14}$$

The equivalent age is the age at which a certain degree of hydration is reached in iso-thermal conditions. The degree of hydration is defined as the ratio of the hydrated cement to the original cement content. Supposing the total amount of producible heat does not change with temperature, this time correction is applied to the hydration heat curve [31].

q and setting time

Initial set has been traditionally linked to somewhere between stage two and three of the heat of hydration evolution (figure 2.8). In the same way, final set has been linked to a point between stage three and stage four. In 2007, Sandberg and Liberman [11] proposed two methods of obtaining setting times from temperature histories:

1. "Fractions Method"- where IST and FST were defined as percentages of the total semi-adiabatic temperature rise. Default values of 21 % and 42 % were defined as IST and FST respectively

2. "Derivatives Method"-defines FST as time corresponding to the maximum slope of the hydration heat and IST is defined as the time corresponding to maximum curvature of the hydration heat.

In 2004 Schindler [32] proposed a maturity-based model in terms of the degree of hydration of a sample. IST and FST were defined as the equivalent age for certain degrees of hydration in function of the W/C ratio. However, this model did not give good results for mixtures containing ground-granulated blast- furnace slag.

For this experimental programme the "Derivatives Method" was proposed at first. to-gether with the age at which q=qmin+0.25 J/gh proposed by Zingg [12] as a good measure for the IST as determined by a Vicat penetration test. Figure 3.8 shows graphically these criteria.

However, as the experimental results were obtained the q curves showed longer dormant periods and its minimum is not clearly defined. This is why for IST reference points qmin+0.2△(qmax-qmin)and qmin+1.5J/gh were considered. Figure 3.9 shows these criteria graphically.
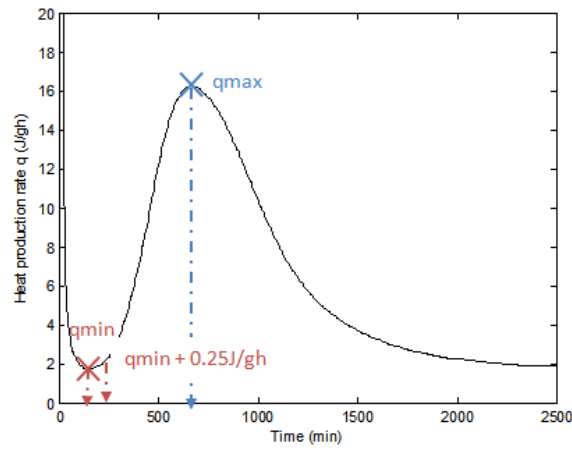
Figure 3.8: *Semi-adiabatic possible indicators for IST (red) and FST (blue).*
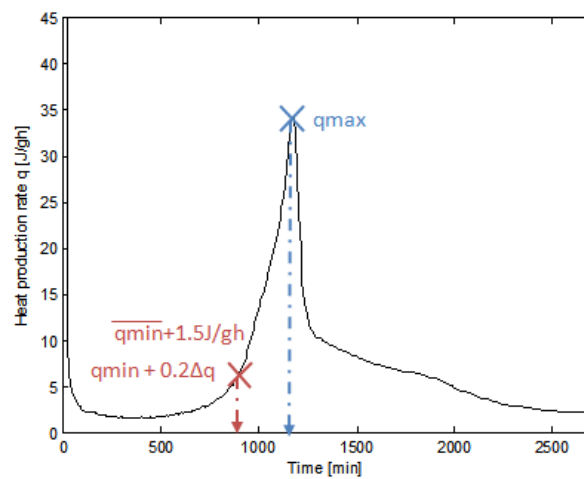
Figure 3.9: *Semi-adiabatic possible indicators for IST (red) and FST (blue).*

3.1.3. Vicat needle test

Both Vicat and penetrometer tests are penetration resistance methods which try to study setting and hardening process from direct measurements. Both of these methods test the ability of a material to resist the penetration of a tool, and setting characteristics can be inferred from the results. However, penetration tests can be labour intensive, dependent on the technician and do not give us any information on the hydration reactions or microstructural changes in the mixture [33].

The Vicat test is standardized in ASTM C187 (Standard test method for normal consistency of hydraulic cement) and EN 196-3 (Methods of testing cement- Part3: Determination of setting times and soundness). The standard followed for this experimental programme was EN 196-3. In this testing method, a needle of 300 g and a diameter of 1.0 mm is dropped and penetrates a sample of cement paste (figure 3.10 shows the equipment used). For standard EN 196-3 IST is defined as the time when the clear distance between the needle and the bottom of the mould is of 6 ± 3 mm, rounded to the nearest 5 min. This distance varies between standards, ASTM C187 sets it to 15 mm, both values serve as convenient points of comparison between samples [13]. Although the standard does define a procedure to determine FST, a needle with ring is required which was not available for this experimental method.

Figure 3.10: *Vicat needle test equipment*

The Vicat needle exerts a force of 2.94 N, the cement paste exerts two reaction forces on

the needle: skin resistance exerted on the "penetrated" surface of the needle which is dictated by shear resistance and a compressive resistance exerted on the tip of the needle [1]. This forces are represented in figure 3.11.
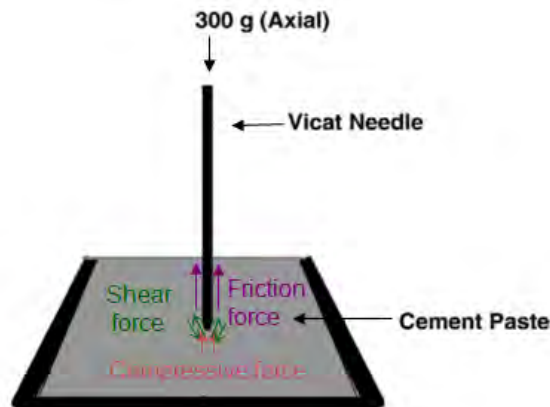
Figure 3.11: *Schematic illustration of the forces involved in the Vicat test [1]*

It is important to note that this test is performed on cement paste instead of mortar. Therefore, an equivalent cement paste had to be determined based on workability equivalence. However, the workability behaviour was drastically different, and after a series of tests slump results were given priority. Figure 3.12 shows the mortar slump and shock test results (blue and pink lines respectively) and the results for the equivalent cement paste.
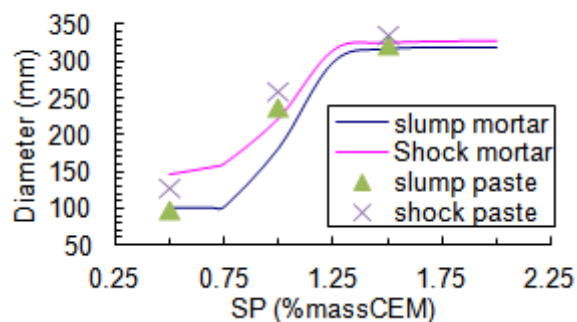
Figure 3.12: *Workability curve for SP, with workability of cement paste*

Data treatment

Standard EN 196-3 does not specify any kind of data treatment criteria, however as experiments were carried out it was obvious there were jumps in the measurements due to air entrapped. For this reason a logarithmic approximation was used, using common sense to exclude these points. Figure 3.13 shows this fit and illustrates *IST* criteria.
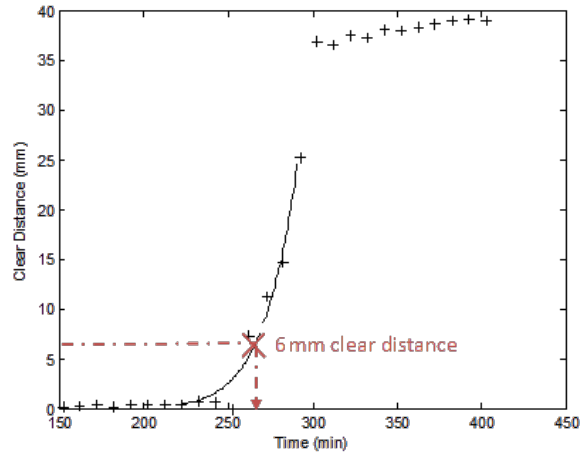
Figure 3.13: *Vicat needle test indicators for IST (red).*

3.1.4. Penetration resistance test

The method for time of setting by penetration resistance is standardized by ASTM C403. A mortar sample of with a dimension of 140 mm (depth)× 150 mm (width)× 150 mm (length) that allows six penetrations throughout one test. Each penetration should have a distance of 2.5 cm of either wall of the container or a clear distance of at least 2.5 cm or two diameters between penetrations. The mortar is penetrated to a depth of 25 mm in 10 s. To avoid the disturbance of bleed water, it is removed before any penetration. Different size needles are used depending on the mixture and its state. The penetration resistance exerted by the mortar is calculated by dividing the force by the cross-sectional area of the needle. The equipment used is shown in figure 3.14.

At a penetration resistance of 3.4 MPa, *IST* is considered to occur. Tuthill and Cordon found that at beyond this penetration resistance concrete can no longer be made plastic by vibration. They also defined that concrete can be considered as completely set as a resistance of 27.6 MPa, at this point concrete has reached a compressive strength of

Figure 3.14: *Penetrometer apparatus*

around 0.6 MPa and could carry some measurable loads. As ASTM C403 explains, data is fitted by a linear regression analysis of the logarithms of the data, verifying the correlation coefficient after removal of outliers is greater or equal to 0.98. An example of the results exemplifying IST and FST criteria is shown in figure 3.15.
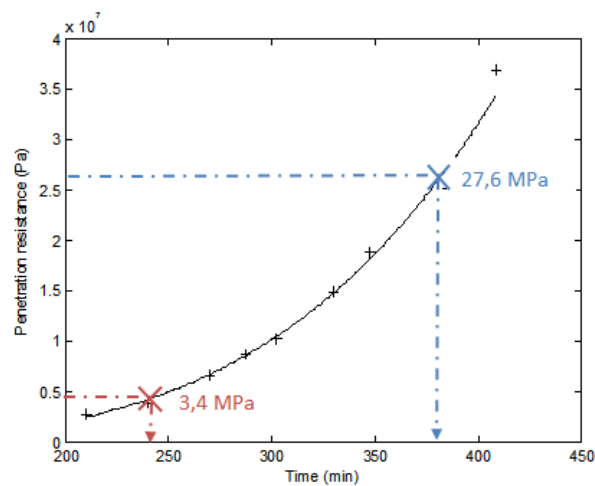
Figure 3.15: *Penetration resistance indicators for IST (red) and FST (blue).*

Forces involved in this process are basically the same as for Vicat tests though the contribution of the compressive and friction forces is higher, as the cross-sectional area of the needles is increased (figure 3.16).
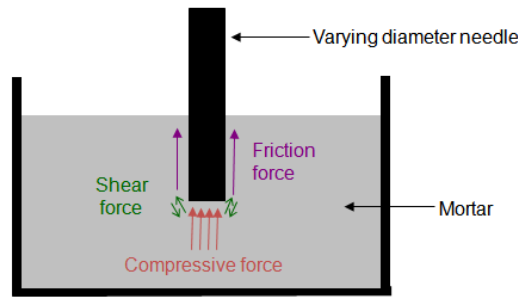
Figure 3.16: *Schematic illustration of the forces involved in the penetrometer test*

Deviation from standard- depth of sample

Penetrometer tests are standardised in ASTM C403. However, this standard states a sample with a depth of 140 mm must be filled in the containers. Due to the limitations of the facilities in the laboratory, a sample with dimensions of 80 mm (depth)× 150 mm (width)× 150 mm (length) is be used.

To verify the effect of the depth, six test specimens were prepared. Samples A, B and C had a depth of 140 mm as established in ASTM C403, while specimens I, II and III had a depth of 80 mm.

To objectively compare the two types of dimensions, a batch of 18 l of mortar was mixed. Mix proportions are listed on table 3.1. Filling was performed on sample I and sample A: then sample II and sample B: finally sample III and sample C in order to ensure similar properties of each pair.

Experimental data was treated using the steps explained in ASTM C403. The results can be observed in figure 3.17, a summary of the numerical results can be observed on table 3.2.

Although the test results were not enough to quantify the effect of depth, a series of conclusions can be reached.

Considering the mixing order and the heterogeneity of the results, its is important to note sample C was filled last and visually there was a difference with the other samples. There-

Table 3.1: *Mix proportions for the test specimens*

Mix design:			Weight		Remarks:
sand 0/5		18	**24300.00**	g	standard sand GR
CBR CEM I 52,5 N	C/S	0.333333	**8100.00**	g	+/- 0,1 g
Water @ 20C	W/C	0.45	**3645.00**	g	+/- 0,1 g
Addition	C/P	1	**0.00**	g	+/- 0,1 g
SP	$SP\%_{CEM}$	0	**0.00**	g	+/- 0,1 g
Acc. (Calcium Nitrate)	$AC\%_{CEM}$	0.4	**32.40**	g	+/- 0,1 g
Ret.(Sodium Gluconate)	$RET\%_{CEM}$	0	**0.00**	g	+/- 0,1 g
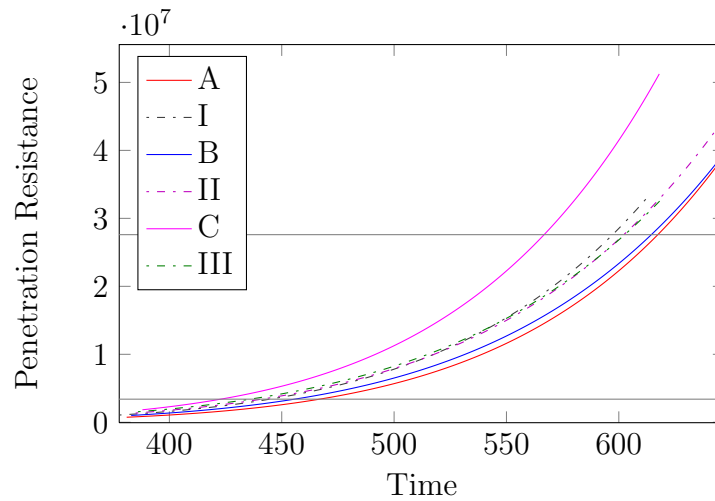
Figure 3.17: *Penetration resistance of test samples in function of corrected time after water addition*

Table 3.2: *Numerical results*

	Best fit line	R^2	IST (min)	FST (min)
A	log(PR)=7,49log(t)-13,47	0,992853	470	615
B	log(PR)=7,01log(t)-12,09	0,995294	455	615
C	log(PR)=7,15log(t)-12,24	0,996519	425	565
I	log(PR)=7,1log(t)-12,27	0,998608	445	595
II	log(PR)=6,72log(t)-11,25	0,992011	440	600
III	log(PR)=6,46log(t)-10,53	0,997796	435	605
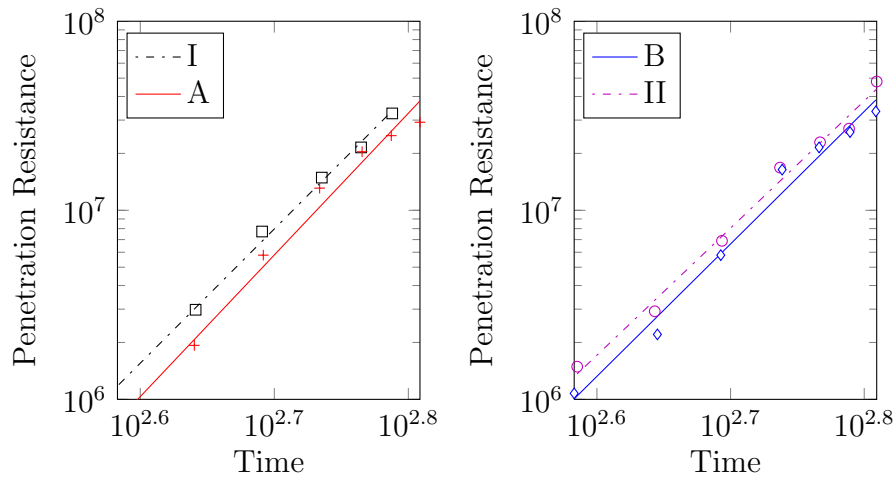
Figure 3.18: *Logarithmic plot of penetration resistance of test samples in function of corrected time after water addition*

fore sample C can be ruled out of the interesting test results. While the filling was made it was obvious the remaining mixture was more dry, thus the higher penetration resistance.

On the other hand, if the pairs of different samples are compared (sample A vs sample I and sample B vs sample II) a exponential offset is observed between the pairs that decreases slightly as the penetration resistance increases. Figure 3.18 shows the logarithmic plot and fit for the experimental data. For the same time it can be observed that 8cm deep samples have higher penetration resistances, this means times for IST and FST are lower than the standard.

3.2. Compositions

Mortar or cement paste was used for this experimental programme, depending on the requirements of the experimental technique.

3.2.1. Cement

The cement used for this research was Holcim CEMI 52.5N, its technical sheet can be seen in annex A. Its chemical composition is stated in table 3.3.

Table 3.3: *Chemical composition of Holcim CEM I 52.5 N MF*

Chemical	Content[%]
CaO	62.9
SiO_2	18.2
Al_2O_3	5.7
Fe_2O_3	4.1
MgO	0.9
Na_2O	0.40
K_2O	0.75
SO_3	3.4
Cl^-	0.06
Ignition loss	1.2
Insoluble residue	0.3

3.2.2. Sand

CEN reference sand as defined in standard EN 196-1 was used. This is a natural, siliceous sand consisting of rounded particles and has a silica content of at least 98%. It was provided in $(1350\pm5)g$ plastic bags. Its particle size distribution is described in figure 3.19.
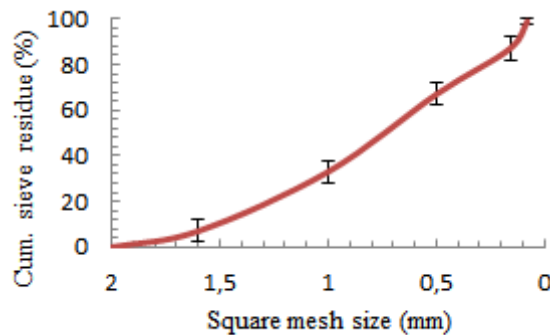
Figure 3.19: *Particle size distribution of the CEN Reference sand*

3.2.3. Fly ash

The fly ash used for this research came from Electrabel's power plant in Langerlo (Genk-Belgium). This fly ash is class C, which is self cementing and hardens without the addition of an activating chemical similar to cement.This setting is primarily due to the hydration of crystalline and amorphous calcium aluminate phases [34]. However, this supplementary cementing material will have little activity during the first days [15]. Therefore the fly ash was considered to be unreactive, acting purely as a filler for our tests.

3.2.4. Superplasticizer

The SP used for this research was a third generation polycarboxyl ether, its molecule representation is shown in figure 3.20. When water is added to the mixture, OPC particles tend to form flocks, which entrap water inside. Polycarboxyl ether's dispersion mechanism is hindrance (see subsection 2.2.5). The side carboxyl groups are adsorbed into the cement particles, these particles are separated due obstruction between the graft chains (figure 3.21).
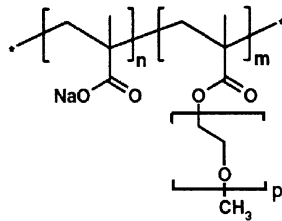
Figure 3.20: *Semi-developed molecular representation of used SP (m:n-1:3;p-23)*

Slump and shock tests were performed to obtain the workability curves (figure 3.22). Activation and saturation points were determined to be approximately 0.75 % and 1.25 % respectively.

3.2.5. Accelerator

For this experimental programme calcium nitrate tetrahydrate $(Ca(NO_3)_2 \cdot 4H_2O)$ was selected as setting accelerator. However, previous research [23] has shown that it has
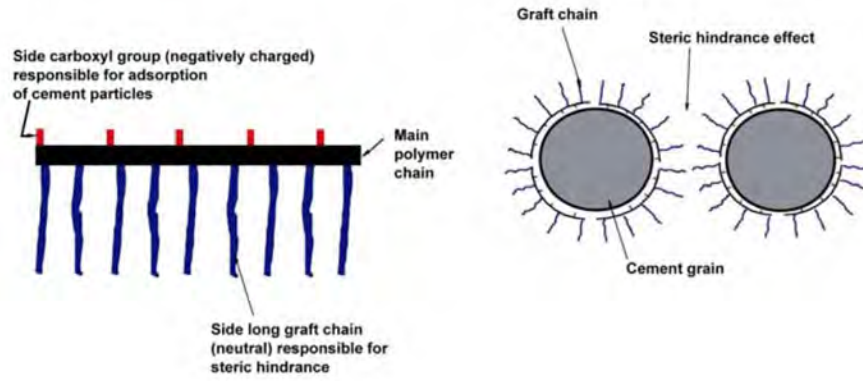
Figure 3.21: *Third generation polycarboxyl ether action mechanism [22]*
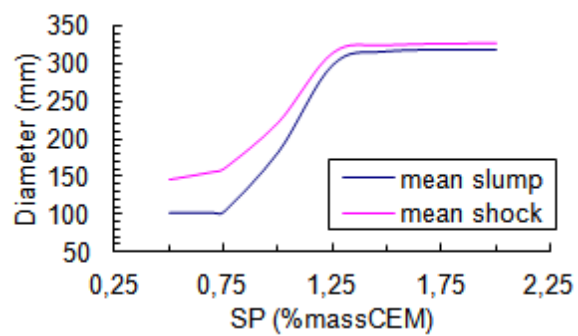
Figure 3.22: *Workability curve for SP*

other simultaneous effects such as:

- Counter-balancing the retardation provoked by SPs without affecting workability (0.2-1%massCEM).

- Long term strength increase (1-3%massCEM).

- Anti-freeze or winter concreting admixture (1–3 % mass CEM).

- Inhibitor against corrosion of steel provoked by chloride (3-4% mass CEM).

For this experimental programme quantities used varied from 0 to 3%massCEM, meaning different side-effects for these compositions would be expected.

3.2.6. Series

Ten different mortar compositions and their corresponding equivalent cement paste were developed for this testing programme. The notation for these compositions will be related to their composition in the following way:

$$\mathbf{S} - SP_{m\%CEM} * 100 - \mathbf{F} - C/P * 100 - \mathbf{A} - A_{m\%CEM} * 100 - \mathbf{R} - R_{m\%CEM} * 100 \quad (3.15)$$

Where:

$SP_{m\%CEM}$: Superplasticizer percentage cement mass.

C/P: Powder-cement ratio.

$A_{m\%CEM}$: Accelerator percentage cement mass.

$R_{m\%CEM}$: Retarder percentage cement mass.

For cement paste, the notation used will corresponds to its equivalent mortar composition. Details of the variations between the mortar and cement paste compositions can be observed in table 3.4.

For this experimental programme, the different compositions were classified into two test series:

- SP **quantity variation** (SP series): Six quantities (0 % massCEM, 0.5 % massCEM, 0.75 % massCEM, 1 % massCEM, 1.25 % massCEM and 1.5 % massCEM). For these compositions, a high powder content corresponding to a C/P ratio of 0.72, except for the 0 % SP quantity. For this case a C/P ratio of 1 was used. This variation was to avoid working with a very dry mixture (due to the water absorption by the fly ash).

- **Accelerator quantity variation** (AC series): Five quantities (0 % massCEM, 0.4 % massCEM, 1 % massCEM, 2 % massCEM and 3 % massCEM). With an SP quantity of 1 % massCEM and a C/P ratio of 0.72.

Exact compositions are tabulated in table 3.4.

Table 3.4: *SP and AC series' mixture proportions*

| | Mortar composition | | | | | | | Cement Paste (mods) | |
| | Sand | Cement | Water | FA | SP | Ac | Ret | Sand | Water |
	±5[g]	±0.1[g]	±0.1[g]	±0.1[g]	±0.001[g]	±0.001[g]	±0.1[g]	±0.1[g]	±0.1[g]
SP series									
S-00-F-100-A-000-R-000	1350	450.0	202.5	0.0	0.000	0	0	0	148.5
S-50-F-72-A-000-R-000					2,250				
S-75-F-72-A-000-R-000				175.0	3.375				
S-100-F-72-A-000-R-000					4.500				
S-125-F-72-A-000-R-000					5.625				
S-150-F-72-A-000-R-000					6.750				
AC series									
S-100-F-72-A-40-R-000	1350	450.0	202.5	175.0	4.500	1.800	0	0	148.5
S-100-F-72-A-100-R-000						4.500			
S-100-F-72-A-200-R-000						9.000			
S-100-F-72-A-300-R-000						13.500			

Testing methods

Three repetitions were fulfilled for each composition in four different methods. Each repetition is named A, B or C. However, not all compositions were tested with all the testing techniques. A summary of the tests performed can be seen on table 3.5

Table 3.5: *Testing techniques performed on each mixture*

	p-wave	Semi-Ad. cal.	Vicat	Penetration
SP **series**				
S-00-F-100-A-000-R-000	YES	YES	NO	NO
S-50-F-72-A-000-R-000	YES	YES	YES	YES
S-75-F-72-A-000-R-000	YES	YES	YES	YES
S-100-F-72-A-000-R-000	YES	YES	YES	YES
S-125-F-72-A-000-R-000	YES	YES	YES	YES
S-150-F-72-A-000-R-000	YES	YES	NO	NO
AC **series**				
S-100-F-72-A-000-R-000	YES	YES	YES	YES
S-100-F-72-A-40-R-0	YES	YES	YES	YES
S-100-F-72-A-100-R-0	YES	YES	YES	YES
S-100-F-72-A-200-R-0	YES	YES	YES	YES
S-100-F-72-A-300-R-0	YES	YES	YES	YES

3.2.7. Mixing procedure

The different constituants are mixed with the aid of the automatic mortar mixer automix 65-L0006/AM, with a 5l bowl capacity and 4 programmable mixing cycles conforming to EN 196-1, EN 196-3, DIN 1164-5 and DIN 1164-7 and 1 mixing cycle programmable by the operator.

As standard mixing procedures do not consider the use of admixtures or supplementary cementing materials. A mixing procedure adapted to this kind of mortars was applied.

The mixing procedure was developed by KV Leuven, Reyntjens (lab for concrete research) and involves the following steps:

1. 00:00(min :s)- 1/2 sand + cement + mineral addition + 1/2 sand

2. 00:00-01:00 (min :s)-Slow dry mixing

3. 01:00-01:30 (min :s)-Add water (Slow mixing)

4. 01:30-02:00 (min :s)-Slow mixing

5. 02:00-02:30 (min :s)-Stop mixing and add SP

6. 02:30-03:00 (min :s)-Fast Mixing

7. 03:00-04:30 (min :s)-Clean bowl and resting

8. 04:30-05:30 (min :s)-Fast Mixing

9. 6:00-06:10 (min :s)-Add accelerator

10. 06:10-08:10 (min :s)-Slow mixing

For this research, time is measured from the time of water addition. In other words, reference time for mixing was considered to be the moment at which water was added, which is the start of hydration.

Penetrometer

For the penetration test 3.5 kg of fresh mortar is needed to fill the moulds. The mixer can only produce a 2 kg batch. Therefore two batches were prepared which were posteriorly mixed by two minutes slow mixing. The moulds were filled with this homogeneous mixture.
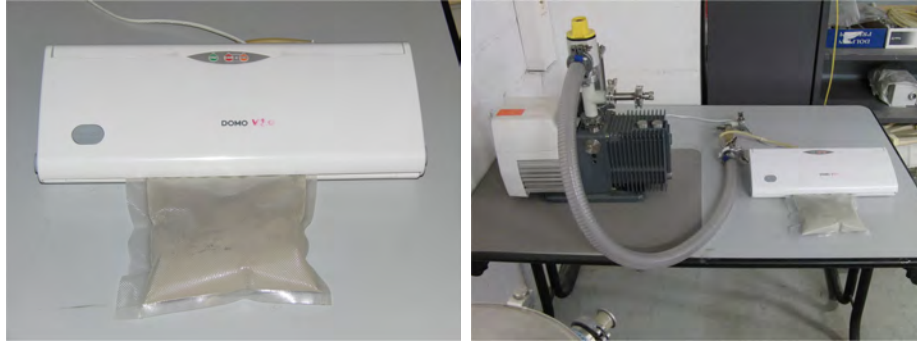
Figure 3.23: *Set-up for cement packaging*

3.3. Environmental conditions

All measurements are subjected to uncertainty, this uncertainty will propagate and affect the accuracy and precision of derived results. In every experimental programme it is important to know the different variables which will affect the results obtained, as disregarding them could lead to false conclusions. Although the objective of this thesis is not to quantify these uncertainties, an assessment on the different sources is made and an attempt to reduce these error sources where possible.

3.3.1. Cement packaging

Relative humidity is critical for the storage of cement, as water in the air will react with the cement modifying its reactivity. This ageing means irregular results for long duration tests. To reduce this effect cement was conserved double sealed vacuum bags. Figure 3.23 shows the set-up for the packaging of cement.

Extreme humidity conditions took place inside the laboratory while packing took place. This could mean that cement exposed to these conditions might have developed some hydration products during this period, retarding hydration reactions, but meaning the microstructure at the start of our tests was also affected.

Bags packed during the last week could not be discarded because there was not enough cement for the research programme. Therefore for careful analysis was made and experiments were repeated when it was considered appropriate.

3.3.2. Laboratory conditions

Temperature and relative humidity are critical variables for this experimental programme. Temperature affects the rate at which hydration reactions take place, while relative humidity will control the amount of water that evaporates during the experiments.

The laboratories where this research was performed did not have any temperature or relative humidity control, meaning they were allowed to vary freely. Standard EN 196, generally states the laboratory where preparation of specimens takes place shall be maintained at temperature of $(20\pm2)°C$ and a relative humidity of not less than 50%. However, EN 196-9 is more restrictive and states the room where the test is carried out shall be maintained at a temperature of $(20,0\pm1,0)°C$. Figure 3.24 shows temperature and relative humidity evolution throughout the months this experimental programme took place, as well as the limits stated by the standards. Temperature in the mixing room generally complies with its restriction, however the experimental room temperature does not, and relative humidity on the two rooms is generally lower than 50 %. To try to reduce the temperature deviation heaters where located in the two rooms, although this was obviously not enough to rise the temperature to adequate levels. To increase relative humidity an open water deposit heated by a resistance was also placed.
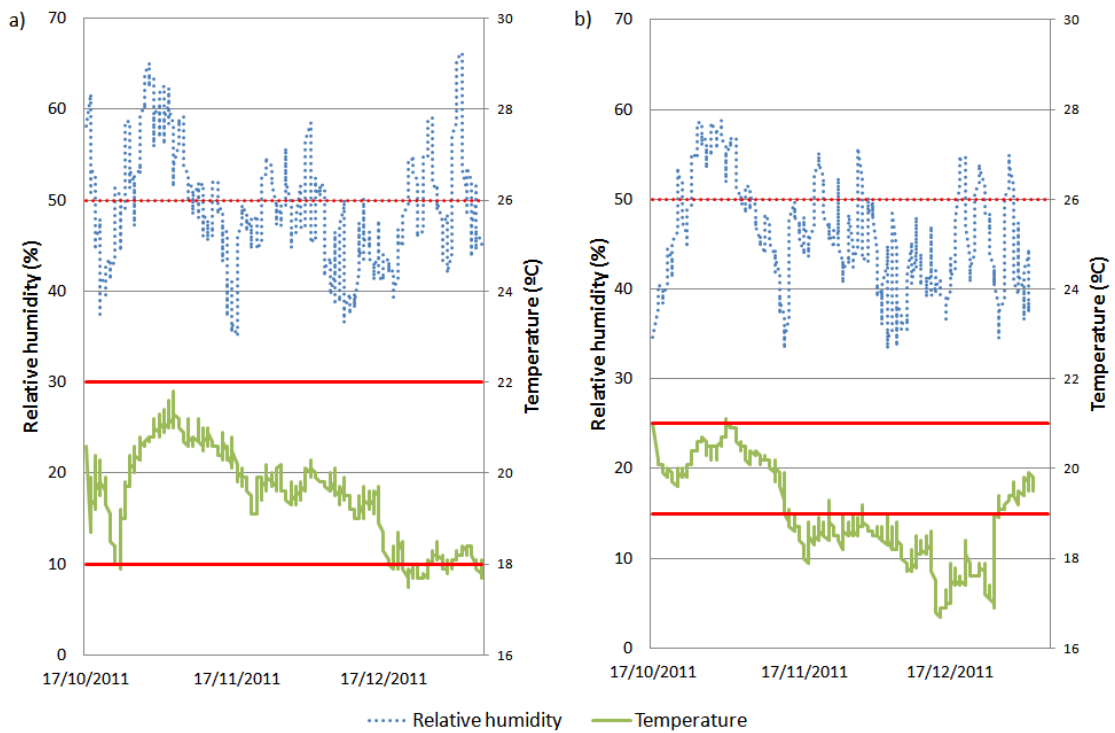
Figure 3.24: *Temperature (solid) and relative humidity (dashed) evolution in a) mixing room and b) experimental room and limits*

4. Results

In this chapter results obtained by the different experimental methods for the different compositions are presented. It is important to note that these results are the averages from the repetitions rounded to the nearest minute. Detailed results can be found in Annexes C and D.

Results are presented for each experimental technique (p-wave transmission test, semi-adiabatic calorimetry, Vicat needle test and penetration resistance test) and for each series. SP series comprises the study of 6 mixtures, containing different SP quantities: 0.00 %, 0.50 %, 0.75 %, 1.00 %, 1.25 % and 1.5% of the cement mass. With this SP quantity a C/P ratio of 0.72 was used, except for the 0.00 %, where a C/P ratio of 1 was used, meaning no fly ash was present to avoid a very dry mixture, which would be very difficult to work with and could influence our results. The AC series comprises the study of 5 mixtures, each containing a different quantity of accelerating agent: 0.00 %, 0.40 %, 1.00 %, 2.00 % and 3.00 % of cement mass. The amount of fly ash was maintained constant with a C/P ratio of 0.72, and SP quantity corresponding to 1.00 %mCEM.

4.1. P-wave transmission test

4.1.1. *SP* series

The splines approximation method (see section 3.1.1) was used to smoothen the raw p-wave velocity curves. This decision was based on two criteria: the root mean square error and standard deviation for the points in the proximity of the inflexion points. Indeed, while the Splines method results in a fit curve with a lot of oscillations at the start and the end of the p-wave velocity curve, it results in a smooth fit with very low RMSE values there where it matters, in the vicinity of the inflexion points.
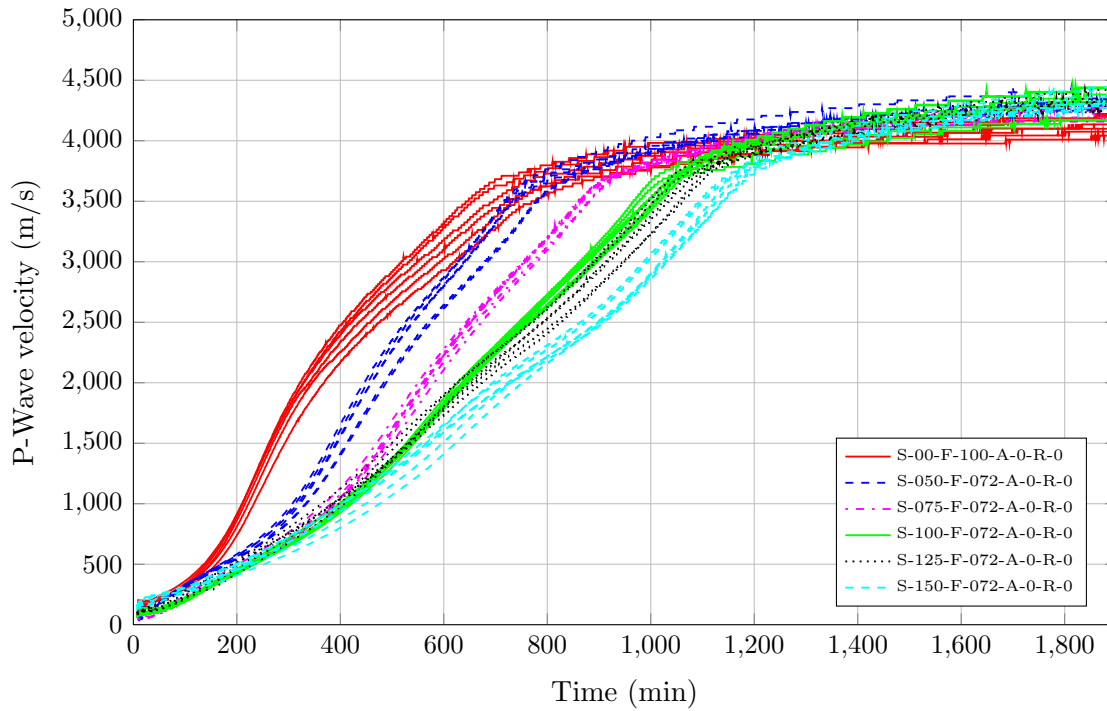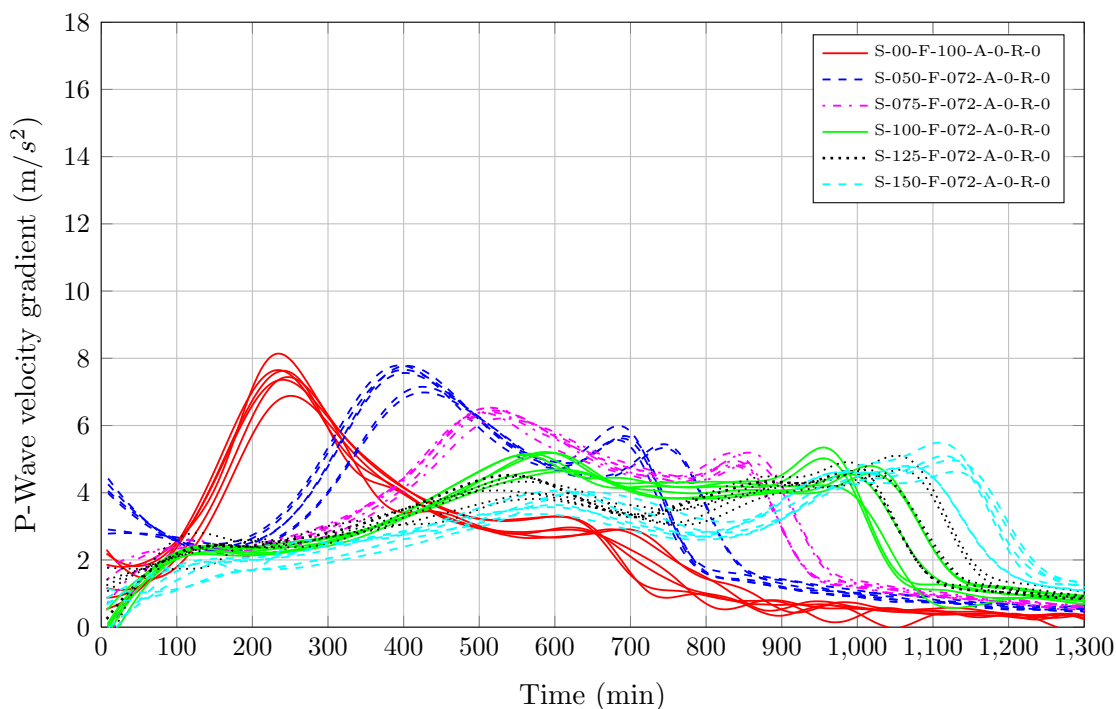
Figure 4.1: *P-wave velocity evolution for the different compositions of the SP series in function of time after water addition*

Figure 4.1 shows the p-wave velocity time histories for the different compositions of the *SP* series. This figure shows two distinct domains, one with a fast increase of p-wave velocity and one with a much slower increase, towards an asymptotic value of 4500 m/s. As *SP* quantity increases, the slope (p-wave velocity gradient) in the first domain decreases, indicating a reduced intensity of the hydration, which can result in a delay of the initial setting and an extension of the duration of the setting.

After 1500 min, curves with more *SP* have higher wave velocities. For example, the black curves (corresponding with *SP* 1.25 %mCEM) are higher than the red curves (*SP* 0.00 %mCEM). A probable explanation is that as *SP* quantity is increased the mortar is less porous, in other words: deareation is improved, meaning a denser final mixture and a stiffer micro-structure. Therefore the velocity after a few hours is higher than that in mortar samples with lower *SP* content.

Figure 4.2 represents the p-wave velocity gradient evolution in function of time after water addition. As explained before, the spines fit is not a good approximation for the edges,

Figure 4.2: *P-wave velocity gradient evolution for splines fit for the different compositions of the SP series in function of time after water addition*

thus, the first 75 min should be disregarded. All the curves show an "M" shape, with 2 maxima. With increasing quantities of *SP*, the first peak decreases in intensity, inferring the first peak is influenced by *SP* quantity. Meanwhile the second peak's intensity remains relatively constant. For an *SP* quantity between 1.00 % and 1.25 %, the second peak is higher than the first. A possible explanation for this is that the repellent effect of the *SP* makes hydration occur slower and in a more constant rate. The second peak seems to be caused by the fly ash, the mixture with no fly ash quantity (S-00-F-100-A-0-R-0) shows a weaker second peak, while for the rest of the mixtures that contain the same quantity of fly ash this second peak remains constant.

Table 4.1 summarizes the mortar ages for the different key points, hile figures 4.3 and 4.4 graphs these results. These values are the averages from the 6 velocity curves, detailed results can be found in annex D. In general, the different indicators show a more or less proportional increase as the quantity of *SP* increases. When observed in more detail, the first inflection point, maximum inflection point and 1500 m/s threshold relations show a bilinear behaviour, where the results for the largest quantities of SP diverge from the other results. For the first inflection point indicator, the gradient of the p-wave velocity is

Table 4.1: *P-wave transmission test key reference concrete ages of the SP series*

Mixture	Max. Infl. point	1st Infl. point	2nd Infl. point	1500 m/s threshold	2975 m/s threshold	2/3 of final velocity	20 % of max gradient
S-000-F-100-A-0-R-0	241	241	635	272	557	510	752
S-50-F-072-A-0-R-0	409	409	706	397	645	644	845
S-75-F-072-A-0-R-0	516	516	844	485	757	735	990
S-100-F-072-A-0-R-0	588	588	981	535	872	872	1189
S-125-F-072-A-0-R-0	1020	554	1020	524	913	912	1278
S-150-F-072-A-0-R-0	1102	607	1102	581	1008	1017	1370
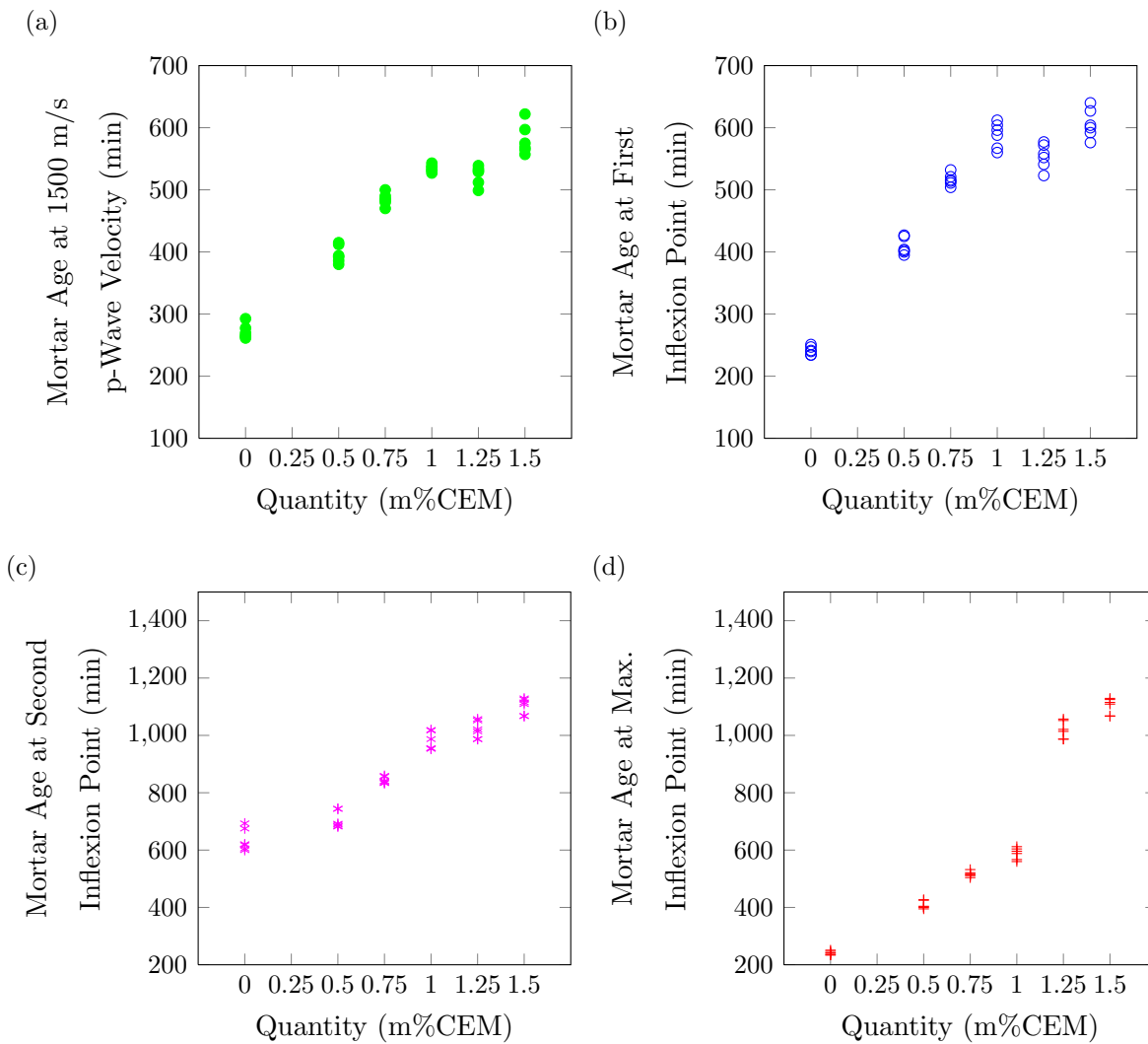
Figure 4.3: *P-wave velocity key mortar ages possible indicators for IST in function SP quantity*

(a)

(b)

(c)

(d)
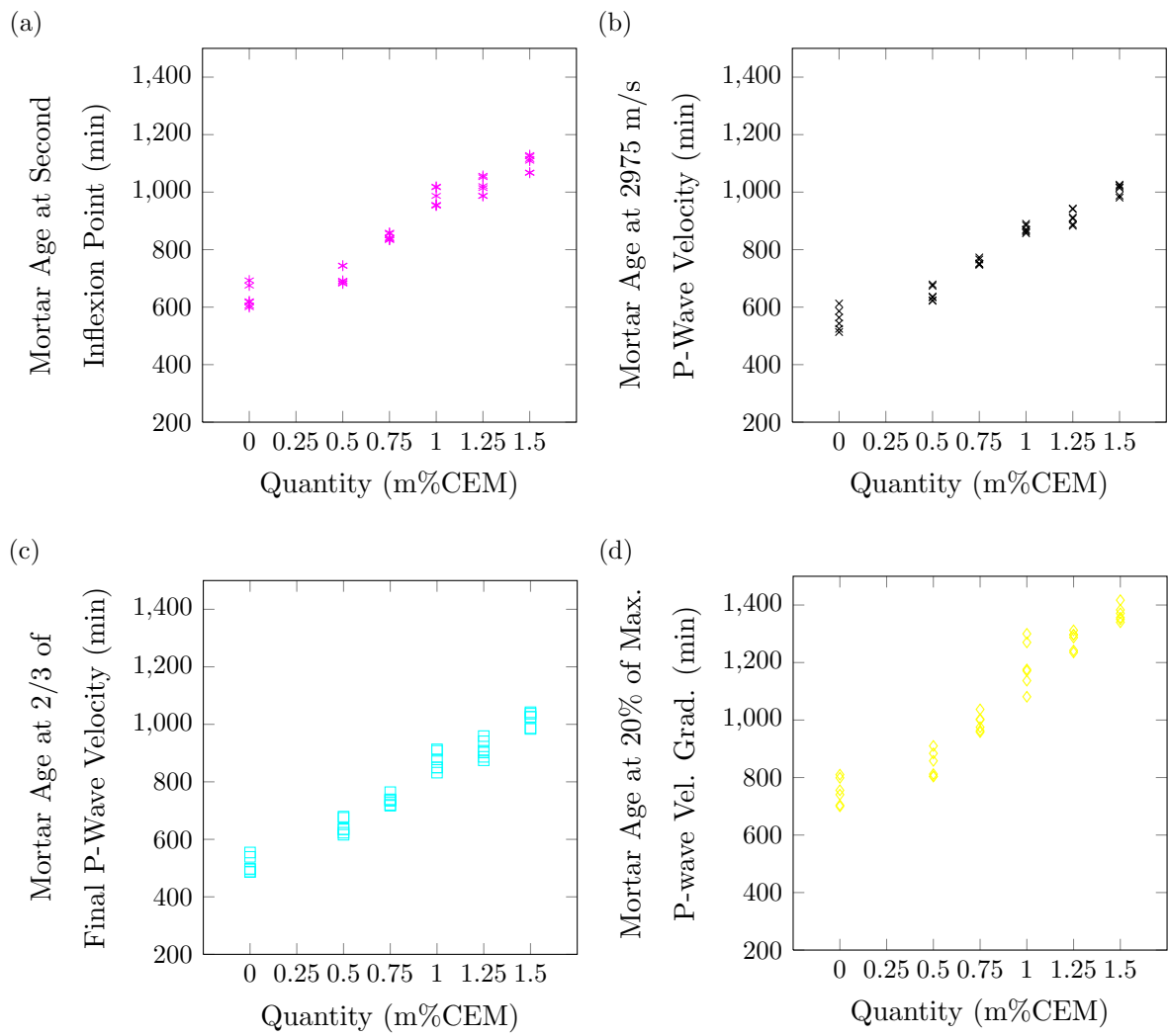
Figure 4.4: *P-wave velocity key mortar ages possible indicators for FST in function SP quantity*

so regular that this inflection point is hardly distinguishable in the curve: it can only be observed as a slight variation. Apart from the fact that this increases the possible error committed by the approximation of the curve and the consequent determination of the maximum gradient. What can be seen can be no more than the impact of the splines approximation on a practically straight curve. However, these two SP values are within the range of the SP saturation point (as obtained from the flow tests), so a certain stabilisation in the impact of the SP on the hydration, as on the workability, could be expected. Regarding the indicator 1500 m/s, the sudden decrease in S-125 is probably related to the fact that the experimental curves for 1.00 % and 1.25 % are quite hazy in the area 0-2000 m/s. It is interesting to note that the second inflection point magnitude ranges around the values for FST indicators, which could imply it is not a good indicator of IST. An equal significant aspect of the FST indicators is that, contrary to IST, the relationship is much more linear. In addition, the composition with no SP shows a slightly different behaviour, this could be due to the fact that this composition does not have any fly ash.

4.1.2. *AC* series

For this series, the polyfit approximation method (see section 3.1.1) was used. The p-wave velocity curves show a quasi-linear behaviour and the polyfit approximation method adjusts better to this kind of curves, which is being reflected by the fact that the root mean square error and standard deviation are smaller. To maintain coherency, results presented here for the reference mixture S-100-F-072-A-0-R-0 are obtained using the Splines fit, as justified in the previous paragraphs.

Figures 4.5 and 4.6 show the p-wave velocity and p-wave velocity gradient respectively for the different compositions of the AC series. From these experimental curves it can be observed that the effect of the accelerator its most important during the first 1000 min: the maximum gradient (shown in figure 4.6) increases with the amount of accelerator added to the mixture. There is a change in shape for both velocity and its gradient. As the quantity of accelerator increases the first inflection point for the p-wave velocity curve is more pronounced while the second one is diminished, showing a more pronounced trilinear behaviour. This increase and decrease of the gradient is very visible in the velocity
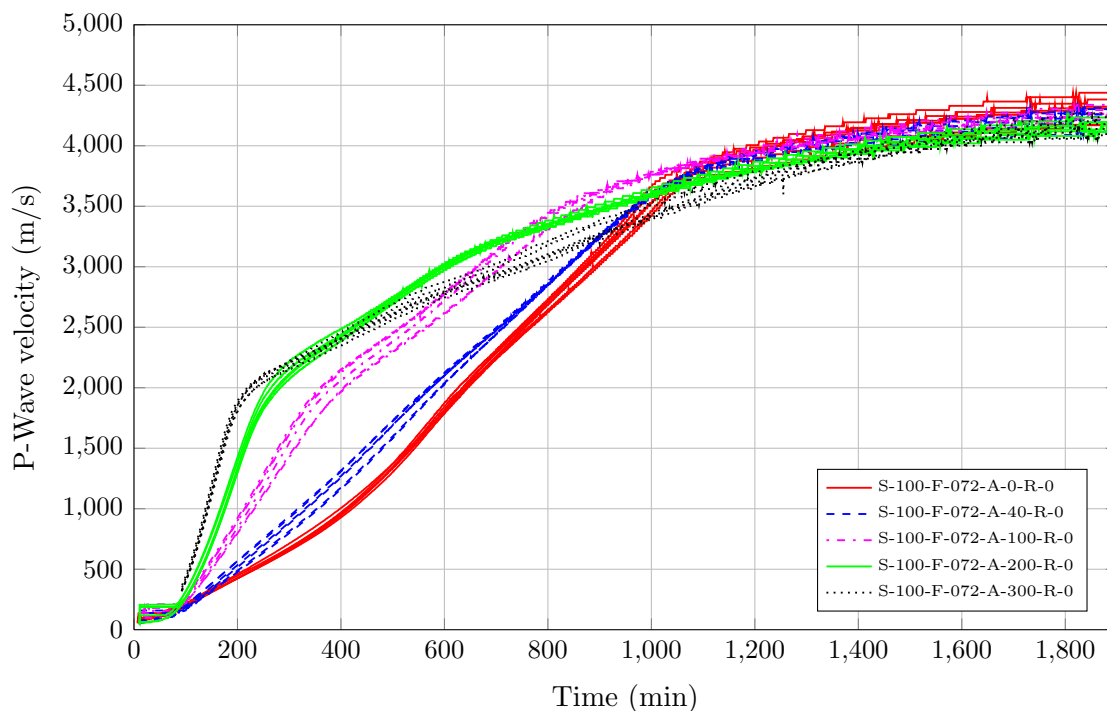
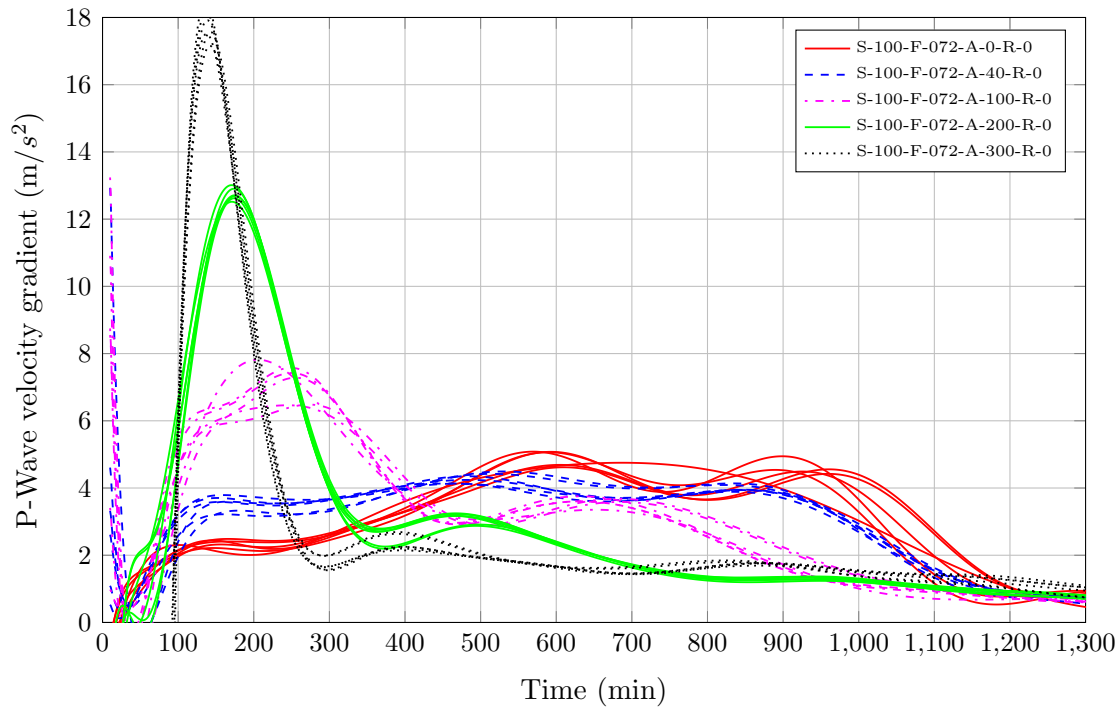**Figure 4.5:** *P-wave velocity evolution for the different compositions of the AC series in function of time after water addition*

gradient curves.

Table 4.2 summarizes the average mortar ages for the different key points. It should be noted that for the A-300 curve the indicator 20 % maximum gradient must be treated with care, $3.6\frac{m}{s^2}$ is never reached after the second inflexion point at least, not within the measured time, contrary to the remaining mixtures.

Figures 4.7 and 4.8 graph the variation of the key mortar ages with accelerator quantity. Although most of the references decrease as the quantity of accelerator increases, this decrease is different for each case. Indicators for *IST* decrease bilinearly (with 1.00 % accelerator as pivot point). *FST* indicators behave in a quadratic way, except for 20 % maximum gradient, that also shows a linear behaviour.

Regarding the *FST* indicator values for the highest accelerator quantity, a number of remarks should be made: first of all, the linear behaviour of the 20 % of maximum gradient curve cannot be certified, since it was already shown that this value is possibly tainted by a high error. While the second inflection point indicator tends to an asymptote, the two

Figure 4.6: *P-wave velocity gradient evolution for splines fit for the different compositions of the AC series in function of time after water addition*

Table 4.2: *P-wave transmission test key reference concrete ages of the AC series*

Mixture	Max. Infl. point	1st Infl. point	2nd Infl. point	1500 m/s threshold	2975 m/s threshold	2/3 of final velocity	20 % of max gradient
S-100-F-072-A-0-R-0	588	588	981	535	872	872	1189
S-100-F-072-A-40-R-0	490	490	837	460	830	819	1207
S-100-F-072-A-100-R-0	247	247	652	292	674	666	952
S-100-F-072-A-200-R-0	173	173	476	213	591	559	577
S-100-F-072-A-300-R-0	139	139	394	171	714	662	249
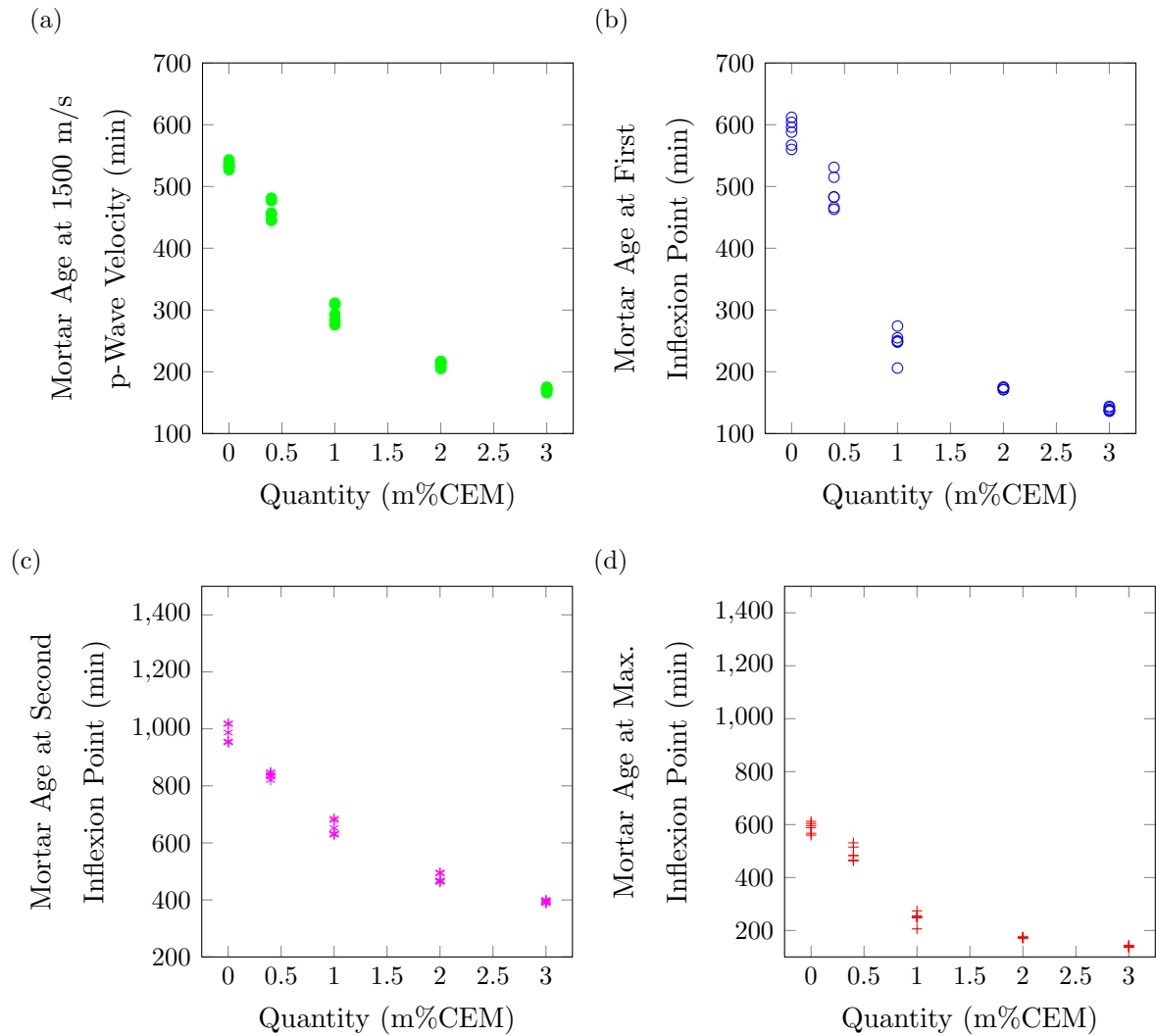
Figure 4.7: *P-wave velocity key mortar ages possible indicators for IST in function Accelerator quantity*

(a)

(b)

(c)

(d)
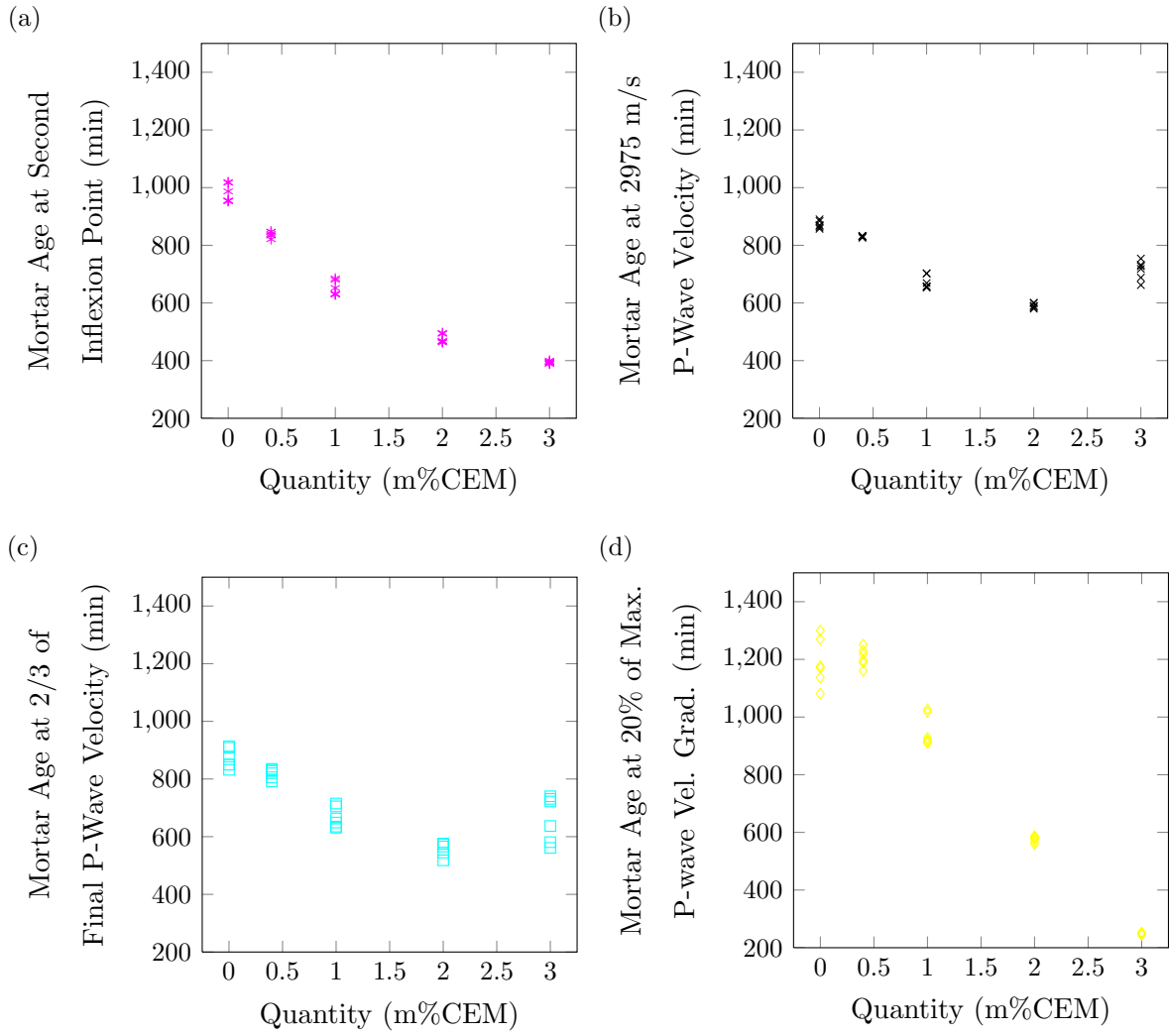
**Figure 4.8:** *P-wave velocity key mortar ages possible indicators for FST in function accelerator quantity*
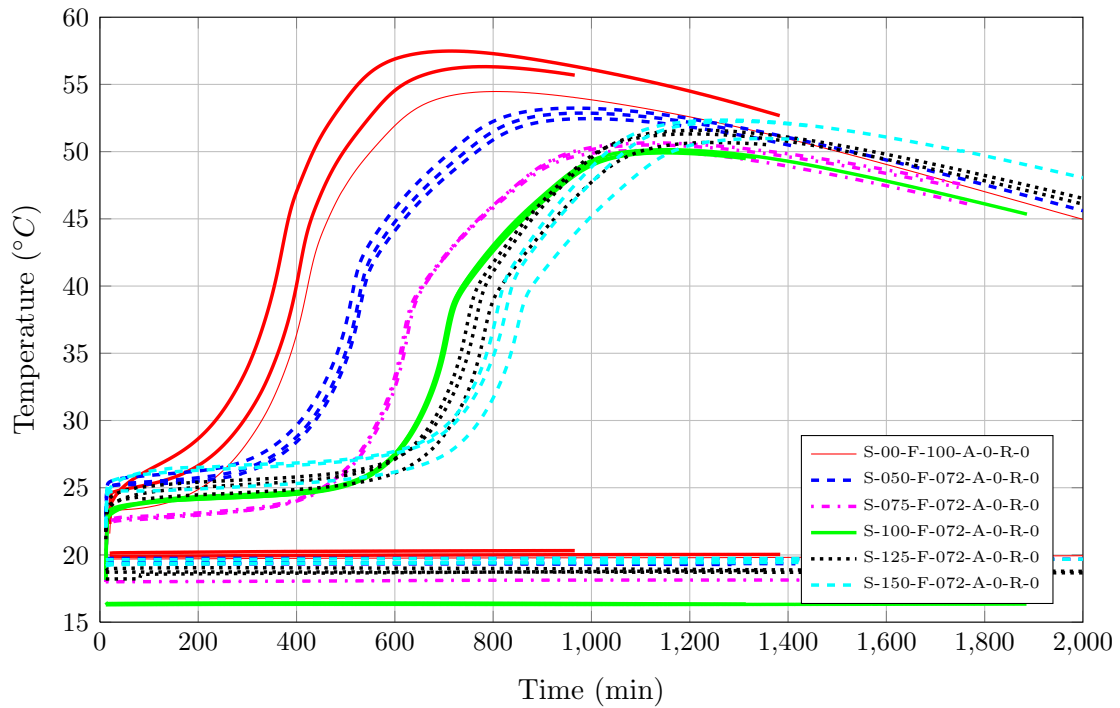
Figure 4.9: *Temperature evolution for semi adiabatic test the different compositions of the SP series in function of time after water addition*

remaining indicators show an increase of their value for the 3.00 % accelerator mixture. This might seem very awkward at first, but given the extreme changes in the shape of the p-wave velocity curve, it could be an acceptable result. It could be that the very fast microstructural formation (that leads to the extremely high slopes in the first 300 minutes) leads to an increasingly difficult or slow continued microstructure formation after the first gradient peak. These two indicators would however need supplementary validation for these extreme compositions. Comparing *IST* and *FST* indicators, it can be observed that *IST*'s are decreasing more rapidly with a rising accelerator content. This results in longer setting times for these mixtures.

4.2. Semi-adiabatic calorimetry test

4.2.1. *SP* series

Figure 4.9 shows the temperature evolution during the semi-adiabatic test in function of time after water addition, while 4.10 shows hydration heat flux in function of *corrected*
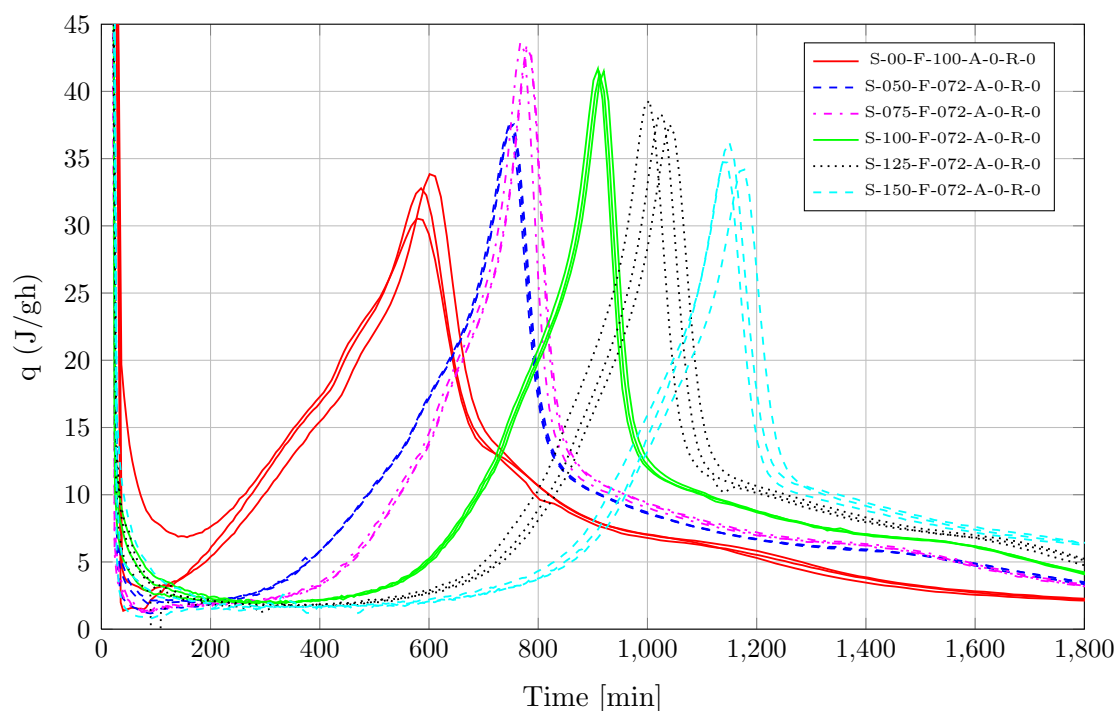
Figure 4.10: *q for the different compositions of the SP series in function of corrected time after water addition*

time after water addition. In general the temperature evolution within the considered time frame is characterised by an exponential increase followed by a linear decrease. As the quantity of *SP* is increased, the temperature rise starts later, which means chemical reactions are postponed. Moreover, the maximum temperature decreases.

On the other hand, figure 4.10 shows an increase and then decrease of the maximum heat flux value, and thus of the maximum chemical activity. This decrease happens more gradually as the quantity of *SP* is increased. This would corroborate the results obtained in the p-wave transmission test, that reactions take place later and in a more constant manner.

Table 4.3 summarizes the reference mortar ages, which are plotted in 4.11 and 4.12. Indicators qmax and qmin+0.2*△q show quite clearly a linear trend, except for S-000 which could be considered an outlier. It is important to note S-000 contains no fly ash, in comparison with the other mixtures which have a C/P ratio of 0.72, this could explain the difference for this point. Disregarding S-000, qmin+1.5 J/gh shows a parabolic or bilinear increase with the *SP* quantity.

Table 4.3: *Key reference concrete ages for the semi-adiabatic calorimetry of the SP series*

| Mixture	qmin+0.2*△q time (min)	qmin+1.5J/gh time (min)	qmax time (min)
S-000-F-100-A-0-R-0	286	249	588
S-50-F-072-A-0-R-0	468	324	751
S-75-F-072-A-0-R-0	546	425	775
S-100-F-072-A-0-R-0	687	544	914
S-125-F-072-A-0-R-0	798	635	1022
S-150-F-072-A-0-R-0	925	645	1155

(a)

(b)
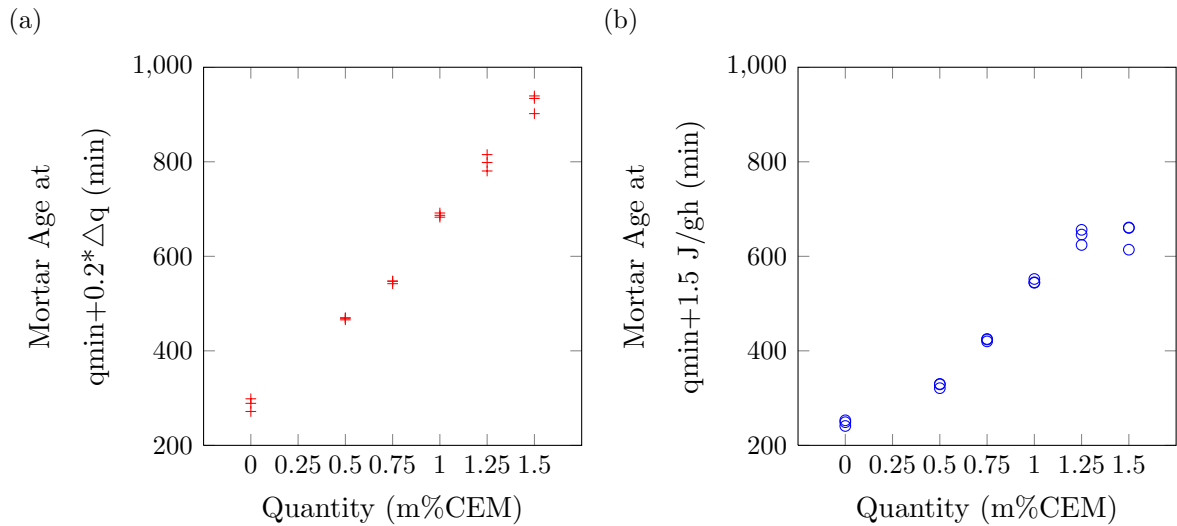
Figure 4.11: *Heat flux key mortar ages possible indicators for IST in function of SP quantity*
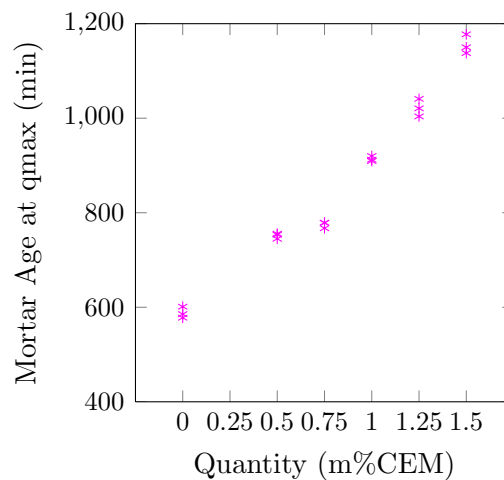
Figure 4.12: *Heat flux key mortar age candidate for FST in function of SP quantity*
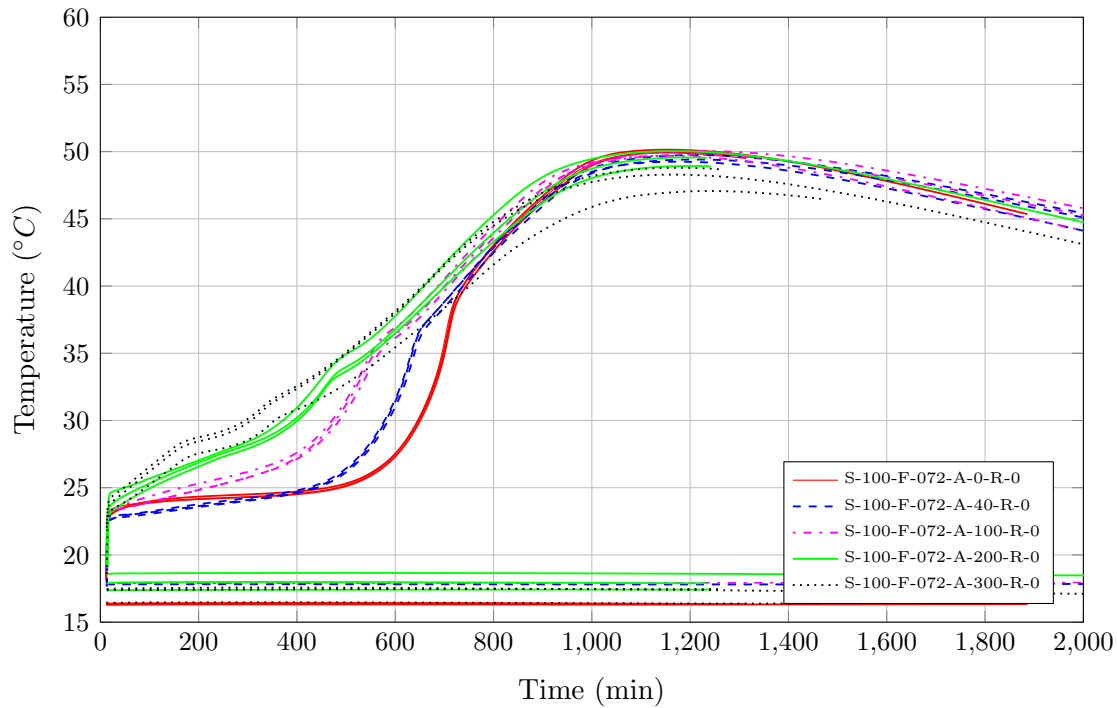
Figure 4.13: *Temperature evolution for semi adiabatic test for the different compositions of the AC series in function of time after water addition*

4.2.2.   *AC* series

Figures 4.13 and 4.14 show the semi-adiabatic calorimetry experimental results for the *AC* series compositions. Figure 4.13 shows temperature starts rising earlier as the quantity of accelerator increases, implying *q* peak occurs earlier as well, although its maximum value decreases. Also, temperature histories show a more gradual increase of temperature, almost eliminating the dormant period. *q* evolution shows the emergence of an initial rise, suggesting a severely shifted reaction chain starts taking place with high accelerator quantities.

Table 4.4 summarizes the possible *IST* and *FST* indicators. Figures 4.15 and 4.16 graph the results obtained for the different quantities. qmin+0.2*△q and qmax show a proportional decrease as the quantity of accelerator increases. The shift in the reaction chain activated by the accelerator clearly contributes to the setting and hardening of the mixture. As soon as the new first "plateau" emerges the *IST* indicators lose a lot of their
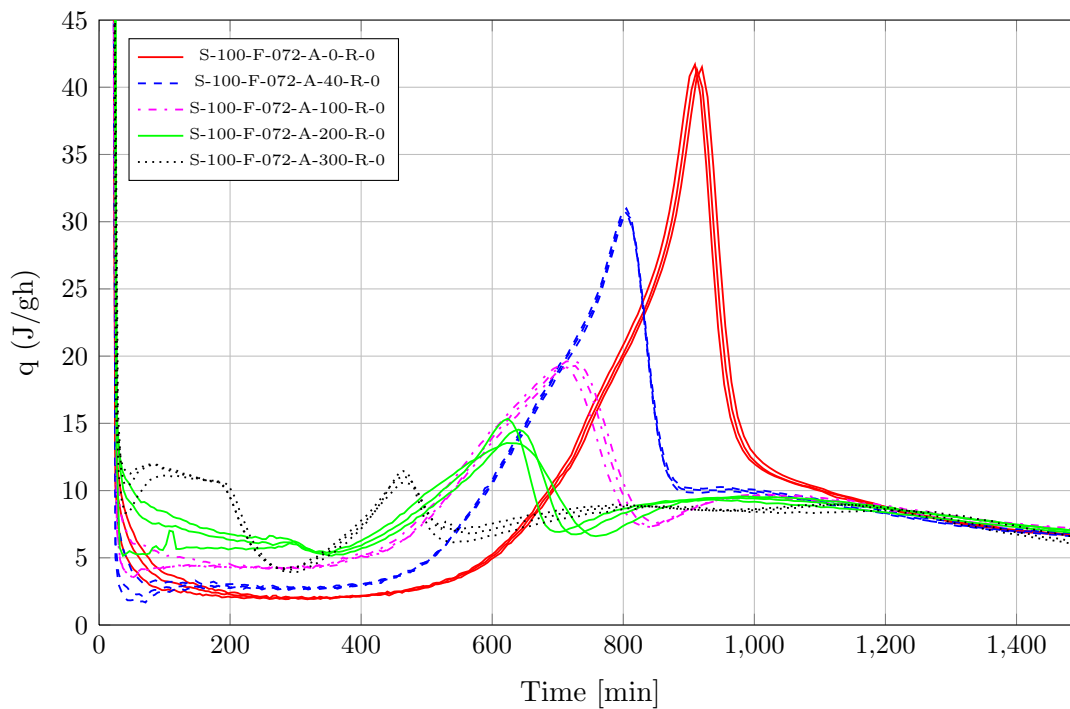
Figure 4.14: *q for the different compositions of the AC series in function of corrected time after water addition*

Table 4.4: *Semi-Adiabatic calorimetry test key reference concrete ages of the AC series*

Mixture	qmin+0.2*△q time (min)	qmin+1.5J/gh time (min)	qmax time (min)
S-100-F-072-A-0-R-0	687	544	914
S-100-F-072-A-40-R-0	567	483	805
S-100-F-072-A-100-R-0	484	297	716
S-100-F-072-A-200-R-0	(450)	(419)	629
S-100-F-072-A-300-R-0	(356)	(392)	(465)

(a)

(b)
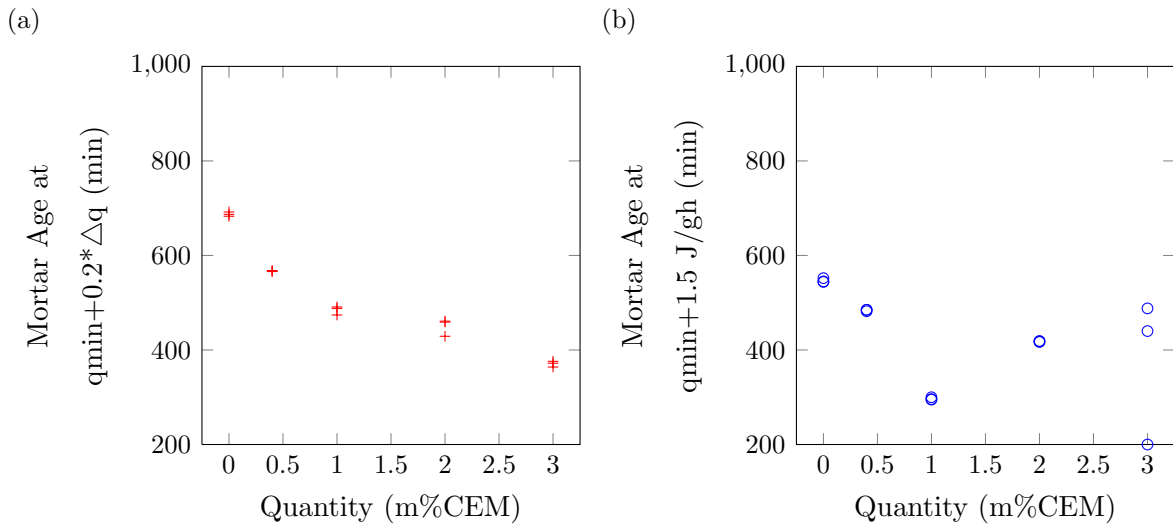
Figure 4.15: *Heat flux key mortar ages possible indicators for IST in function of accelerator quantity*
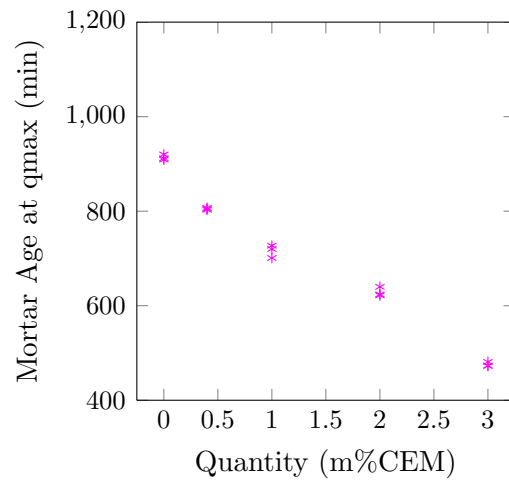
Figure 4.16: *Heat flux key mortar age candidate for FST in function of accelerator quantity*

meaning, since the curve shape in which the concept of qmin is based is completely absent. In the case of A-200, this effect only affects start of setting. However for A-300, where the reaction is clearly activated, the semi-adiabatic indicators proposed for *IST* and *FST* are not plausible. Considering this, qmin+1.5 J/gh shows also a proportional decrease as the quantity of accelerator is increased.

4.3.   Vicat needle test

4.3.1.   *SP* series

Figure 4.17 shows the Vicat needle penetration depth for the different compositions of the *SP* series. In general, the curves have an exponential increase followed by a linear increase. It is important to note there is a high variability of the results obtained, although it can be observed that an increasing amount of *SP* results in a displacement of the curves to the right, especially between S-050 and S-075. This results in a delay in the *IST*.

As the amount of *SP* is increased, the penetration depth for a fixed time is reduced. In other words, the development of the penetration resistance is also retarded, which is coinciding with that the hydration reactions and evolution of the elastic properties have been retarded. As expected, the bigger the quantity of *SP*, the longer the time to attain a certain hardness, as shown in the results of table 4.5 and figure 4.17. It is hard to draw any conclusions from these results as there is a high variability and only 4 successful data points. However, S-75 shows a higher setting time than S-100, indicating it could be an outlier for these results. It is important to remember Vicat needle tests are performed on cement paste, although the compositions of the paste were determined by equivalent workability, S-75 was not tested for slump and shock tests, and it is quite possible that this composition behaves differently.
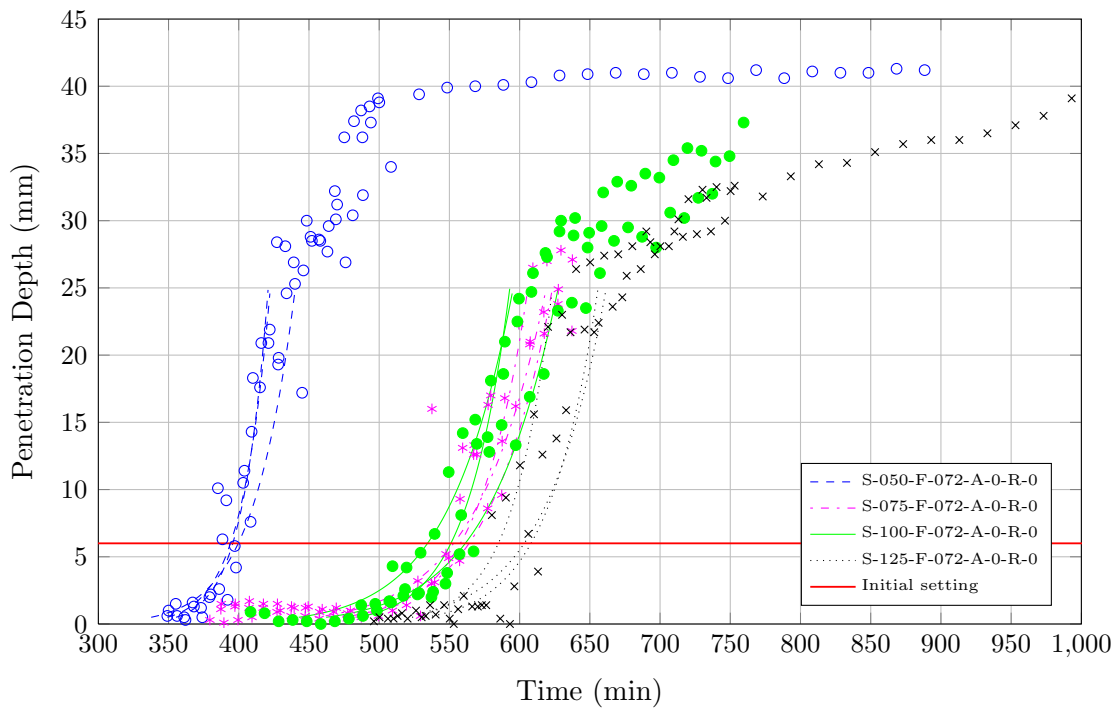
Figure 4.17: *Penetration depth for the different compositions of the SP series in function of time after mixing*

Table 4.5: *Summary of IST experimental results for Vicat needle test for all SP series compositions*

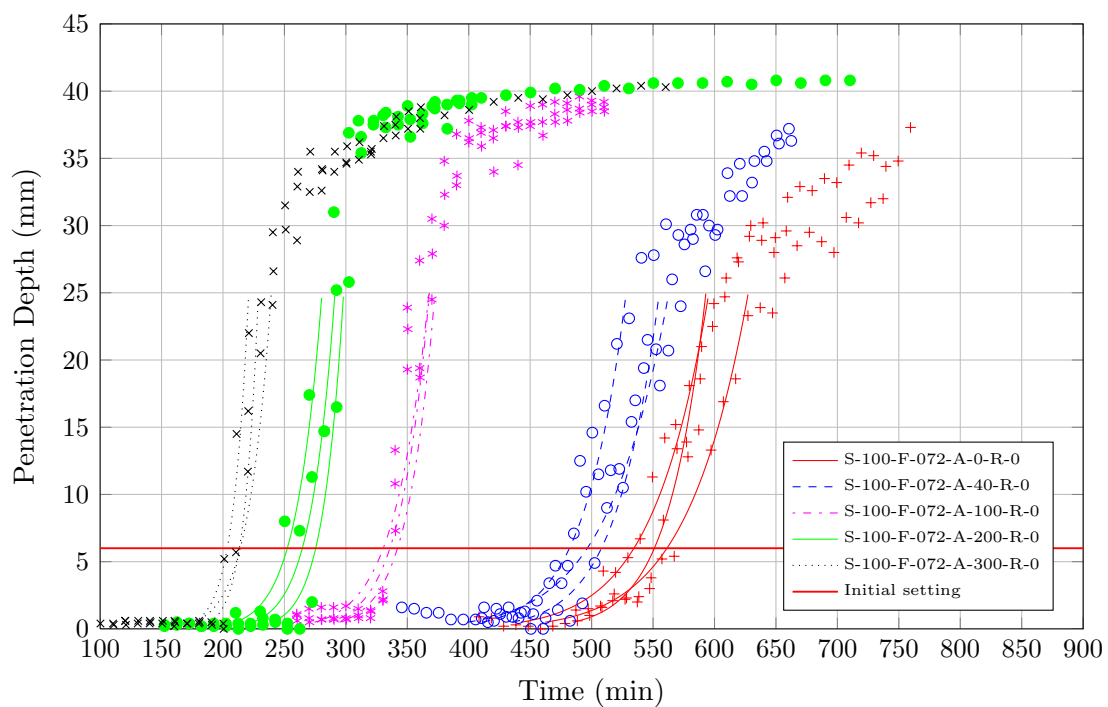|	IST
Mixture	(min)
S-000-F-100-A-0-R-0	
S-50-F-072-A-0-R-0	397
S-75-F-072-A-0-R-0	560
S-100-F-072-A-0-R-0	548
S-125-F-072-A-0-R-0	600
S-150-F-072-A-0-R-0	
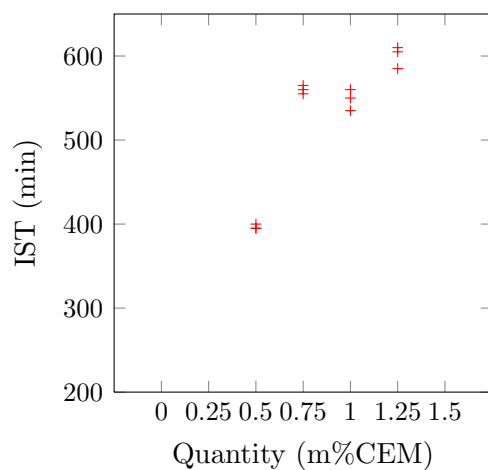
Figure 4.18: *Vicat needle test IST in function of SP quantity*

Figure 4.19: *Penetration depth for the different compositions of the AC series in function of time after mixing*

Table 4.6: *Summary of IST experimental results for Vicat needle test for all AC series compositions*

	IST
Mixture	(min)
S-100-F-072-A-0-R-0	548
S-100-F-072-A-40-R-0	495
S-100-F-072-A-100-R-0	335
S-100-F-072-A-200-R-0	263
S-100-F-072-A-300-R-0	212
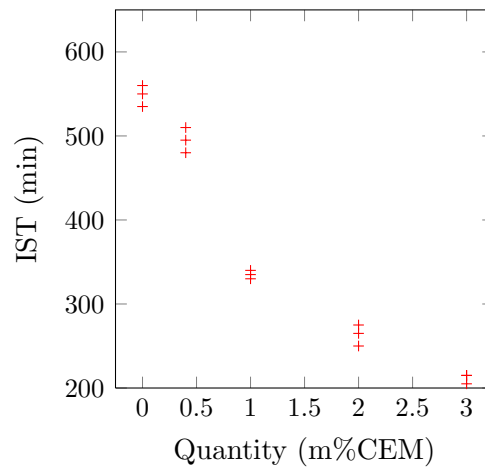
Figure 4.20: *Vicat needle test IST in function of accelerator quantity*

4.3.2. *AC* series

Figure 4.19 shows the results for the penetration depth of the Vicat needle for the different compositions of the *AC* series. In general, curves show an exponential increase followed by a linear behaviour. As the amount of accelerator is increased the linear behaviour becomes more horizontal. Furthermore, as the amount of accelerator is increased the time for a fixed penetration is decreased. As the hydration reactions have been accelerated, the development of the penetration resistance is also accelerated, displacing the curves to the left. This displacement is not constant, the displacement between 0.40 %mCEM and 1.00 %mCEM is proportionally greater than the displacement between the other results.

Figure 4.20 and table 4.6 show the variation for the standardized *IST* in function of the
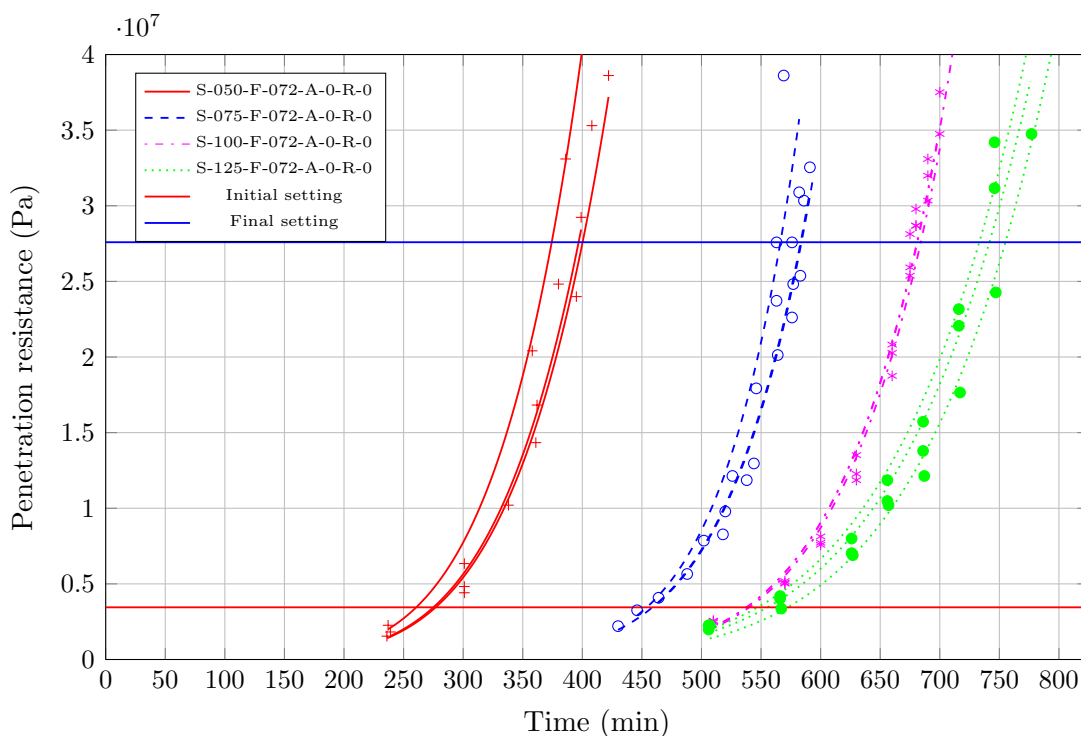
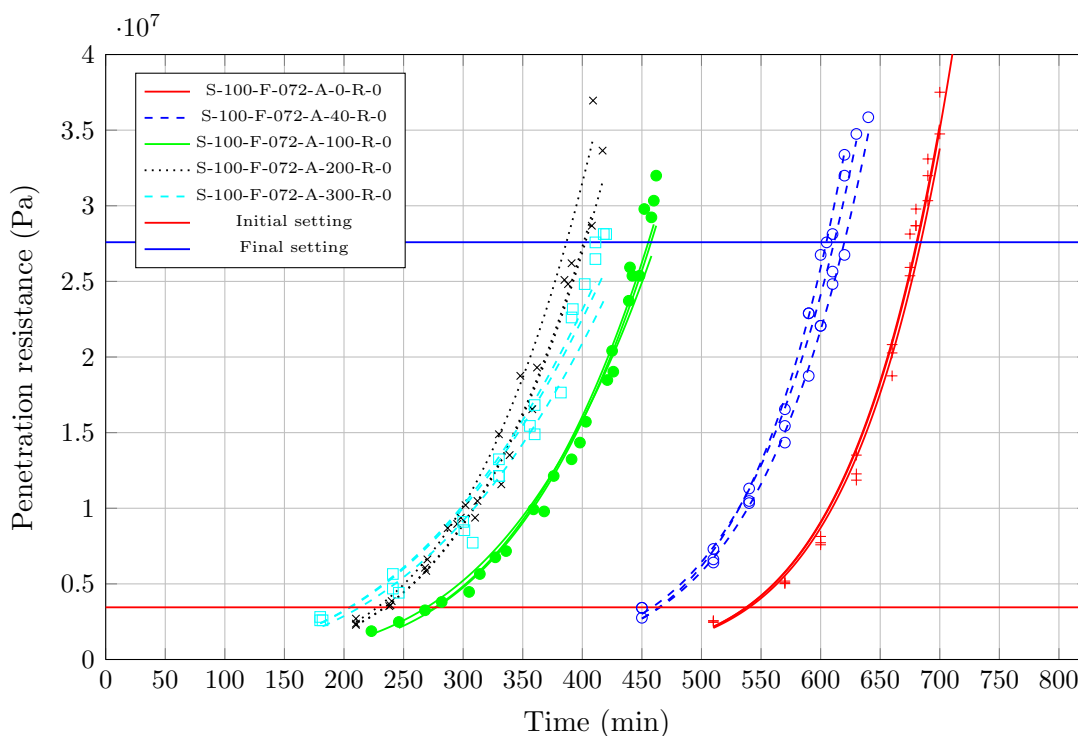**Figure 4.21:** *Penetration resistance for different SP quantities in function of time after mixing the two batches*

accelerator quantity. As the quantity of accelerator increases there is an exponential decrease in the indicator, of course given the reduced number of data and the high margin of error, the exact nature of the decrease could be different.

4.4. Penetration resistance test

4.4.1. *SP* series

Figure 4.21 shows the penetration resistance evolution for the different *SP* series compositions. All the curves show an exponential increase with time. An increasing amount of *SP* results in a displacement of the curves to the right. This results in a delay in the *IST* (3.45 MPa) and *FST* (27.59 MPa), as shown in table 4.7. Setting time duration is also increased with *SP* quantity. As expected, the higher the quantity of *SP*, the longer the time to attain a certain mechanical resistance.

Studying table 4.7 and figure 4.22 can see that S-50 does not behave consistently with

Table 4.7: *Summary of IST and FST experimental results for Penetration test for all SP series compositions*

	IST	FST
Mixture	(min)	(min)
S-000-F-100-A-0-R-0	-	-
S-50-F-072-A-0-R-0	270	390
S-75-F-072-A-0-R-0	458	578
S-100-F-072-A-0-R-0	538	682
S-125-F-072-A-0-R-0	557	743
S-150-F-072-A-0-R-0	-	-

(a)   (b)
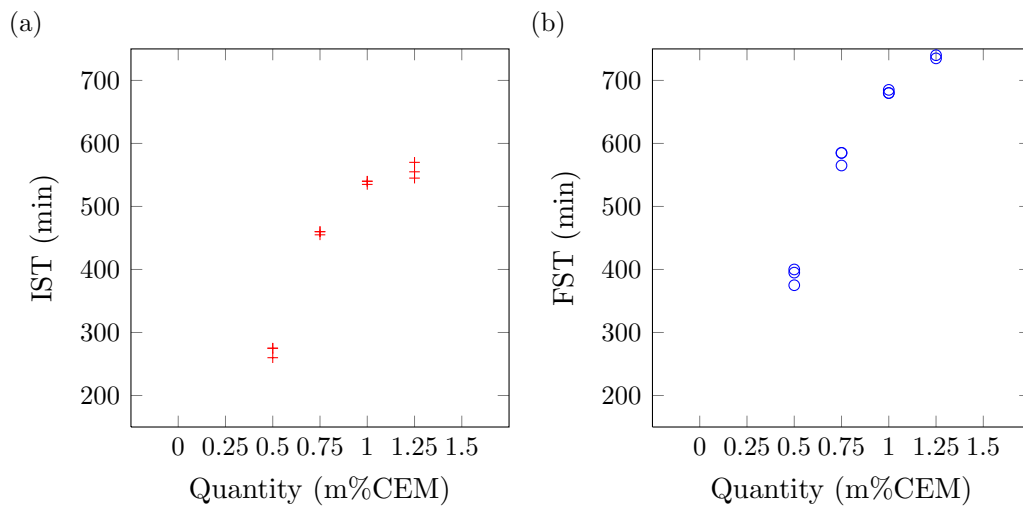
Figure 4.22: *a) IST b)FST penetration resistance results in function of SP quantity*

Figure 4.23: *Penetration resistance for different accelerator quantities in function of time after mixing the two batches*

the other quantities. This variation coincides with the plateau where *SP* has little effect on workability. For mortar composition S-50-F-072-A-0-R-0 it makes sense that if the *SP* is not lubricating the mixture, friction between sand grains could result in greater penetration resistance values, as a result lower setting times are obtained than for the rest of the series. However, there are only 4 points in these graphs and to reach more accurate conclusions more quantities should be tested.

4.4.2. *AC* series

Results for the penetration resistance test are shown in figure 4.23. It can be observed that curves displace to the left as the quantity of accelerator increases. Moreover, this displacement seems to reach an asymptote. It is possible that the accelerating agent used has a saturation point beyond which an increase in the amount does not decrease the *IST* and *FST*. Generally, the curves are less steep with greater accelerator quantities. This is confirmed by the decrease of the slopes of the fits on logarithmic axes, displayed in annex D. These decrease in the slope means even if the mechanical properties development

Table 4.8: *Summary of IST and FST experimental results for Penetration test for all AC series compositions*

| | IST | FST |
Mixture	(min)	(min)
S-100-F-072-A-0-R-0	538	682
S-100-F-072-A-40-R-0	463	612
S-100-F-072-A-100-R-0	275	458
S-100-F-072-A-200-R-0	233	397
S-100-F-072-A-300-R-0	208	432

starts before, the rate at which they develop decreases with accelerator quantity. It can be noted these results show a peculiarity of this accelerating agent: for higher quantities, it accelerates *IST* (and thus shortens the time for which concrete can be put in place), but smaller accelerating effect for *FST*, which results on longer setting durations. Indeed, calcium nitrate used has the peculiarity of accelerating setting but not hardening.

The trend shown between A-100, A-200 and A-300 is quite interesting. While increasing setting duration is a trend with increasing accelerator quantity, as inferred from the results listed in table 4.8, A-100 and A-200, show a decrease in setting duration. Furthermore, curves for accelerator quantities 2.00 % and 3.00 % cross each other. *IST* is reached earlier for A-300, but *FST* happens later than for A-200. This results in a longer setting duration for A-300. This changes in the behaviour could be provoked by the changes in the reaction chain shown in the semi-adiabatic tests.

Figures 4.24 a) and b) show *IST* and *FST* in function of accelerator quantity. It can be seen what could be a second degree correlation between the variables. The results show, as explained earlier a re-increase in *FST* for A-300. This is not impossible, but it would be more intuitive to obtain a plateau. It would be necessary to perform further testing with greater accelerator quantities to confirm the results.

(a)

(b)
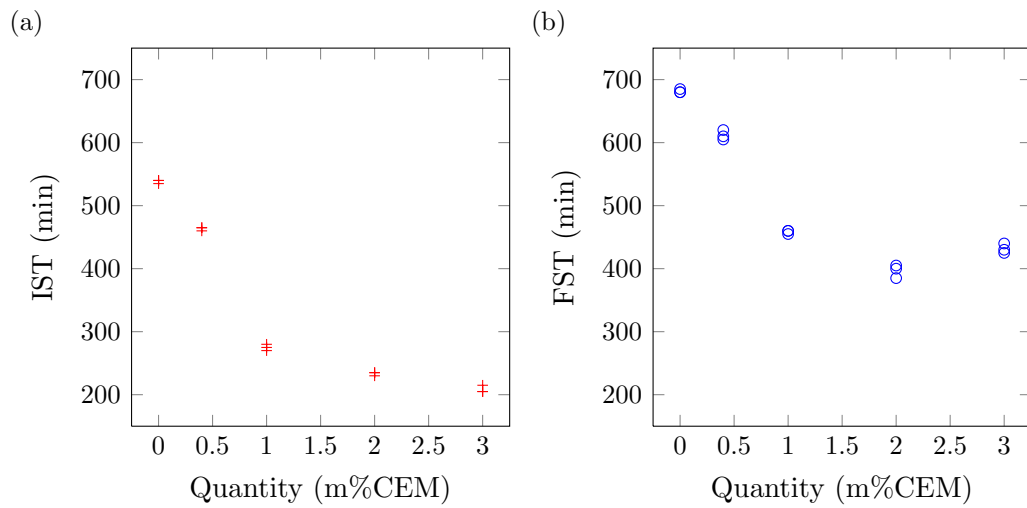
Figure 4.24: *a) IST b)FST penetration resistance results in function of accelerator quantity*

5.   Analysis

Eleven different types of mortar compositions have been tested in the development of this parametric experimental programme. These mortar compositions comprise different quantities of a third generation polycarboxylic ether *SP* and calcium nitrate (accelerator).

This chapter will analyse the results obtained from the parametric experimental programme. By analysing the data of the different experimental methods, possible correlation factors between the hydration characteristics and *IST* and *FST* for these experimental techniques will be sought. As explained before, the Vicat needle test only determines *IST*, thus the correlations pursued with this experimental technique will only involve *IST*. For practical reasons only the most significant cases are presented in this chapter. All the analysed correlations can be found in annex E.

5.1.   Procedure

Different key mortar ages for each experimental technique have been proposed in the previous chapters. These mortar ages will be treated to compare them against each other and try to obtain correlations between each other. The best possible outcome is obtaining a relationship y=x, which means that both indicators are related in the same way to the mortar hydration proving the indicator as valuable as the reference result to directly determine setting. However, the indicator could show an offset or a different sensitivity to the sought characteristic, in this case, generalized linear relationships (y=mx+c) and parabolic correlations (y=ax^2+bx+c) are considered. Higher degree polynomials are not studied due to the lack of points to determine a good correlation between variables. The criterion used to determine a good fit was a coefficient of determination (R^2) greater than 0.9.

Data obtained is divided into three separate sets: SP series data, AC series data and all data. Although the best result would be to obtain good correlations considering all the data, it cannot be neglected that the two series might behave dissimilarly due to the differences in their chemistry.

5.2. Correlation overview

R^2 is an adimensional measure that quantifies the dependence or relation between the data. It determines the proportion of the variance of the dependent variable that is explained by a statistical model. R^2 values range from 0 to 1, with 1 representing a perfect fit between the data and the line. Negative values are mathematically possible when fitting certain trends to data, these values will be showed as 0. R^2 is calculated with the equation:

$$R^2 = 1 - \frac{\sum(y_i - f(x_i))^2}{\sum(y_i - \overline{y})^2} \tag{5.1}$$

For a simple linear regression model,R^2 equals the square of the correlation coefficient between the dependant variable and the fitted values [35].

Tables 5.1, 5.2, 5.3 and 5.4 show the different R^2 obtained for the linear fit with all data (including SP and AC series) and the R^2 between the data and a y=x fit. As explained before, while the R^2 between the data and a simple linear regression will give us a quality of fit measure, high values would indicate the reference is a valuable indicator for setting. The R^2 between the experimental data and y=x will quantify if the two variables could be measuring the same hydration characteristic, which is the best case scenario. As R^2 is a summary measure of the dispersion structure and it is always convenient to plot the graph. The study of the relation will be completed by both.

As a first approximation to acceptable correlations these R^2 values are convenient tools. Correlations with low R^2 values for y=mx+c and y=x as shown in figure 5.1a) can be discarded, as the data does not fit well with a linear model. On the other hand if the correlation has a low R^2 for y=x but high for y=mx+c as in figure 5.1b) the data shows a
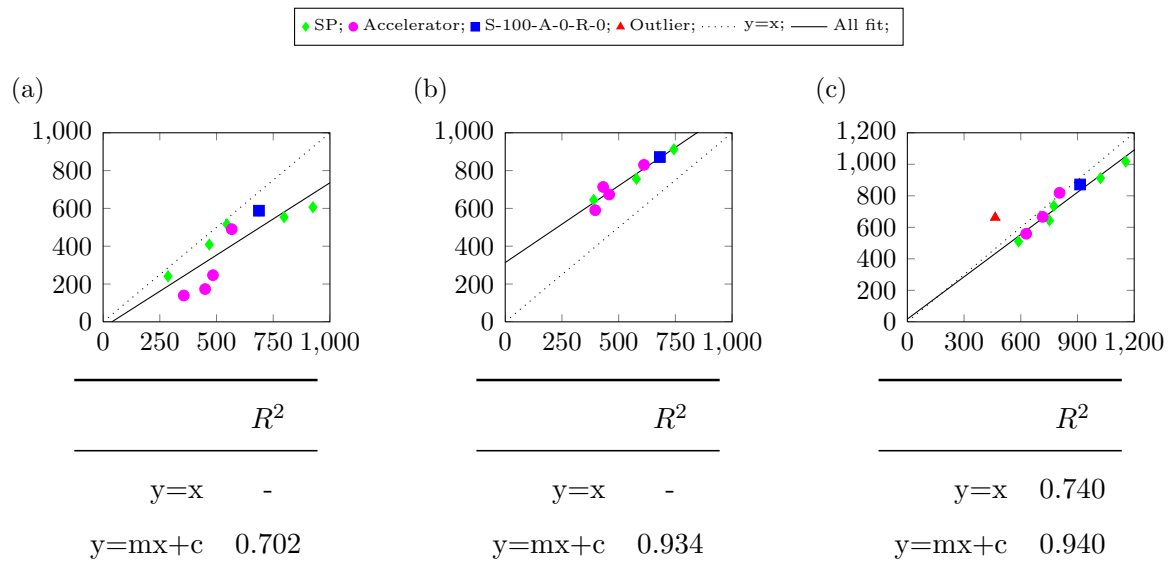
Figure 5.1: R^2 *examples a) low y=x, low y=mx+c, b)low y=x, high y=mx+c, c)low y=x, high y=mx+c*

strong linear behaviour but not centered around y=x, indicating an offset and/or a different sensitivity to the characteristic point, this would make a suitable indicator. Best case scenario would be a y=x correlation, which has a high R^2 value for both fits, as illustrated in figure 5.1c). Nevertheless this criteria serves only for a first approximation as graphs have to be analysed on the whole, and in some cases correlations with less favourable R^2 values have been chosen.

In the next sections only one selected indicator is shown for each setting time. However not all the indicators were good references, as illustrated by figure 5.2,this figure graphs the qmin+0.2$\triangle$q indicator from the semi-adiabatic test against the *IST* obtained by the penetration resistance test, it is apparent there is a big dispersion in the results. The experiments measure the variation of different variables, that do not necessarily show relationships between each other.

Table 5.1: *IST key mortar ages correlations, R^2 value for linear fit*

	Penetrometer-*IST*	Vicat-*IST*
Vicat-*IST*	0.983	-
SA- qmin+0.2△q	0.872	0.893
SA- qmin+1.5 J/gh	0.911	0.979
Pw- Max inf	0.862	0.958
Pw- First Inf	0.979	0.952
Pw- 2nd Inf	0.997	0.953
Pw-1500 m/s	0.976	0.967

Table 5.2: *IST key mortar ages correlations, R^2 value for y=x*

	Penetrometer-IST	Vicat-*IST*
Vicat-*IST*	0.942	-
SA- qmin+0.2△q	0	0
SA- qmin+ 1.5 J/gh	0.868	0.902
Pw- Max inf	0.818	0.871
Pw- First Inf	0.929	0.879
Pw- 2nd Inf	0	0
Pw-1500 m/s	0.972	0.867

Table 5.3: *FST key mortar ages correlations, R^2 value for linear fit*

	Penetrometer-FST
Pw-2975 m/s	0.934
Pw-2/3 final	0.941
Pw-20%	0.889
Pw-2nd inf	0.914
SA-qmax	0.945

Table 5.4: *FST key mortar ages correlations, R^2 value for y=x*

	Penetrometer-FST
Pw-2975 m/s	0
Pw-2/3 final	0
Pw-20%	0
Pw-2nd inf	0.061
SA-qmax	0

(d)

	Polinomial	r2
SP	y=1.58x-164	0.992
AC	y=0.828x+202	0.931
y=x	y=x	0
All	y=0.982x+145	0.893

Outliers: S-075-F-072-A-0-R-0
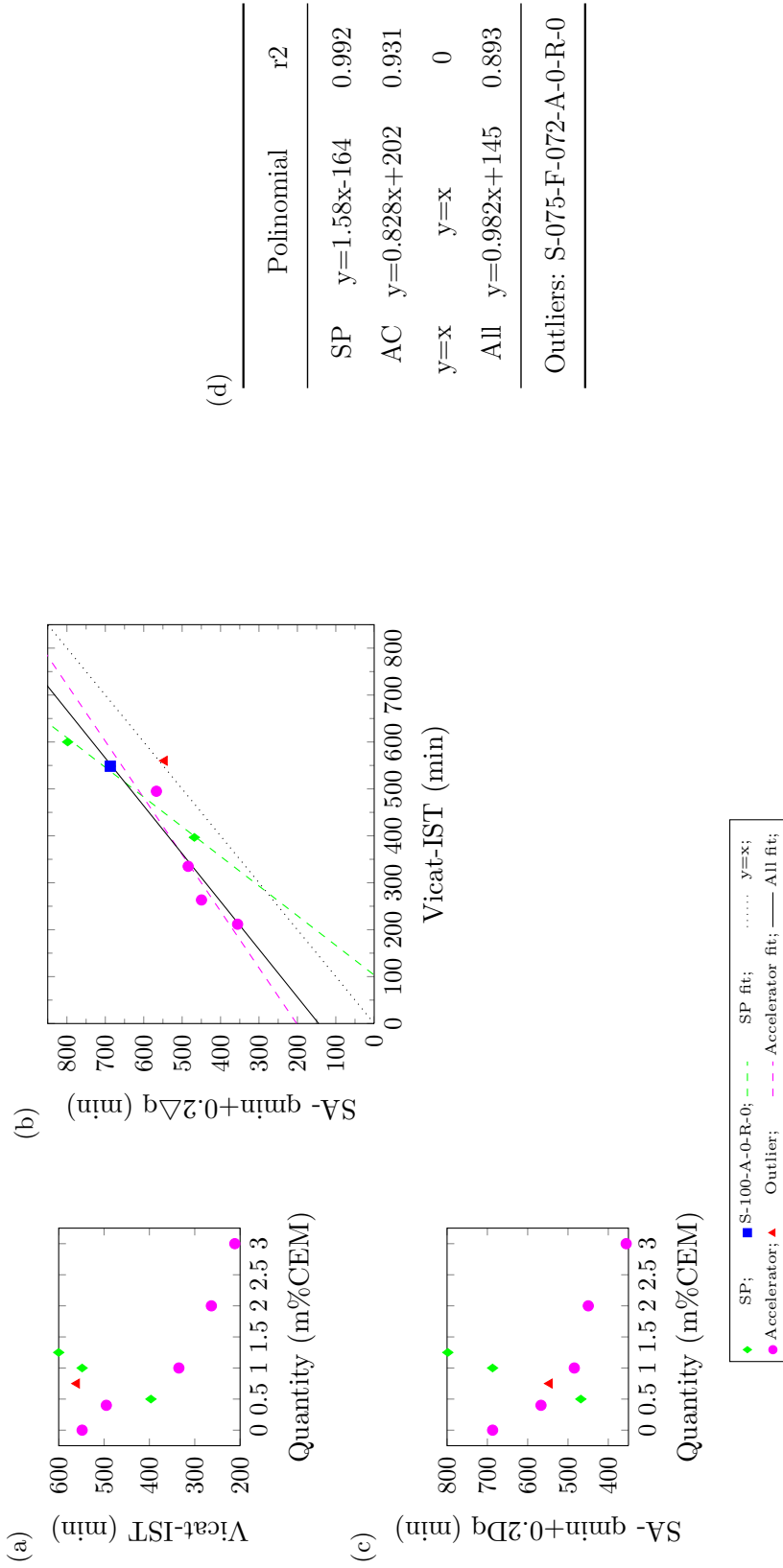
Figure 5.2: *Vicat-IST vs Semi adiabatic- Mortar Age at qmin+0.2△q*

5.3. Correlations with regard to *IST*

5.3.1. Penetration resistance test versus Vicat needle test

Figure 5.4 graphs the results for *IST* between the two standardized tests: penetration resistance and Vicat needle. Figures 5.4 a) and b) illustrate the variation of the results for each test in function of admixture quantity. The behaviour for the *SP* series is dissimilar between the tests. However, for the *AC* series there is an exponential decrease with accelerator quantity for both cases.

Figure 5.4 c) shows both tests plotted against each other, the best fit line y=1.01x+27.4 shows that as other authors [13] have already highlighted, although the criterion for *IST* are dissimilar, they serve as convenient points of comparisons between samples. Indeed, even using different standards, there is a y=x correlation with a 27 min offset. The Vicat needle results being less conservative, as times given for *IST* are higher, which would mean the workable time is greater.
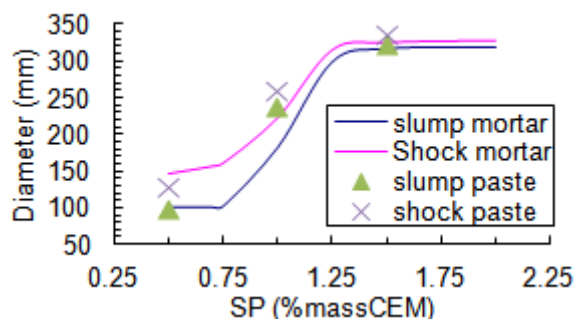
Figure 5.3: *Workability curve for SP, with workability of cement paste*

Although the results obtained are very positive, there are two outliers for this correlation: S-050-F-072-A-0-R-0 and S-075-F-072-A-0-R-0. Both outliers come from the *SP* series tests, leaving little data to analyse for this series. However, S-050 is repeatedly an outlier for penetration resistance correlations while S-075 also seems to be related to an experimental technique, in this case Vicat.

S-50 does not behave consistently with the other quantities for the penetration resistance

test. This variation coincides with the plateau where SP has little effect on workability, as shown in figure 5.3. For this mortar composition as the SP is not lubricating the mixture, friction between sand grains could result in greater penetration resistance values, as a result lower setting times than for the other data of the series are obtained .

For the Vicat test, S-75 shows a higher setting time than S-100, indicating it could be an outlier for these results. It is important to remember Vicat needle tests are performed on cement paste, although the compositions of the paste were determined by equivalent workability, S-75 was not tested for slump and shock tests (figure 5.3), and it is quite possible that this composition behaves differently. Moreover, it cannot be forgotten that these test are very susceptible to air entrapped, as SP quantities are lower the fluidity of the mixture is diminished and more air bubbles are entrapped. Air entrapped would increase the penetration depth, as a result higher setting times would be retrieved.

	Polinomial	r2
SP	y=2.82x-969	1
AC	y=0.975x+35.4	0.977
y=x	y=x	0.942
All	y=1.01x+27.4	0.983
Outliers:	S-050-F-072-A-0-R-0,	
S-075-F-072-A-0-R-0		

(d)

(a) (b) (c)
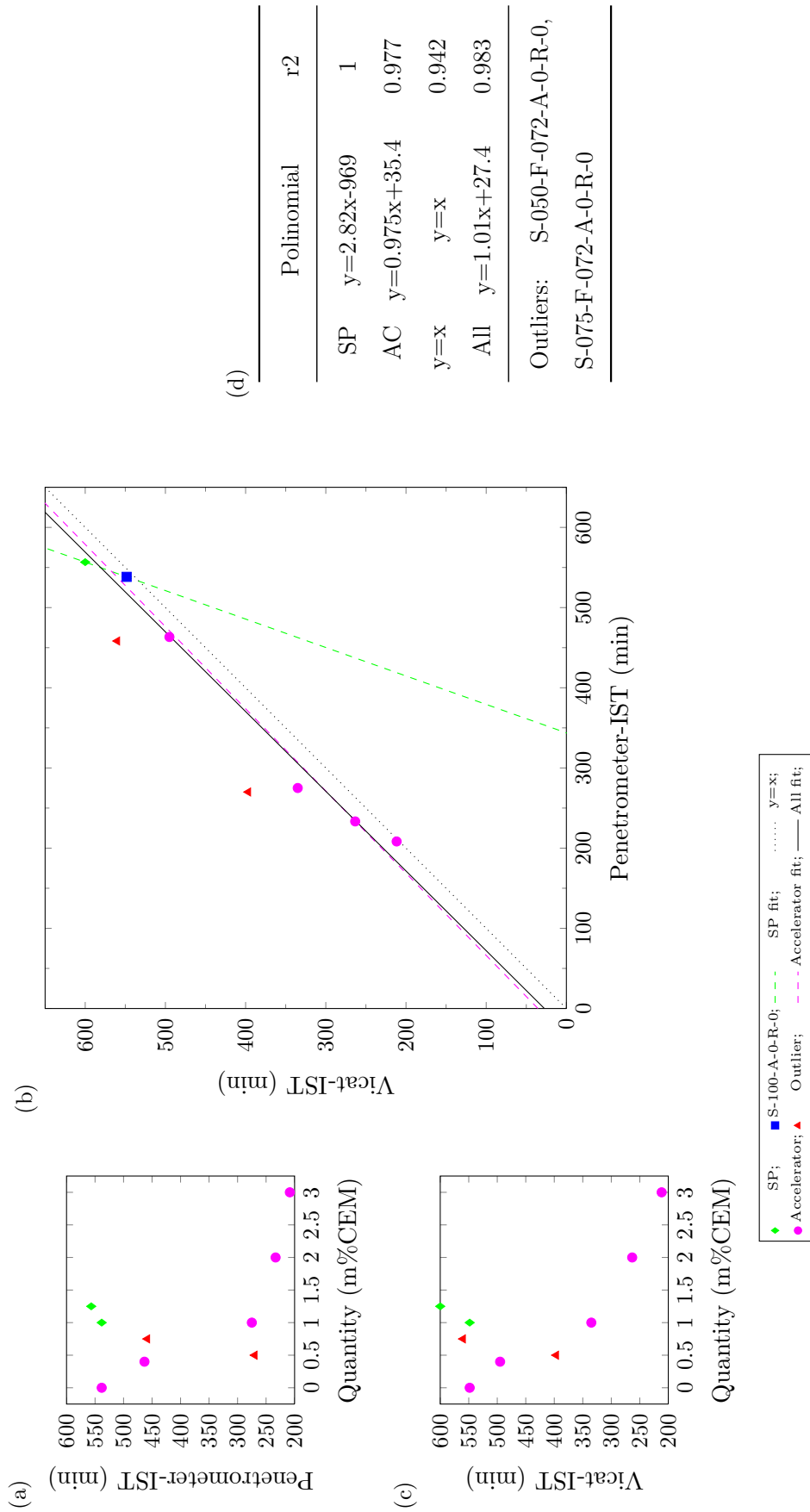
Figure 5.4: *Penetrometer-IST vs Vicat-IST*

5.3.2. p-wave transmission test- Mortar age at 1500 m/s velocity threshold

Standards determine *IST* by penetration resistance, which is directly linked to the compression and shear resistance of the mortar at certain ages. p-wave velocity depends on the changes of the elastic properties, which is also directly linked to mechanical properties changes. Two of the mortar ages proposed as indicators for *IST* show a good correlation with the results obtained from the penetration resistance test and Vicat needle test, as shown in annex E. Indeed first inflection point and 1500 m/s velocity threshold show acceptable correlations. However, second inflection point has a slope of 1.5 (min/min) and an offset of 97 min when compared to the Vicat needle test. This, of course, means the maximum inflection point is not an adequate indicator.

Mortar age at p-wave velocity first inflection point results in R^2 of 0.929 for a y=x is obtained comparing to the penetration resistance tests, but the results obtained with the Vicat needle test show higher dispersion and an 118 min offset.

The best correlation with both standards (ASTM C403 and EN196-3) is obtained with the mortar age at 1500 m/s p-wave velocity threshold. Figures 5.5 and 5.6 graph this indicator against the *IST* obtained by the penetration resistance test and the Vicat needle test.

Figures 5.5 a) and b) show a similar behaviour for the different mortar compositions except for S-050-F-072-A-0-R-0, as discussed previously the penetrometer resistance point for this mixture is an outlier. The fit y=x has a R^2 of 0.972 for the penetrometer , which would mean the same hydration point is being measured.

Figure 5.6 c) shows the correlation with the Vicat needle test. Considering the *SP* and *AC* series separately, different behaviours are apparent. However with such small samples, more tests would have to be performed to confirm the different behaviours. Taking into account all the experimental data the *SP* series data fits quite well with the *AC* series data, although it modifies the fit, the final result gives a y=0.957x-23.3 linear regression, which makes sense considering there is a 27 min offset between the Vicat needle test and the penetration resistance test.
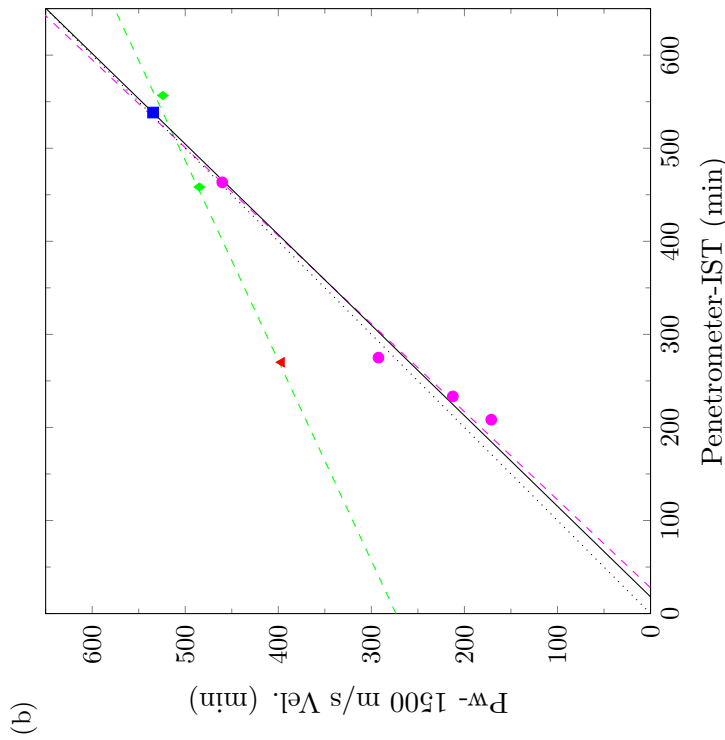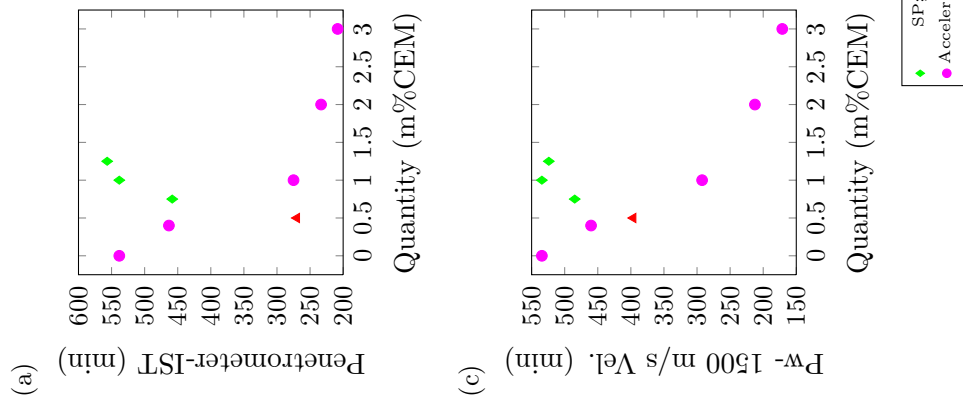
Figure 5.5: *Penetrometer-IST vs P-wave- Mortar Age at 1500 m/s Velocity Threshold*

	Polinomial	r2
SP	y=0.465x+274	0.864
AC	y=1.06x-29.2	0.986
y=x	y=x	0.972
All	y=1.03x-18.5	0.976
Outliers: S-050-F-072-A-0-R-0		

(d)

	Polinomial	r2
SP	y=0.647x+145	0.846
AC	y=1.08x-65.4	0.997
y=x	y=x	0.867
All	y=0.957x-23.3	0.967
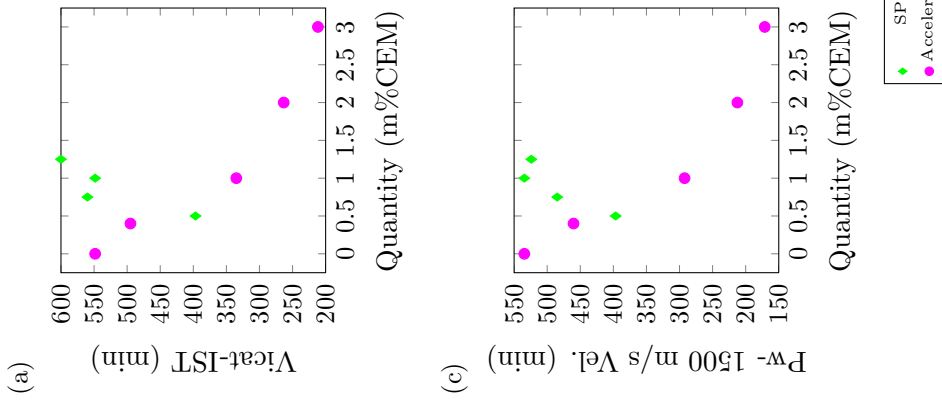
Outliers:

Figure 5.6: *Vicat-IST vs P-wave- Mortar Age at 1500 m/s Velocity Threshold*

5.3.3. Semi-adiabatic calorimetry- Mortar age at qmin+ 1.5 J/gh

As shown in annex E, no perfect correlations for *IST* are obtained with the criteria proposed for this experimental work. $qmin + 0.2 \triangle q$ gives an acceptable R^2 value of 0.872 for a linear regression against penetration resistance, but with a 251 min delay, this indicates that the heat flux variation is probably too big. Results with the Vicat needle test give poor correlations.
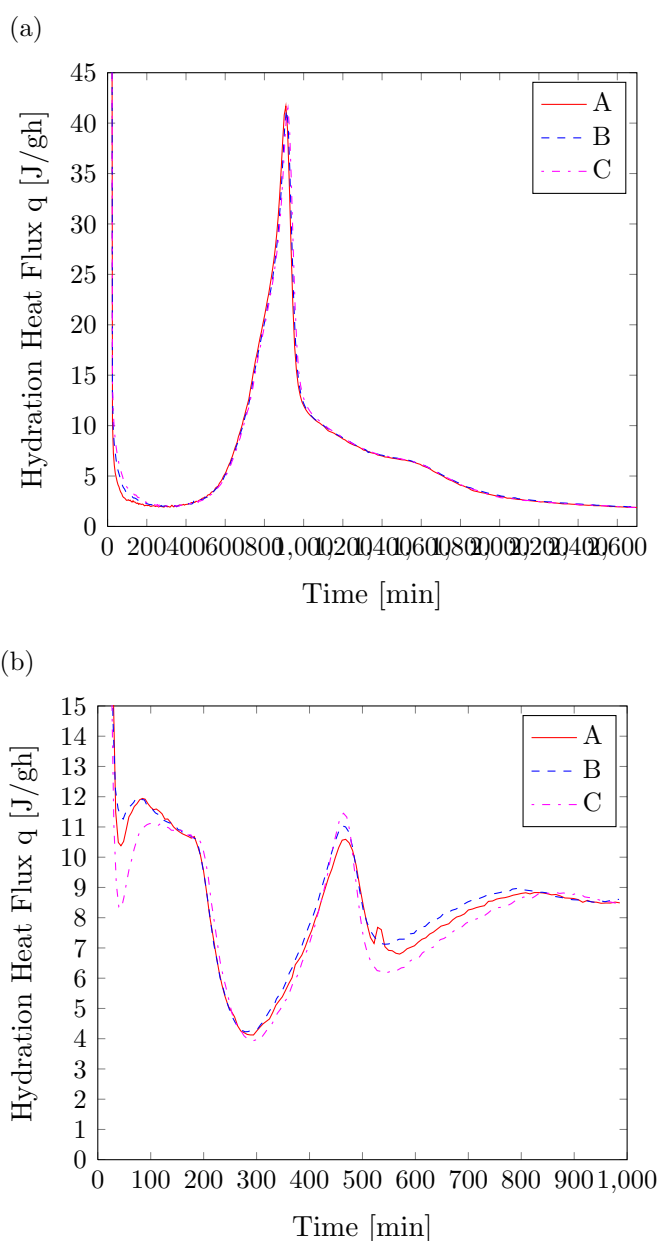
Figure 5.7: *Hydration heat flux in function of corrected time after water addition for a) S-100-F-072-A-000-R-0 b)S-100-F-072-A-300-R-0*

qmin+ 1.5J/gh gives mores acceptable results. Figures 5.8 and 5.9 show the correlations between this mortar age and the standardized *IST*s. S-100-F-072-A-200-R-0 and S-100-F-072-A-300-R-0 are outliers for this correlation. Indeed, due to the chemical changes in this composition qmin+1.5 J/gh is not a plausible indicator. Figure 5.7 shows the hydration heat flux evolution in function of corrected time after water addition for the composition and for S-100-F-072-A-0-R-0. As the graph shows, a severely shifted reaction chain seems to be activated by the accelerator, this reaction apparently contributes to the hardening and setting, as other indicators show *IST* occurs nearly at the end of the first plateau.

Figure 5.8 a) and c) illustrates the variation of the indicators with the admixture quantities. Data from both series behave linearly with admixture quantity. On the other hand, figure 5.9 b) shows the correlation between this indicator and the Vicat results follow a y=x fit with an R^2 of 0.902. It can be observed from figure 5.8 b) that the correlation with the penetrometer test shows a an R^2 of 0.911 with an offset of 31.8 min, which is consistent with the offset between the penetrometer and Vicat tests.
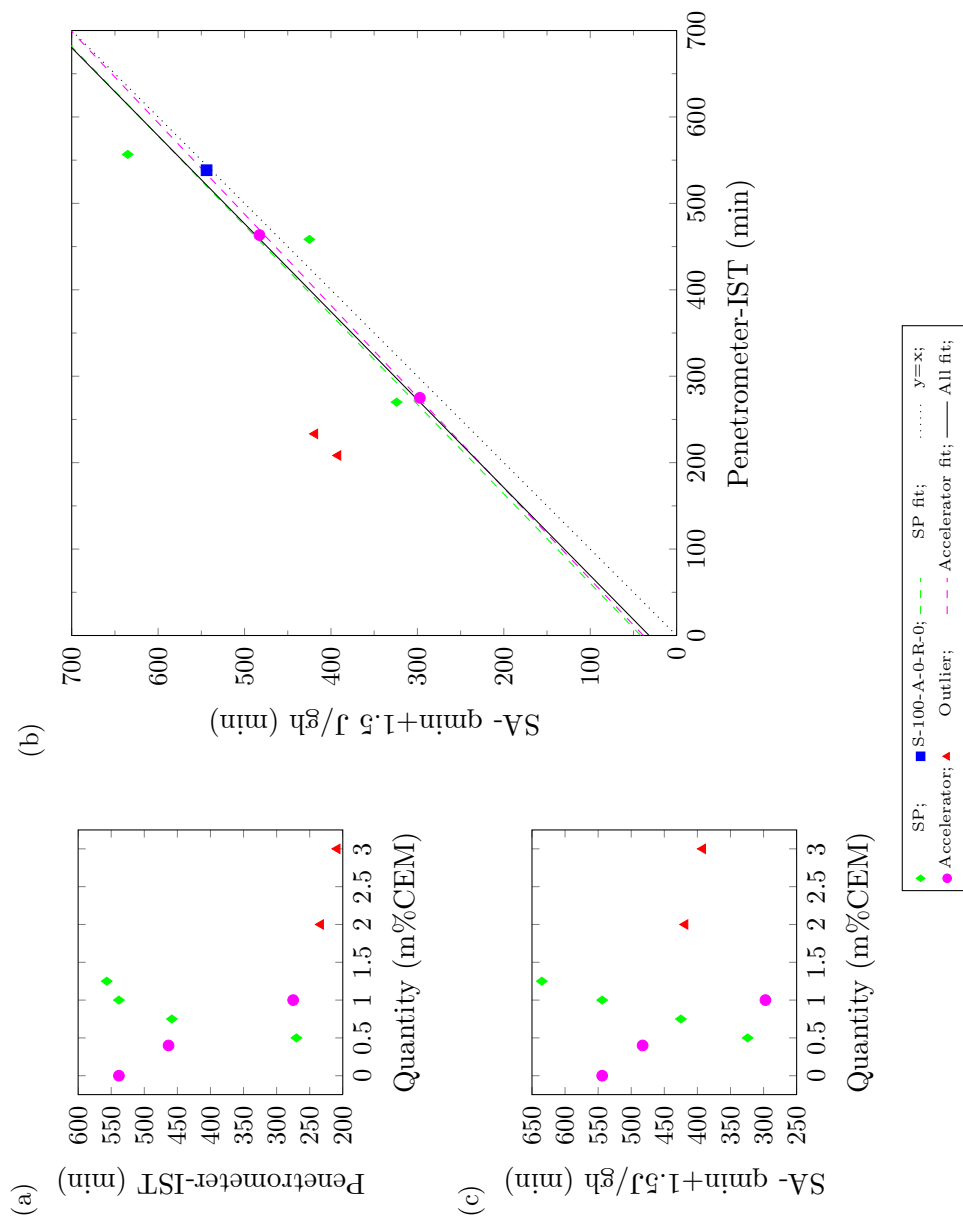
Figure 5.8: *Penetrometer-IST vs Semi adiabatic- Mortar Age at qmin + 1.5 J/gh*
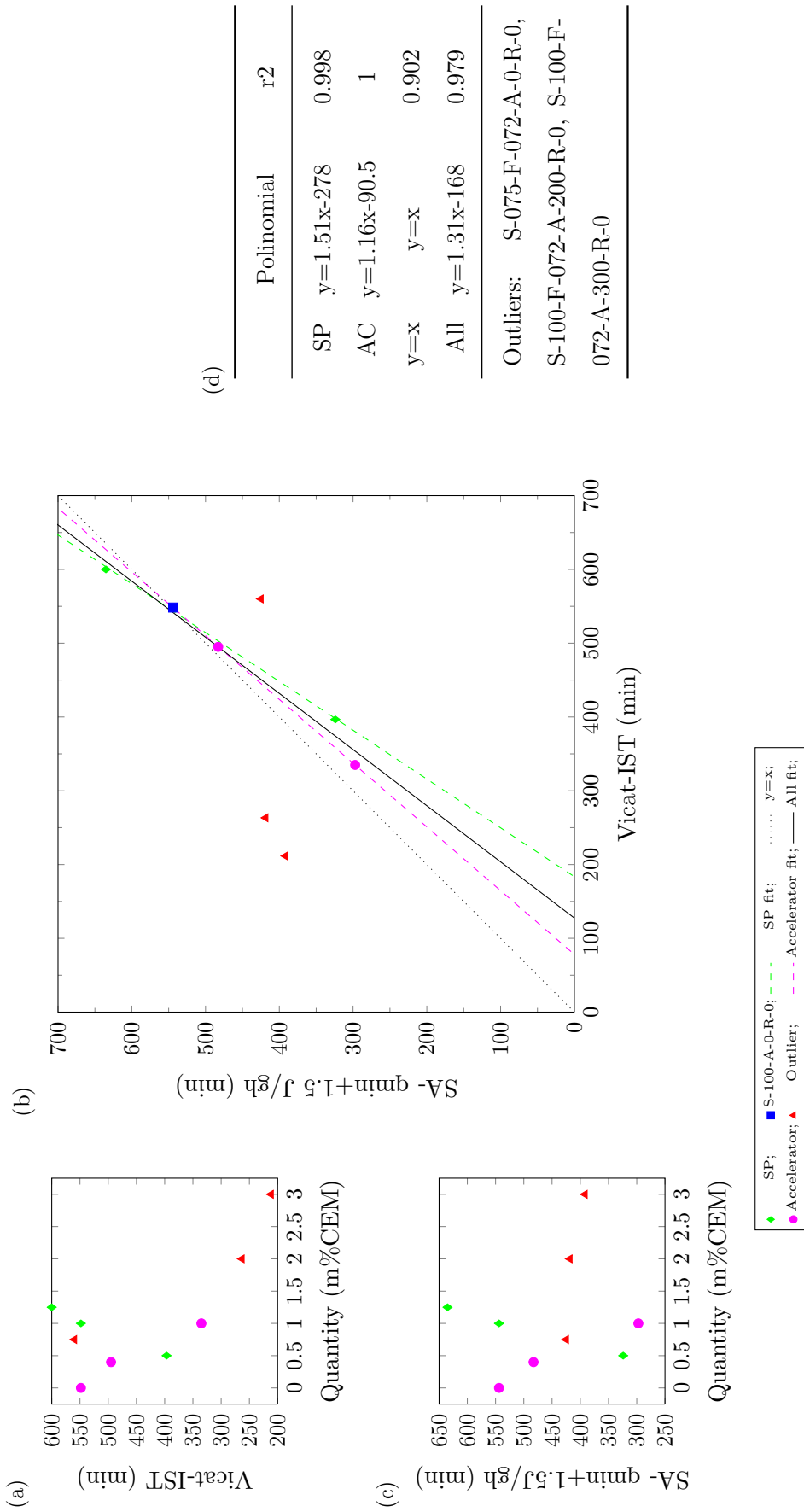
Figure 5.9: *Vicat-IST vs Semi adiabatic- Mortar Age at qmin+1.5J/gh.*

5.4.   Correlations with regard to *FST*

5.4.1.   p-wave transmission test- Mortar age at 2/3 of final velocity

As shown in annex E, the indicators proposed for the p-wave transmission test give acceptable correlations with *FST* except for the 20% of maximum velocity gradient. The second inflection point gives a good linear regression, but totally off the y=x+200 fit. The 2975 m/s threshold gives a good correlation, but not as good as the 2/3 of final velocity threshold, which has a higher R^2 for y=x+200.

Figure 5.11 a) and c) graph the variation of the indicators with admixture quantity. S-100-F-072-A-300-R-0 shows an increase in *FST*, while it would be expected a similar *FST* to S-100-F-072-A-200-R-0. However in figure 5.11 c) this data fits in the correlation. The slope obtained is 0.879 (min/min) and the offset is 262 min. However if the offset is fixed to 200 min an R^2 of 0.941 is obtained.

5.4.2.   Semi-adiabatic calorimetry- Mortar age at qmax

Figure 5.12 shows the correlation between standardized ASTM C403 *FST* and the indicator qmax from the semi-adiabatic calorimetry test. In figure 5.12 c) it can be observed that the behaviour of S-100-F-072-A-300-R-0 would seem to be the expected, however as it has already been discussed the semi-adiabatic indicators are not plausible with high accelerator quantities. The value obtained for qmax for S-050-F-072-A-0-R-0 is clearly an outlier for the trend observed for the *SP* series in figure 5.12 c), as explained before, this could be because of the workability behaviour of the mixture. Figure 5.12 b) illustrates a y=x+200 trend for the remaining data.

Figures 5.11 and 5.12 show a 200 min offset between the standardized ASTM C403 *FST* value and the proposed indicators from the p-wave velocity and semi-adiabatic calorimetry tests. This offset could be due to the indicators chosen or to external factors. Due to the big differences in size between the samples of different tests, in the case of the penetration resistance samples, which are the biggest in size and mass (as exemplified in figure 5.10), the temperature variation is more significant than for the p-wave velocity tests.
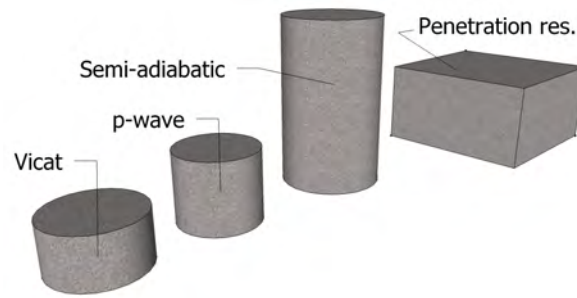
Figure 5.10: *Volumes of the samples for the different tests*

Even though the process followed for the acquisition of the penetration resistance data followed the standard ASTM C403, to perform a more adequate comparison with the other experimental techniques, the maturity adaptation correction for the time series should have been applied. The time series adaptation would result in an equivalent age at which a certain degree of hydration is reached in isothermal conditions. For *IST*, the rise in temperature is negligible (as shown in semi-adiabatic calorimetric tests), thus results obtained are valid. However for *FST*, since in general there are no energetic variations between the compositions tested, this adaptation could be equivalent to a 200 min offset.

	Polinomial	r2
SP	y=0.781x+323	0.953
AC	y=1.01x+195	0.961
y=x+200	y=x+200	0.922
All	y=0.879x+262	0.941
Outliers:		

(d)
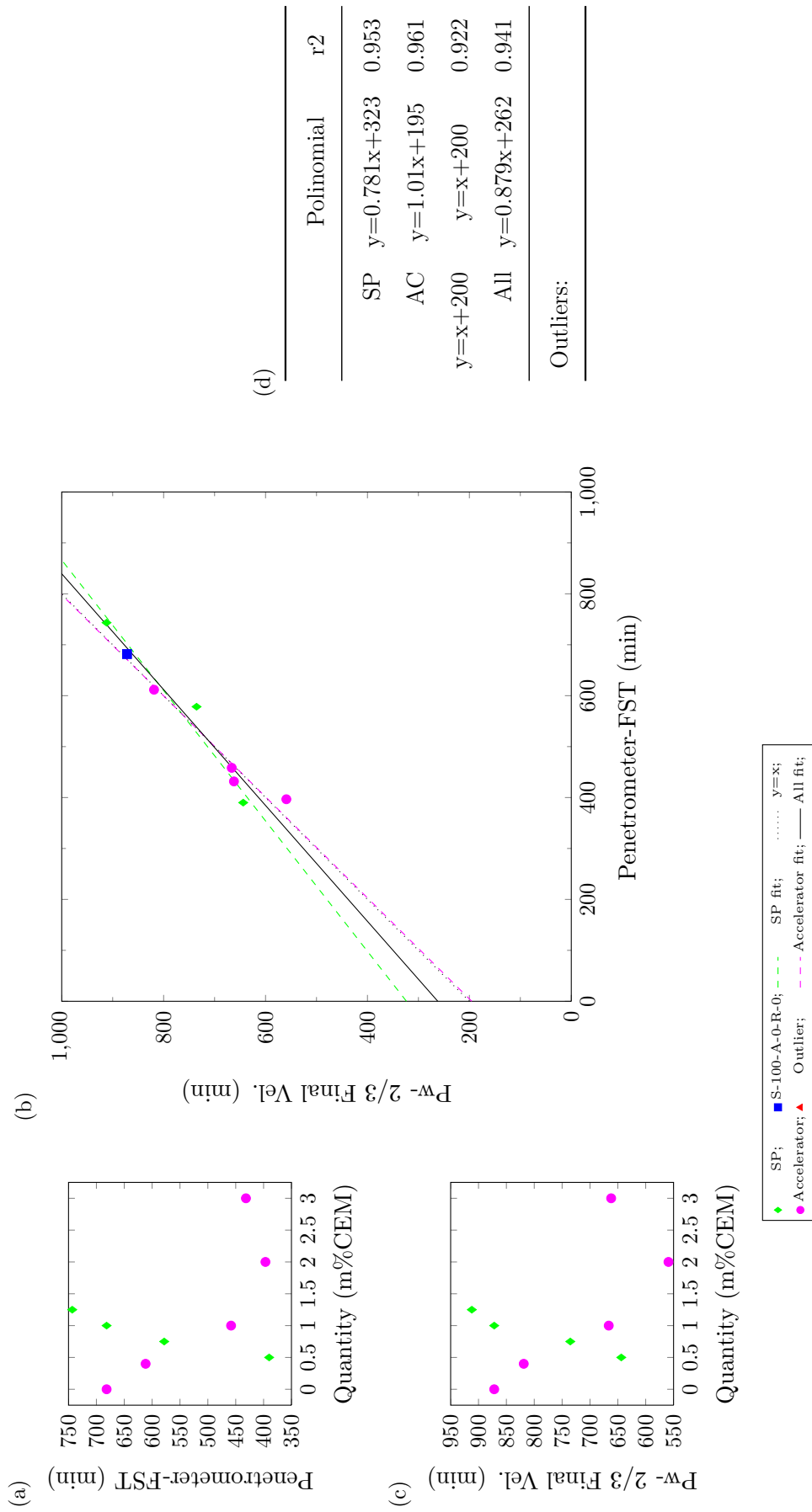
Figure 5.11: *Penetrometer-FST vs P-wave- Mortar Age at 2/3 of Final Velocity*
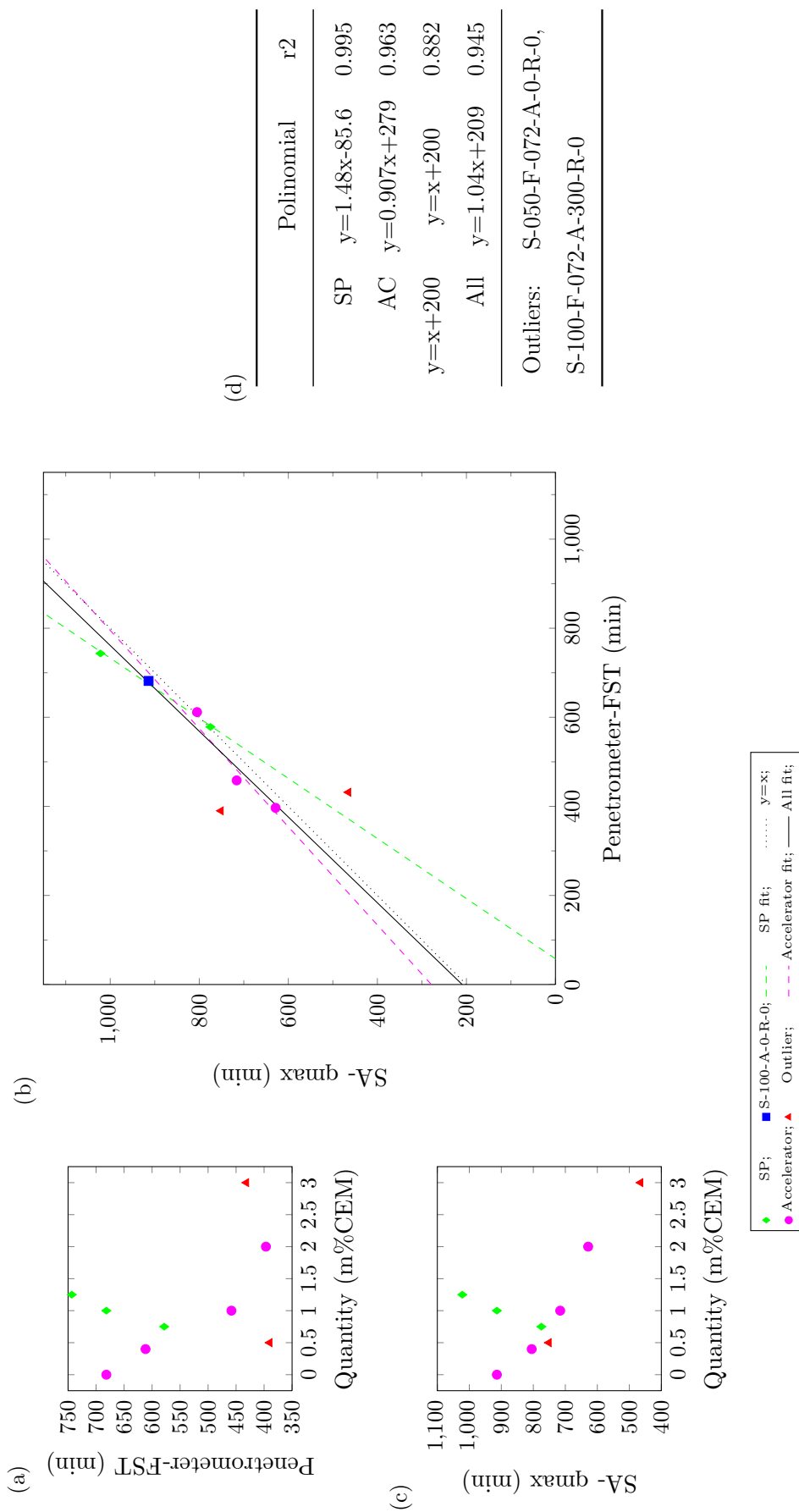
Figure 5.12: *Penetrometer-FST vs Semi adiabatic- Mortar Age at qmax*

5.5. Summary

Useful correlations were found between the p-wave transmission test and the semi-adiabatic calorimetry test and the standardized tests for setting times (penetration resistance and Vicat needle). These valuable correlations illustrate the meaningfulness of the p-wave velocity curve and hydration heat flux parameters to *IST* and *FST*. The best possible correlation is a relationship y=x, which means both indicators are related in the same way to the mortar hydration proving the indicator as valuable as the reference result to directly determine setting. However, some indicators show an offset (c) or a different sensitivity (m) to the sought characteristic, giving linear relationships y=mx+c, this correlation is still valuable.

IST correlations show sensitivities close to 1 and low offsets (0 to 31 min). Where as *FST* correlations show a high offset of approximately 200 min, this offset could be the result of the indicators chosen or the lack of maturity adaptation to the penetration results.

From the p-wave velocity curve the mortar ages at: 1500 m/s, 2975 m/s and 2/3 of final p-wave velocity thresholds proved valuable indicators for setting. On the other hand mortar ages at first, second and maximum inflection points and 20 % maximum p-wave velocity gradient did not prove to be good reference indicators for setting times.

For semi-adiabatic calorimetry, qmin+1.5 J/gh and qmax proved to be reliable indicators for start and end of setting respectively. However qmin+0.2△q did not prove to be a good indicator.

These correlations relate compositions with extreme values for both accelerator and *SP* admixtures, however the results show that not all the indicators are plausible for its experimental technique and composition. Experiments that depend directly on the shear and compression resistance (penetration resistance test and Vicat needle test) are more prone to irregular results in the case of low workabilities (low *SP* quantities). Semi-adiabatic calorimetry test indicators suggested for this experimental programme lose a lot of their meaning for high accelerator quantities, since the reaction chain is severely shifted and the curve shape in which the concept of qmin is based is completely absent.

This means that even though the correlations obtained are valuable, further testing with more compositions and different indicators to try to comprise extreme values are necessary.

6. Conclusions and future lines of work

The objective of this work was to develop and execute a parametric experimental programme for different mortar compositions. By analysing the data of the different experimental methods, possible correlation factors between the hydration characteristic points and IST and FST were sought.

The hydration of two series of mortars have been subjected to: p-wave velocity, semi-adiabatic calorimetry, penetration resistance and Vicat needle tests. The two series are self compacting mortars which differ from each other in the nature of their admixtures. The SP series comprises 6 different mortars with different SP quantities that vary from 0.00 to 1.50 %mCEM. The AC series uses a mortar with 1.00 %mCEM of SP and a varying quantity of accelerator from 0.00 to 3.00 %mCEM.

As primary conclusions regarding the main topic of the work:

- Direct correlations are obtained between standardized IST and FST and characteristic points of the p-wave velocity test and semi-adiabatic calorimetry test. These valuable correlations illustrate the meaningfulness of the p-wave velocity curve and hydration heat flux parameters to IST and FST.

- Not all the characteristic points proposed were suitable references for setting. From the p-wave velocity curve the mortar ages at: 1500 m/s, 2975 m/s and 2/3 of final p-wave velocity thresholds proved valuable indicators for setting. While for semi-adiabatic calorimetry, qmin+1.5 J/gh and qmax proved to be reliable indicators for start and end of setting respectively

Furthermore, a number of important conclusions can be made regarding the experiments:

- High accelerator quantities severely shift the reaction chain affecting setting and hardening. Semi-adiabatic calorimetry test indicators suggested for this experimental programme lose a lot of their meaning, since the curve shape in which the concept of qmin is based is completely absent.

- Correlations with regard to FST show an offset approximately equal to 200 min when comparing the penetration resistance test to p-wave or semi-adiabatic. This offset could be the result of the indicators chosen or the lack of maturity adaptation to the penetration results.

- Experiments that depend directly on the shear and compression resistance (penetration resistance test and Vicat needle test) are more prone to irregular results in the case of low workabilities.

- The polycarboxylate ether SP used in this experimental programme makes hydration take place later and at a more constant rate.

- The accelerator (calcium nitrate) makes hydration take place before and has a greater impact during the first 1000 min, counteracting the effect of the SP.

To allow the development of truly general indicators for IST and FST, the following studies should be carried:

- Further testing with more admixtures and different cements to determine if these correlations are still valid.

- Repetition of the penetration resistance test with temperature measurement to apply the maturity adaptation.

- Investigating generally useful indicators, that comprise extreme admixture quantities.

- Full study to obtain equivalent cement paste composition for the Vicat needle tests.

- Because it was noticed that the the vacuum preservation of the cement presented some flaws, a study of the efficiency of the vacuum preservation of cement and its effects on the early hydration of fresh mortar.

Bibliography

[1] G. Sant, C. F. Ferraris, and J. Weiss, "Rheological properties of cement pastes: a discussion of structure formation and mechanical property development," *Cement and concrete Research.*, vol. 38, pp. 1286–1296, 2008.

[2] G. Trtnik, G. Turk, F. Kav?i?, and V. B. Bosiljkov, "Possibilities of using the ultrasonic wave transmission method to estimate initial setting time of cement paste," *Cement and Concrete Research*, vol. 38, no. 11, pp. 1336 – 1342, 2008. [Online]. Available: http://www.sciencedirect.com/science/article/pii/S0008884608001531

[3] B. Desmet, K. Atitung, M. Abril Sanchez, J. Vantomme, D. Feys, N. Robeyst, K. Audenaert, G. De Schutter, V. Boel, G. Heirman, z. Cizer, L. Vandewalle, and D. Van Gemert, "Monitoring the early-age hydration of self-compacting concrete using ultrasonic p-wave transmission and isothermal calorimetry," *Materials and Structures*, vol. 44, pp. 1537–1558, 2011, 10.1617/s11527-011-9717-x. [Online]. Available: http://dx.doi.org/10.1617/s11527-011-9717-x

[4] H. Lee, K. Lee, Y. Kim, H. Yim, and D. Bae, "Ultrasonic in-situ monitoring of setting process of high-performance concrete," *Cement and Concrete Research*, vol. 34, no. 4, pp. 631 – 640, 2004. [Online]. Available: http://www.sciencedirect.com/science/article/pii/S0008884603003697

[5] T. Voigt, Z. Sun, and S. P. Shah, "Comparison of ultrasonic wave reflection method and maturity method in evaluating early-age compressive strength of mortar," *Cement and Concrete Composites*, vol. 28, no. 4, pp. 307 – 316, 2006, ¡ce:title¿Non-Destructive Testing¡/ce:title¿. [Online]. Available: http://www.sciencedirect.com/science/article/pii/S0958946506000242

[6] H. Reinhardt and C. Grosse, "Continuous monitoring of setting and hardening of mortar and concrete," *Construction and Building Materials*, vol. 18, no. 3, pp. 145 – 154, 2004, ¡ce:title¿3rd Kumamoto International Workshop on Fracture, Acoustic Emission and NDE in Concrete (KIFA-3)¡/ce:title¿. [Online]. Available: http://www.sciencedirect.com/science/article/pii/S095006180300117X

[7] N. Robeyst, E. Gruyaert, C. U. Grosse, and N. D. Belie, "Monitoring the setting of concrete containing blast-furnace slag by measuring the ultrasonic p-wave velocity," *Cement and Concrete Research*, vol. 38, no. 10, pp. 1169 – 1176, 2008. [Online]. Available: http://www.sciencedirect.com/science/article/pii/S000888460800104X

[8] A. Herb, "Indirekte beobachtung des erstarrens und erhrtens von zementleim, mrtel und beton mittels schallwellenausbreitung," Ph.D. dissertation, Universitt Stuttgart, Holzgartenstr. 16, 70174 Stuttgart, 2003. [Online]. Available: http://elib.uni-stuttgart.de/opus/volltexte/2003/1509

[9] N. Robeyst, "Monitoring setting and microstructure development in fresh concrete with the ultrasonic through-transmission method," Ph.D. dissertation, Magnel Laboratory for Concrete Research, Ghent University, 2009.

[10] A. G. Brooks, A. K. Schindler, and R. W. Barnes, "Maturity method evaluated for various cementitious materials," *Materials in civil engineering*, pp. 1017–1025, 2007.

[11] L. S. Sandberg, J P, "Monitoring and evaluation of cement hydration by semi-adiabatic field calorimetry," in *Concrete Heat Development: Monitoring, Prediction & Management*, K. W. A. K. Schindler, Ed. American Concrete Institute, 2007, pp. 13–23.

[12] A. Zingg, F. Winnefeld, L. Holzer, J. Pakusch, S. Becker, R. Figi, and L. Gauckler, "Interaction of polycarboxylate-based superplasticizers with cements containing different c3a amounts," *Cement and Concrete Composites*, vol. 31, no. 3, pp. 153–162, 2009.

[13] D. Lootens, P. Jousset, L. Martinie, N. Roussel, and R. J. Flatt, "Yield stress during setting of cement pastes from penetration tests," *Cement and concrete Research.*, vol. 39, pp. 401–408, 2009.

[14] C. J. Prof. G. Hammond. (2008) Inventory of carbon and energy (ice). Department of Mechanical Engineering (University of Bath). [Online]. Available: http://www.bath.ac.uk/mech-eng/sert/embodied/

[15] P. S. B. Prof. K. Scrivener, "Cementitious material hydration," in *Cementitious Material Hydration*, 2011.

[16] M. Shetty, *Concrete Technology Theory and Practice*. Rajendra Ravindra Printers, 2005.

[17] J. Illston and P. Domone, Eds., *Construction Materials their Nature and Behaviour*. Spon Press, 2001.

[18] G. De Schutter, J. Gibbs, P. Domone, and P. Bartos, *Self-compacting concrete*. Whittles, 2008.

[19] R. Gheysens, Ed., *Technologie de Beton*. Groupement Belge du Beton, 2006.

[20] S. H. Kosmatka and M. L. Wilson, *Design and Control of Concrete Mixtures,*, P. C. Association, Ed., 2011.

[21] J. Newman and B. S. Choo, Eds., *Advanced Concrete Technology*. Butterworth-Heinemann, 2003, vol. Constituent Materials.

[22] M. Collepardi, "Admixtures-enhancing concrete performance," 2005.

[23] H. Justnes, "Calcium nitrate as a multifunctional concrete admixture."

[24] P. Taylor, S. Kosmatka, and G. Voigt, *Integrated Materials and Construction Practices for Concrete Pavement: A State-of-the-Practice Manual*. Federal Highway Administration, Office of Pavement Technology, 2006.

[25] S. Shah and M. Konsta-Gdoutos, *Measuring, monitoring and modeling concrete properties: an international symposium dedicated to Professor Surendra P. Shah, Northwestern University, U.S.A.* Springer, 2006. [Online]. Available: http://books.google.es/books?id=6tDBt5_b9nkC

[26] A. Aguado, R. Gettu, and S. Shah, *Concrete technology: new trends, industrial applications : proceedings of the International RILEM Workshop*

on Technology Transfer of the New Trends in Concrete, ConTech '94, ser. RILEM proceedings. E & FN Spon, 1995. [Online]. Available: http://books.google.es/books?id=Xd5ZkLw4tFgC

[27] L. G. HERNNDEZ, "Desarrollo y anlisis de pavimentos industriales desde el punto de vista del acabado superficial," Ph.D. dissertation, Universidad de Cantabria, 2007.

[28] *Matlab R2012a Documentation.*

[29] B. Lempriere, *Ultrasound and elastic waves: frequently asked questions.* Academic Pr, 2002.

[30] P. Livesey, A. Domnnelly, and C. Tomlinson, "Measurement of the heat of hydration of cement," *Cement and concrete composites*, vol. 13, pp. 177–185, 1991.

[31] H. L. N.J. Carino, "The maturity method: From theory to application," in *Proceedings of the 2001 Structures Congress & Exposition, May 21-23, 2001, Washington, D.C., American Society of Civil Engineers, Reston, Virginia*, P. C. C. , Ed. National Institute of Standards and Technology, 2001, p. 19.

[32] A. Schindler, J. Weiss, K. Kovler, J. Marchand, and S. Mindess, "Prediction of concrete setting," in *International RILEM Symposium on Concrete Science and Engineering: A Tribute to Arnon Bentur.* RILEM Publications SARL, 2004.

[33] R. W. Weakley, "Evaluation of semi-adiabatic calorimetry to quantify concrete setting," Ph.D. dissertation, Faculty of Auburn University, 2009.

[34] R. Hill and K. Daugherty, "The interaction of calcium nitrate and a class c fly ash during hydration," *Cement and concrete Research.*, vol. 26, pp. 1131–1143, 1996.

[35] P. V. G. Snchez. (2004) Apuntes estadstica i universidad carlos iii de madrid-tema 2: Medidas de dependencia lineal. AulaGlobal. Universidad Carlos III de Madrid.

List of Figures

Nuria Ortiz Taboada

List of Tables

Annexes

A. Cement technical sheet

CEM I 52,5 N MF
Ciment haute performance

Le produit et ses applications

Le ciment CEM I 52,5 N MF est un ciment portland dont l'unique "constituant principal" est le clinker portland (K). La teneur en clinker est supérieure à 95 %.

Domaines d'application préférentiels

- Bétons en milieu non agressif (classes d'environnement E0, EI et EE selon la norme NBN B15-001), demandant un décoffrage, une manutention ou une mise en service courant ou rapide
- Bétons de classes de résistance moyenne ou élevée
- Bétonnage en période hivernale
- Maçonneries, particulièrement en période hivernale
- Mortiers de rejointoiement
- Préfabrication de produits en béton

Contre-indications

- Bétons en milieu agressif (classes d'environnement EA2 et EA3 selon la norme NBN B15-001)
- Bétons pour constructions massives
- Utilisation de granulats sensibles à la réaction alcalis-granulats pour les bétons en milieu humide

Résistances béton

Evolution de la résistance à la compression d'un béton standard *
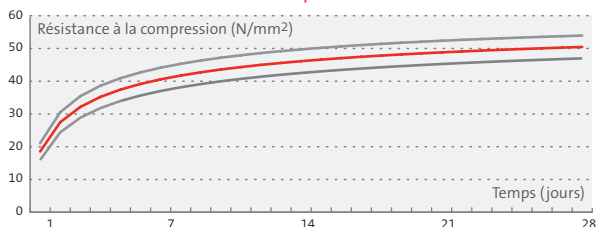
La figure donne l'évolution de la résistance à la compression sur cubes de 150 mm d'arête, obtenue dans notre laboratoire sur un béton à base du CEM I 52,5 N MF. Les caractéristiques principales du béton sont :

- granulométrie continue : concassé calcaire 4/20 + sable de rivière gros
- dosage en ciment : 300 kg/m^3
- fluidité : affaissement (slump) de 80 mm
- facteur E/C : environ 0,58

PAYS	NORME	DÉNOMINATION	MARQUE
Belgique	NBN EN 197-1 PTV 603	CEM I 52,5 N MF	Benor
France	NF EN 197-1 NF P15-318	CEM I 52,5 N CP2 "MF"	NF
Pays-Bas	NEN EN 197-1	CEM I 52,5 N (MF)	KOMO

Avantages du CEM I 52,5 N MF

- Durcissement rapide
- Résistance élevée à courte et à moyenne échéance

Spécifications techniques

Caractéristiques mécaniques et physiques **

	UNITÉS	RÉSULTATS	SPÉCIFICATIONS EN 197-1 ET PTV 603
Prise			
Besoin en eau	%	28	-
Début	hh:mm	2:45	≥ 0:45
Fin	hh:mm	3:30	≤ 12:00
Stabilité	mm	≤ 1	≤ 10
Résistance à la compression			
1 jour	N/mm^2	21	
2 jours	N/mm^2	34	≥ 20
28 jours	N/mm^2	62	≥ 52,5
Surface spécifique Blaine	m^2/kg	375	-
Masse volumique absolue	kg/m^3	3140	-
Masse volumique apparente	kg/m^3	1092	-
Refus au tamis de 200 µm	%	≤ 0,1	≤ 3,0
Valeur C	-	1,1	-

Composition chimique **

	RÉSULTATS (%)	SPÉCIFICATIONS (%) EN 197-1
CaO	62,9	-
SiO$_2$	18,2	-
Al$_2$O$_3$	5,7	-
Fe$_2$O$_3$	4,1	-
MgO	0,9	-
Na$_2$O	0,40	-
K$_2$O	0,75	-
SO$_3$	3,4	≤ 4,0
Cl$^-$	0,06	≤ 0,10
Perte au feu	1,2	≤ 5,0
Résidu insoluble	0,3	≤ 5,0

* Remarque : La résistance d'un béton dépendant de beaucoup de facteurs, la courbe de la figure n'est pas nécessairement représentative pour l'évolution des résistances d'un béton quelconque à base de CEM I 52,5 N MF.

** Remarque : Les résultats repris dans les tableaux sont basés sur des valeurs moyennes et sont donnés à titre purement indicatif et n'ont en aucun cas un caractère contractuel. En conséquence, ils ne sauraient engager la responsabilité de Holcim (Belgique) s.a.

La fiche MSDS de ce produit est disponible sur www.holcim.be

B. Lab Procedures

Mortar Lab

Standards and Procedures

1. Index

2. Working standards and Procedures

2.1. EN 1015-3: Methods of test for mortar for masonry- Part3: determination of consistence of fresh mortar (by flow table). Flow test and shock test.

link to standard

The Flow value is measured as the diameter of the test sample of fresh mortar which has been placed on a flow table disc by means of a defined mould and given a number of vertical impacts by raising the flow table to a given height and dropping it.

2.1.1. PROCEDURE

2.1.1.1. Preliminary steps:

1. Write down the T (°C) and RH (%) from the weather station to the right of the mixing machine.

2. APPARATUS

    a. Mixer bowl (mixing)

    b. Sand (mixing)

    c. Cement (mixing)

    d. Measuring cylinder (scale)

    e. Water bottle (scale)

    f. Jug (sink)

    g. Shock table

    h. Mould (2 parts) Truncated conical mould (shock table)

    i. Callipers (big one in wooden box in first black cupboard) (shock table)

    j. Tamper (shock table)

    k. Trowel (shock table)

    l. Scoop (shock table)

2.1.1.2. Mixing:

This mixing procedure is for standard EN 196 please consider if you need another procedure.
This is for a standard mortar – be careful for other mixtures (especially for the quantities and composition)

1. Turn on mixing machine (button is in the rear of the machine-right hand side)

2. Check the machine is set in standard EN-196, if otherwise press select.

3. Push the lever outwards and down to lower the bowl plateau

4. Place the beater (push up and turn)

5. Open cement bag and put it in the mixer bowl (DO NOT OPEN AND LEAVE IT FOR A MORE THAN 15 MIN IF POSSIBLE)

    a. In the case you're using a packaged cement sample, off course. Anyway, it would be better to check the cement quantity, even if it comes from a vacuum bag. This can be done by putting the bowl on the scale and taring.

6. Open sand bag, twist the top part and empty on the funnel on the top-left hand side, we do it like this so min quantity of fine sand is lost (DO NOT THROW AWAY THE BAG- WE WILL USE IT LATER)

7. WATER

    a. Play with the tap putting the probe in the water stream to take the water to 20.2°C (if room temp is below 20°C) - 19.8°C (if room temp is above 20°C)

    b. Fill the jug while stirring with temp probe to obtain a mixture of the desired temp.

    c. Rinse the measuring cylinder (fill it with water and then empty)

    d. Weigh 225g of water (use the distilled water for fine tuning) **if W/C=0.5**
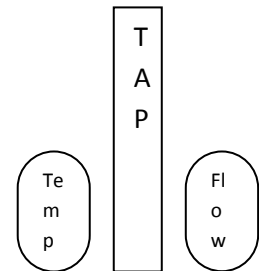
8. Humidify the metal slope for adding water of the mixing machine (top right) using the water. (use some tissue to collect the water)

9. Place the mixing bowl

10. Push the lever up and inwards

11. Press the START button for around 2sec- Write the TIME OF WATER ADDITION on the TEST SHEET

    a. Slowly add the water (20s-30s)

    b. After adding the sand and the fast mixing starts the time to "clean" the bowl

        i. Pull down the lever.

        ii. Use the spatula to clean the bowl and beater.

        iii. Don't forget the sand that lies on top of the beater.

       iv. Push up the lever before the end of the resting time and the start of fast mixing.

  c. When the test is completed

       i. Press the STOP button for 2s to reset

       ii. Pull down the lever

       iii. Take out the mixer bowl

       iv. Place the sand bag so it collects any dripping mortar from the beaters.

2.1.1.3. Procedure:

1. Wipe the disk and inner surface of the mould with oil.

2. Place the mould centrally on the disk

  a. Using the little scoop to fill the lower ½ of the mould with the fresh mortar <u>while holding the mould down</u>

       i. Using the tamper to compact the mortar (at least 10 times)

  b. Repeat for the top half of the mould

  c. Clean the disk if any leakages go out with oil.

  d. Take away the top part of the mould and check the level is correct- use the trowel to level the surface.

3. After aprox 15s raise the mould vertically

4. Measure the biggest and smallest diameter using the calliper, remember the disk can be turned- WRITE DOWN THE RESULT- Flow test

5. Turn the wheel 15 times (1 per second)

6. Measure the biggest and smallest diameter using the calliper, remember the disk can be turned- WRITE DOWN THE RESULT- Shock test

7. Clean the calliper to take away any rests of fresh mortar

8. Clean

  a. First use tissue to remove all possible solid mortar

  b. Clean with water in sink

  c. REMEMBER to leave sink clean

2.2. EN 1015-6: Methods of test for mortar for masonry- Part6: determination of bulk density of fresh mortar.

link to standard

Bulk density is defined by the quotient of the mass and the volume as sample of mortar occupies when it is introduced in a prescribed manner into a measuring vessel of a given capacity.

The procedure varies depending on the type of mortar!

2.3. EN 1015-7: Methods of test for mortar for masonry- Part7: Determination of air content of fresh mortar.

link to standard

Pressure of the pressure chamber is transmitted to the mortar by the incompressible layer of water on top of it. The mortar compresses as an effect of the pressure exerted on it – it is to say: the air bubbles in the mortar compress, since all other components are considered incompressible (at least, in comparison to the air)

Method A. - Only applicable to mortars with less than 20% air content.

SEE ALSO 12350-7 for the large scale version for concrete.

2.3.1. Procedure for density and air content

2.3.1.1. Preliminary steps:

1. Write down the T (°C) and RH (%) from the weather station to the right of the mixing machine.

2. APPARATUS

    a. Mixer bowl (mixing)

    b. Sand (mixing)

    c. Cement (mixing)

    d. Measuring cylinder (scale)

    e. water bottle (scale)

    f. Measuring vessel

    g. Scoop

    h. Tamper

    i. Big scale
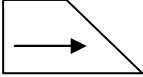
j.   Big ruler

2.3.1.2. Mixing as specified in paragraph 1.1.1.2

2.3.1.3. Procedure for density:

1. Humidify the interior of the mould and the glass plate with a humid tissue

2. Weigh the mould with the glass plate on top (next to the big scale)

3. Fill in the mould

    a. Using the little scoop fill 1/4 of the mould with the fresh mortar

        i.   Compact the mortar using the tamper

        ii.   Repeat

    (The norm states an alternative way using the vibrating table)

    b. Use the big "ruler" to level the mortar in this direction

    c. Clean the edge with humid tissue or finger and make sure there is no mortar outside

    d. Use the glass plate to confirm the mould is correctly filled up - if otherwise remember to clean the plate between each try. You have to see the rim, establish contact between plate and mortar on the whole surface (without major bubbles) and is not movable

3. Weigh the mould full of mortar with the plate on top- The volume of the mould is 1l!!

4. Turn off the scale

2.3.1.4. Procedure for air content:

1. Take the plate off and clean the rim with moist paper. If needed, add some extra mortar (in case too much stuck to the glass plate, for example)

2. Check that the edges of the cover assembly are clean and the two valves are closed (perpendicular to the pipe)

3. Fix the container to the cover assembly, closing both clamps at the same time.

4. Check the % is at the highest point- press the green button

5. open both valves

6. With the help of another person put water through one of the pipes (you have to push the tube downwards for this to happen)

7. When water starts to come out through the other pipe, tilt the device so the valve through which the water exits is vertical.

8. When no more air bubbles come out, close both valves simultaneously while still pumping water.

9. Pump air into the device with the red piston until the indicator goes past the red line

10. Use the black button to place the indicator in the middle of the red line, tap the display to ensure a stable measurement.

11. Press the green button for 10s- check that the indicator stays stable (if it doesn't then there is a leak and you cannot take the measurement down)- WRITE DOWN THE RESULT

12. Open one of the valves covering the pipe with a tissue as some water will come out

13. Press the green button (test) to reduce the pressure

14. Open the device

    a. Clean the rim of the cover assembly and dry it

15. Clean

    a. First use tissue/trowel to remove all possible solid mortar

    b. Clean with water in sink

    c. REMEMBER to leave sink clean

2.4. EN 196-9: Methods of testing cement – Part 9: Heat of hydration – Semi-adiabatic method

link to standard

Method of measuring the heat of hydration of cements by means of semi-adiabatic calorimetry, also known as the Langavant method. The aim of the test is the continuous measurement of the temperature released during the hydration of the mortar for the first few days (a standardized test is 7 days). With this temperature evolution, we will be able to calculate the heat of hydration, <u>expressed in joules per gram of cement</u>.

The semi-adiabatic method consists of introducing a sample of freshly made mortar into a calorimeter in order to determine the quantity of heat emitted in accordance with the development of the temperature. At a given point in time the heat of hydration of the cement contained in the sample is equal to the sum of the heat accumulated in the calorimeter (mortar box, mortar and chamber) and the heat lost into the ambient atmosphere throughout the period of the test.

The temperature rise of the mortar is compared with the temperature of a totally hydrated mortar sample in a reference calorimeter. The temperature rise depends mainly on the characteristics of the cement and is normally between 10 K and 50 K.

2.4.1. Procedure

2.4.1.1. Preliminary steps:

1. Write down the date, T (°C) and RH (%) from the weather station to the right of the mixing machine.

2. APPARATUS

    a. Prepare the vibrating table

        iii. Turn on the red switch

        iv. Try if it works (white and then red button)

        v. Check the time setting is on 1.5 (15s)

    b. Hammer (mixing)

    c. Mixer bowl (mixing)

    d. Sand (mixing)

    e. Cement (mixing)

    f. Mortar box (stored behind the column where the measuring cylinders) (scale)

    g. Measuring cylinder (scale)

      h.   Water bottle (scale)

      i.   Jug (sink)

      j.   Temperature probe (sink)

3. Weigh the mortar box and write value in EMPTY (bottom left of the TEST SHEET)

4. Take the mortar box without the lid and place it on the scale- TARE

5. Prepare the oil (in this case SIKA-DECOFFRE) (other side of the scale)

      k.   Put some in beaker

      l.   Take around 2.5-3 ml with the syringe

      m.   LEAVE IT NEXT TO THE SCALE

6. COMPUTER – next to the coffee table

      a.   Turn on computer (langavant-ConcretE)

      b.   Desktop -> Test 2011-SA (top right hand corner) – check there are no .PLW on root.

      c.   Create new folder: Desktop -> Test 2011-SA (top right hand corner) ->Finalised (EG: Autres-> T7-A-SA) use short names and avoid spaces

      d.   Start -> programs -> pico tech -> pico technology

            i.   Normal

            ii.   Check channel 1 (measuring) and channel 2 (reference) are in a 1K order.

           iii.   New file – select Test 2011-SA - file name (EG. T7-A-SA-A1.PLW)

2.4.1.2. Mixing as specified in paragraph 1.1.1.2

2.4.1.3. Procedure:

1. Immediately after mixing weigh (1 575 ± 1) g of mortar into the box, every couple of if necessary hit the box to try to compact the mortar- clean the sides of the top rim with a tissue

2. Place the box on the vibrating table (HOLD IT DOWN) and turn it on.

3. Place the lid on the box and hammer it in place by hitting the rims- use the narrow part of the hammer to push the top as if to open the rims.

4. Weigh the mortar box full- write it down in the FULL box of the TEST SHEET.

5. Insert the oil in the little pipe of the lid.

6. Weigh the mortar box full + oil - write it down in the FULL+OIL box of the TEST SHEET.

7. Wait until you have reached the time for putting the mortar box in the calorimeter (do NOT put it in before time)

8. Use the hook next to the calorimeter to place the mortar box inside the Dewar flask in CHANNEL 1 – be careful the flask is very fragile and can be dangerous if it breaks.

9. Place the lid and screws (tighten).

10. Insert the PT 100 (Platinum resistance thermometer) – push it down to verify the correct placement and tighten the top opening.

11. Go to the computer and press start recording – write down the START TIME or the DELAY of the TEST SHEET.

12. Write down any remarks in the remarks section

13. Clean

    a. First use tissue to remove all possible solid mortar

    b. Clean with water in sink

    c. REMEMBER to leave sink clean

14. Turn off scale and cover

2.4.1.4. Data saving:

1. COMPUTER – next to the coffee table

    a. Press view graph

    b. Stop the test when OK

    c. Views per sheet and press the button of a blue box to select all data.

    d. Write to disk -> Nuria test -> *.txt

    e. Start -> new office document- excel

    f. Open file -> *.txt -> next… next

    g. Rename the tab to "data", check we have values for all the data (if there is no value just put the precedent)

    h. Fill in our weighing values of our test sheet in the following way:

        i. D4 = EMPTY

        ii. E4= FULL

iii. <u>F4= Delay</u>

i. Save as <u>A.xls/ B.xls/ C.xls</u>

j. Copy the files in the folder in the computer (*.plw, *.xls, *.txt)

2. Go to calorimeter- CHANNEL 1

   a. Take off the lid, there will be a Plexiglas disk left behind – take it and put it back at the bottom of the lid

   b. Place the lid on the screws so the PT-100 does not touch the table

   c. Use the hook to take the mortar box out- CAREFUL, it is hot!

   d. Weigh the mortar box - write it down in the END+OIL box of the TEST SHEET.

      i. The standard states that if the difference between FULL+OIL and End+oil is greater than 2g the experiment is not valid.

   e. Label the mortar box and put it under the table.

2.4.1.5. Data treatment:

1. Copy the folder *-SA to concryd\SA*

2. Open matlab- execute run Mainmenu in command window

3. Click on Semi Adiabatic-> treatment

a. Click browse and select folder

b. Choose treatment option:

    i. with maturity adaptation (considers effect of temperature on mortar's properties)- will require activation energy (for OPC 33.5 kJ/mol)- or without maturity adaptation-> click on TREAT-> SAVE

    ii. Autotreatment will run "without maturity adaptation" and "maturity adaptation" scripts with activation energy 33.5kJ/mol.

c. Hydration rate

    i. EXPLANATION ON HYDRATION RATE

4. If you go back to the semi adiabatic and click on RESULTS you can view the results with the different treatments.

Ultrasound

2.4.2. Procedure

2.4.2.1. Preliminary steps:

1. Write down the T (°C) and RH (%) from the weather station to the right of the mixing machine.

2. APPARATUS

   a. Mixer bowl (mixing)

   b. Sand (mixing)

   c. Cement (mixing)

   d. Measuring cylinder (scale)

   e. Distilled water (scale)

   f. Jug (sink)

   g. Temperature probe (sink)

   h. 4 Plexiglas lids (IP8)

   i. Silicon lubricant (IP8)

   j. Little scoop (IP8)

   k. Tamper (IP8)

   l. Silicon (IP8)

   m. Duct tape

3. Setup sensors on molds and take down the channel number for each mixture

4. COMPUTER – next to the IP8

   a. Turn on computer (administrator-ConcretE)

   b. Create new folder: Desktop -> Test 2011- IP8 (top right hand corner) ->Finalised (EG: SP-> T7-A-IP8)

   c. Desktop -> Test 2011- IP8 - overwrite the files with our new names (EG: T7-A-IP8-A, T7-A-IP8-B, T7-A-IP8-C, T7-A-IP8-D), leave

   d. IP8 program (bottom of desktop)

      i. Functionality check

1. Top tab- TEST

2. Press channel n° (1,2,3,7) time around 140μs (if you already greased it, it should be around170-190μs)

3. Check probes are OK (screwed correctly)

5. <u>Grease all the interior surface of the sensors with the silicon spray</u>

2.4.2.2. Mixing as specified in paragraph 1.1.1.2

2.4.2.3. Procedure:

1. Go to IP8

2. Fill the moulds

   a. Using the little scoop fill ½ of the mould with the fresh mortar

      i. Using the tamper compact the mortar (10 times).

   b. Using the little scoop fill the mould completely with fresh mortar

      i. Using the tamper compact the mortar (10 times).

   c. <u>Try to not fill the moulds more than level with the mould surface</u>.

   d. Tap the sides of the moulds gently with the tamper.

3. COMPUTER

   a. Click on Start for the corresponding channel- try not to have two channels going at the same time

4. Write down the DELAY time in the test sheet

5. Use finger to smoothen the surface and remove any mortar rests from the top surface of the mould.

6. Draw a circle with the silicon on the mould top

7. Place the Plexiglas lids (push and turn to ensure a good insulation) without tape

8. Close the holes with tape

9. Check the computer is taking the measurement OK and press the LCD-OFF.

10. Clean

   a. First use tissue to remove all possible solid mortar

   b. Clean with water in sink

  c. REMEMBER to leave sink clean.

2.4.2.4. Data saving:

1. FRESHCON COMPUTER – next to IP8 device

  a. Choose channel 1 -> STOP -> stop and save (yellow)

    i. Repeat this with channels 2, 3 and 7

  b. Copy the files in the folder in the computer Desktop -> Test 2011- IP8 (top right hand corner) ->Finalized (EG: Autres-> T7-A-IP8 -> T7-A-IP8-A, T7-A-IP8-B, T7-A-IP8-C, T7-A-IP8-D)

2. Go to sensors

  a. Take off Plexiglas lid and scrape off the silicon with a palette knife and with the scrubber

  b. Wiggle the probes to detach them from the mortar

  c. Twist the probes following the arrows and take them out of the moulds- clean the top metallic part with the scrubber (this has to be really clean) place them in the wooden stand:

| S1 | S2 | S3 | S4 | | R1 | R2 | R3 | R4 | |
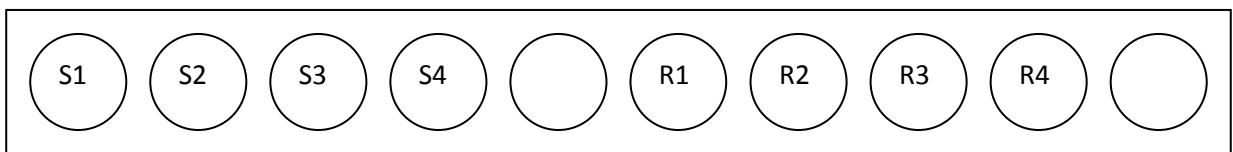
  d. Take the mortar out of the mould and place it in the same spot

  e. Take the calliper out of the black cupboard

    ii. To reset push the on/off button

    iii. Measure the distance between the centre of the sensors

  f. Mark the samples with the correspondent name (e.g. T7-A-G) and store them under the table

  g. Clean the working area

  h. Clean the moulds

    a. Check for any fissures in the moulds which could influence the results.

    i. Clean any remains in the horizontal holes with the fingers and with the rounded palette knife and the rim with edgy palette knife

    ii. Take silicon off the top, push the metal rods down (every 20 times take them out and clean them with tissue)

    iii. Clean the outside and inside with tissue

  i. Place the moulds in place, put the probes back on and organize the cables parallel to each other and spaced out.

2.4.2.5. Data treatment:

1. Copy the folder *-IP8 to concryd\IP8*

2. Open the IPV8 program

    a. Click on analysis-> select the files

    b. Click on "to .xls"

    c. Name the file data.xls

        i. For each sheet enter the following data:

            1. E4- Distance

            2. H4- Delay time

        ii. check you have the same number of data (cell E6 will tell you the number of measurements) for all and delete last values were necessary

        iii. Check all the cells have info

3. Open MATLAB- execute run Mainmenu in command window

4. Click on IP8-> treatment
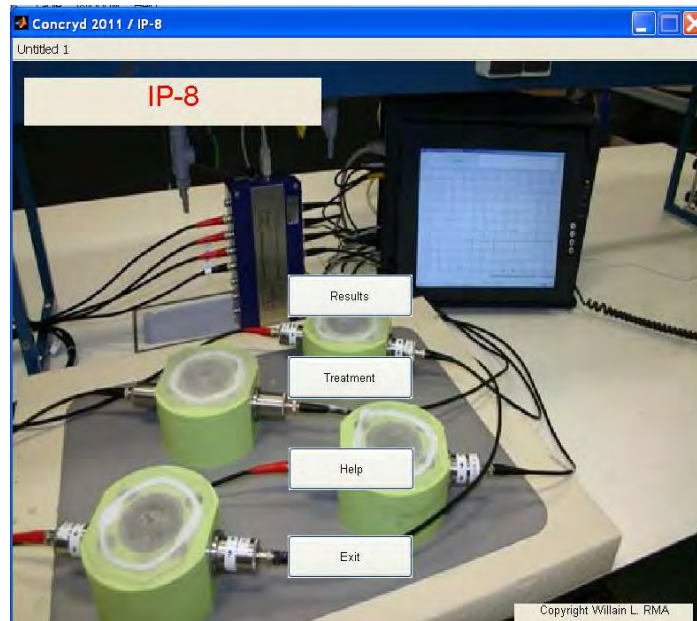
a. Click browse and select folder

b. CORRECT-> select channel and edit the values DO NOT COPY PASTE

    i. Press correct in the middle

    ii. If you screwed up you can select the channel and click on reset

    iii. SAVE and BACK

c. Click on REFRESH to get the modifications

d. Deselect individual curve treatment and mean curve treatment and press on automatic treatment- do not do anything else with MATLAB at the same time- this way we get the results for all the options.

    i. Two study options:

        1. Individual curve- each line is studied separately

        2. Mean curve- take the mean for each point

    ii. Three different curve fitting options

        3. Multilogistic

        4. Polyfit

        5. Spline

e. It will show a warning then EXIT

5. Click on IP8-> results

6. Take results into the excel summary file.

2.5. EN 196-3: Methods of testing cement- Part3: Determination of setting times and soundness. (Vicat)

link to standard

Cement paste of standard consistence has a specified resistance to penetration by a plunger. The setting time is determined by observing the penetration of a needle into cement paste until it reaches a specified value.

2.5.1. Procedure

2.5.1.1. Preliminary steps:

1. Write down the date, T (°C) and RH (%) from the weather station to the right of the mixing machine.

2. APPARATUS

   a. Mixer bowl (mixing)

   b. Cement (mixing)

   c. Measuring cylinder (scale)

   d. Distilled water (scale)

   e. Jug (sink)

   f. Temperature probe (sink)

   g. Little scoop (VICAT)

   h. Tamper (VICAT)

   i. Oil (VICAT)

   j. Silicon (VICAT)

   k. Vicat conical mould (VICAT)

   l. Vicat plate (VICAT)

3. Preparations

   a. Prepare the mould

      i. Put as little as possible silicon on the narrow side, centre it on the mould and push and turn

      ii. Remove any remains of silicon in the inside of the mould with the help of an ear cotton

      iii. Humidify the inside with some oil

b. Clean the needle.

c. NEEDLE CALIBRATION

      i. Place the mould in place in the device, untight the needle screw and put a small piece of paper in the mould just bellow the needle

      ii. INSTRUMENTS MENU -> NEEDLE CALIBRATION

      iii. Check the needle gets to the top of the plate without scratching it (this is why you put the paper), if otherwise use the screws with the hexagonal inserts so the needle just skims the glass without hitting it- tighten the needle screw.

      iv. OK

d. INSTRUMENTS MENU -> RESET POSITIONING

2.5.1.2. Mixing as specified in paragraph 1.1.1.2<u>: cement paste!!</u>

This standard is defined for cement paste only- so an equivalent cement paste composition should be used!

2.5.1.3. Procedure:

1. Using the little scoop fill ½ of the mould with the fresh cement paste

    a. Using the machine in "next" to the SA vibrate it 15 s

      a. Turn the time wheel until it turns on and the other way around

2. Using the little scoop fill ½ of the sensors with the cement paste

    a. Using the machine in "next" to the SA vibrate it 15 s

      i. Turn the time wheel until it turns on and the other way around

3. Position the mould and fill the sides of the mould with water to a depth of at least 5 mm over the surface of the cement paste.

4. Go to TEST EXECUTION

    a. Test number- name

    b. Kind of test- EN (for more than 4h setting time, otherwise EN-196-3 2005)

    C. Specimen time- time of water addition (this is used as the reference time) <u>START DELAY TAKES AS REFERENCE THE WHEN THE MACHINE IS TURNED ON.</u>

With **TIME FIRST PENET.**, the start time for the test can be set. **(NB. Check the machine clock has been set or consult the paragraph menu options and set the time and date).**
As an alternative to the above-mentioned function, which allows a time delay of the test at a defined time, with the **START DELAY** function it is possible to set a time delay for the start of the test from 0 to 999 minutes. One function automatically excludes the other.
The specimen time function memorizes the preparation start time of the mix to be tested.

ATTENTION	The benchmark SPECIMEN TIME is extremely important because it corresponds to the correct time to consider as test time and it corresponds to the mixing time of the water and the mixture. Based on the judgement of the operator, the Vicatronic appliance visualises the time taken to prepare the mixture (SPECIMEN TIME) or the time taken from the start of the machine.

    d.   Time type- FIXED

FIXED, ZONES, THRESHOLD, COMBINED, MANUAL
The **FIXED** modes, sets an interval between one probing and another in a constant and repetitive manner of the set interval (e.g. 10 minutes) with a range between 0.5:999 minutes (30 seconds : 16.65 hours).
The **ZONES** mode divides the test cycle penetrations set in penetration phases with different interval times for every phase. There are 5 different phases available. A programming example follows:

After having selected **INTERVAL TYPE** and **ZONES** and confirmed the **START OF SETTING READING** (YES or NO) if the test profile ASTM has been selected, which consists of 41 penetrations, the display shows the acronym

ZONES

```
ID              TIME [m]
41       o           1
41       o           1
41       o           1
01
```

    e.   Final setting-> NO
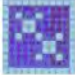
    f.   Confirm- Confirm

2.5.1.4. Data saving:

1.   Start computer next to stress machine (User- ConcretE)

    a.   Start the VicatWin program.

2.   Go to machine- FILE TEST

    a.   Used to delete all the archive test

    b.   for obsolete data in memory to be deleted. By selecting the required test number and activating the suitable control memory space will be freed up

    c.   (DATA) gives the numerical data for the selected test and also makes the menu run so the settings can be viewed again

    d.   (MEASURES) shows the test graphics. The display shows the probing sequences, as they would appear on a traditional pen tracing vicat. By pressing the knob one enters the graphic and by running the highlighted cursor the data can be viewed (time P-I-F, penetration number, penetration size) on any probing.

        i.   P- time from water addition RED LINE IN COMPUTER

        ii.   I- from test start YELLOW LINE IN COMPUTER

        iii.   F- time till end
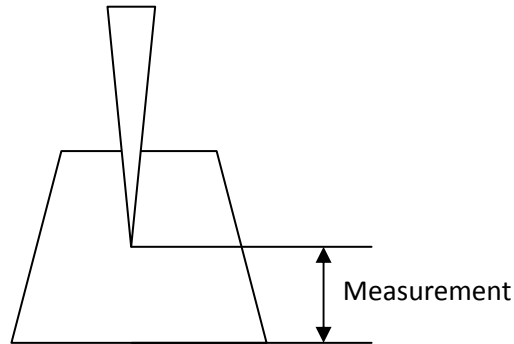
Measurement

    iv. The measurement must be around 3-9mm for setting time.

e. (COMMUNICATE) the data transmission is activated on the PC via the RS232 port (see photo1 ref. Z), the data is transferred to the PC and can be managed via (MS HYPER TERMINAL) or by means of the VICAT-WIN or VICAT- NET software.

    i. Confirm serial -> communication complete

    ii. Go to computer

        1. options-> port COM 2

        2. option->chart-> scale X-40

        3. FOR SETTING measurement =3-5mm

        4. SAVE as txt

f. activates the thermal printer on the Vicatronic with the option of reduced printing (paper saver) or complete print

g. Go back to general menu and turn off

2.5.1.5. Data treatment:

7. Copy the folder *-vicat to concryd\Vicat*

8. Open the .txt with excel

    d. Rename the sheet to data

    e. Save as <u>A/B/C/D.xls</u> and CLOSE

9. Open MATLAB- open Vicat.m

    h. For dname put the folder of the file you want to treat in the form Vicat\series\mixture

    i. Step=0;

        i. Press on run- plot for all the results can be seen- decide on what data is interesting

ii. Open A/B/C/D.xls and

iii. To take outliers just delete de corresponding lines in A30:C55

j. Step=1;

    i. Press on run- plot for all the results on logarithmic scale with interpolation line

    ii. To take outliers just delete de corresponding lines in A30:C55

    iii. Repeat this until you are satisfied

k. Step=2;

    i. Press on run- plot for all the results with interpolation line and results are saved.

2.6. ASTM C403: Standard test method for time of setting of concrete mixtures by penetration resistance.

link to standard

This test method covers the determination of the time of setting of concrete, by means of penetration resistance measurements on mortar. The mortar is placed in a container and stored at a specified ambient temperature. At regular time intervals, the resistance of the mortar to penetration is measured. From a plot of penetration resistance vs elapsed time, the times of initial and final retting are determined.

Stadard specifies the depth of the mortar should be 150mm, however, and because each mixing batch will only prove about 4 cm depth, we used 8 cm mortar depth by mixing two batches.

2.6.1. Procedure

2.6.1.1. Preliminary steps:

1. Write down the date, T (°C) and RH (%) from the weather station to the right of the mixing machine.

2. Turn on the vibrating table

3. APPARATUS

    a. Mixer bowl (mixing)

    b. Cement (mixing)

    c. Measuring cylinder (scale)

    d. Distilled water (scale)

    e. Jug (sink)

    f. Temperature probe (sink)

    g. Little scoop (mixing)

    h. Container (mixing)

    i. Pipette (Pen)

    j. Glass panel (Pen)

2.6.1.2. Mixing as specified in paragraph 1.1.1.2

2.6.1.3. Procedure:

5. Two batches will have to be mixed together in the lowest possible fixed time- 2 min slow mixing.

6. Using the little scoop fill the container with the fresh mortar to the line

    b. Compact the sample using the vibrating table

    c. Some space between the mortar surface and the top edge should be provided for the collection and removal of bleed water (the standard specifies13 mm)

7. Keep the specimens covered with the glass panel and humid tissue at all possible times

8. Penetration:

    a. Remove bleed water from the surface. Fort his tilt the specimen to an angle of about 10˚ from the horizontal by placing a block under one side 2min prior to the removal of the water and then remove it with the help of the pipette.

    b. Insert a needle of appropriate size- Record the type of needle used.

    c. Gradually and uniformly (10s) apply a vertical force downward until the mark on the needle is reached.

    d. Record the force required to produce the penetration and the time of application.

    e. Take out the needle and clean.

    f. For subsequent penetration the clear distance between needle impressions shall be at least two diameters of the needle but not less than 15 mm. The clear distance between any needle impression and the side of the container shall be 25 mm.

    g. Mould should be penetrated in the following order
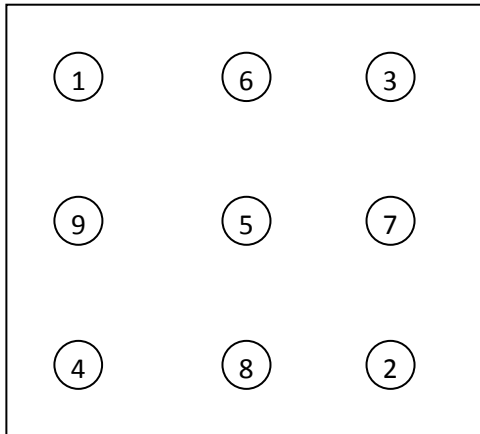
9. Recommendations from the standard- REMEMBER you need results in the range 400-4000:

   a. Make penetration tests at hourly intervals for normal mixtures and normal temperatures, the initial test being made after an elapsed time of 3 to 4 hours. For accelerated mixtures or high temperatures, it maybe advisable to make the initial test after an elapsed time of 1 or 2 hours and subsequent tests at ½ hour intervals. For low-temperature conditions or retarded concrete mixtures, the initial penetration test maybe deferred for an elapsed time of 4 to 6 hours and perhaps longer. Subsequent tests maybe made at intervals of 1 hour unless the rate of increase in penetration resistance indicates that shorter intervals are desirable.

   b. Not less than six penetration resistance determinations shall be made in each rate of hardening test. And the time intervals between penetration resistance determinations shall be such as to give a satisfactory rate of hardening curve, as indicated by equally spaced points. Continue the test until one penetration resistance of at least 4000 psi (27.6 MN/m2) is reached.

2.6.1.4. Data Treatment:

1. Input the data into the <u>excel file of the series</u>

2. Open *\concryd\penet\generate.xls

   a. Input the series file and the mixture short name

   b. Click on just do it

3. Run Penetrometer.m and open GUI

4. Click on browse and select folder - Direct Fitting of a power function is used $PR=ct^d$.

      ii. PR Penetration resistance

      iii. T elapsed time

            iv.   c and d regression constants

    l.   Verify that the data obey this relationships by verifying the correlation coefficient after removal of outliers is greater than 0.98.

5.   If any outliers present simply open data.xls/ * and delete from H5:I14

3.   The variation of the results should not exceed 16% of the average (from standard).

2.7. Vacuum

Air humidity can start the hydration reactions in cement; to avoid this the cement is packed in vacuum bags. This procedure refers to 450g bags, lengths of the bags should be adjusted if other quantities want to be packed.

2.7.1. Procedure

2.7.1.1. Preliminary steps:

1. APPARATUS

   a. Cement

   b. Little scoop

   c. Plastic bags

2.7.1.2. Procedure:

1. Cut 2 20cm long parts from the plastic roll

2. turn on the sealing device

   a. (if during the course proceedings the device is too hot, unplug it and leave it for 10 min)

3. Sealing (this has to be done on both bags, but only on one side)

   a. Place the uneven side of the bag down and position it so it goes over the brown tape (sealing ribbon) but not into the black rectangle (vacuum chamber)

   b. Push a little bit down the top with both hands and press the vacuum immediately followed by the seal button

   c. When the light stops blinking it is finished

4. Fill 1 bag with the desired quantity considering 1-2g for losses

5. Check that the border of the bag that will be sealed, is clean. Use a brush to clean if necessary

6. Vacuum + sealing (do this first on the cement bag then place the bag inside the second one and repeat)

   a. Connect the pump and leave it on for a bit to allow it to clean

   b. Place the uneven side of the bag down and position it so it goes over the sealing ribbon and into the vacuum chamber (this is easier if you leave the cement to rest on your lap)

c. Connect the pump to the rubber hose

d. Push a little bit down the top with both hands , massage if necessary for a good vacuum

e. When the vacuum is complete press vacuum and immediately afterwards seal

f. When the light stops blinking it is finished

g. Open the cylindrical valve and then uncouple the pipe

a. Clean the vacuum chamber

2.8. Vacuum Oven

2.8.1. Procedure

1. Open the door with the handle

2. Use the bottom tray (do not change the tray's positions)

    a. The upper plate prevents any water droplets to enter the vacuum valve which is placed on the top.

3. Close the door with the handle

4. Valves on the right-side:

    a. Top perpendicular to the floor

    b. Bottom parallel to the floor

5. Turn the handle on the left-hand side (general switch) so it is placed on 1

6. Press the Pompe and Marche switch on the front panel

7. Do whatever

8. Shut off Pompe and Marche switch

9. Bring the pressure GRADUALLY down

    a. Turn top valve 10° and leave until 350

    b. Turn top valve 20° and leave until 100

    c. Open valve completely

10. Turn the handle on the left-side so it is placed on 0

2.9. Packaging

2.9.1. Future improvements for packaging

- Preparation of bags (cutting and sealing) BEFORE the arrival of cement

- Packaging of different amounts (not only 450g, but multiples for one-day tests).

- Numbering the bags and putting it in the label.

- Higher control of environmental conditions- turn off water bath and cover some days before.

- Considering the series of experiments- try to pack as quickly as possible cement for the same series.

3. Other related standards

3.1. EN 1015- 11: Methods of test for mortar for masonry – Part 11: Determination of flexural and compressive strength of hardened mortar

link to standard

The flexural strength of mortar is determined by three points loading of hardened moulded mortar prism specimens to failure. The compressive strength of the mortar is determined on the two parts resulting from the flexural strength test.

The flow value of the mortar in the bulk test sample shall be determined in accordance with EN 1015-3 and reported.

The test specimens shall be prisms 160 mm x 40 mm x 40 mm. Three specimens shall be provided. For the compressive strength test, break the prisms into two halves to provide six half prisms.

Modification has suggested loading rates!

3.2. EN 12350-2: Testing fresh concrete – Part 2: Slump test

link to standard

The sample of the concrete shall be obtained in accordance with EN 12350-1:1999.

The sample shall be re-mixed using the remixing container and the square mouthed scoop before carrying out the test.

The test is only valid if it yields a true slump, this being a slump in which the concrete remains substantially intact and symmetrical as shown in Figure 1(a).

If the specimen shears, as shown in Figure 1(b), another sample shall be taken and the procedure repeated.

3.3. EN 12350-5: Testing fresh concrete – Part 5: Flow table test

link to standard

This standard specifies a method for determining the flow of fresh concrete. It is not applicable to foamed concrete or no-fines concrete, nor to concrete with maximum aggregate size exceeding 63 mm.

This test determines the consistency of fresh concrete by measuring the spread of concrete on a flat plate which is subjected to jolting.

3.4. EN 196-1: Methods of testing cement- Part1: Determination of strength.

link to standard

Compressive and flexural strength of cement mortar

4. General remarks

Mixer

- Once in a while the plunge, the rails and the hole for the beater need to be lubrified, the silicon spray can be used for this.

- Remaining powder should be cleaned (check on top of the sand funnel's tunnel).

- The plexiglass "shield" should also be cleaned once in a while.

IP8

- The moulds should be checked for fissures which could influence the results.

- Once a while the steel rods have to be cleaned.

- The tape on the sensors should be replaced when it gets too puffy.

Lab

- The following equipment has a normal-ready to use- weight of:

    o Cement and Fly ash jugs: 108.7g

    o Water cylinder: 103.3g

    o Syringe (5ml): 4.413g

- White cloth to dry things- "orange" towel for hands.

- Once a week the water bath should be filled (be careful that the hose does not wet all the lab when turned on and that the water does not overflow).

- The cement and fly ash jugs should be wiped with tissue when they have too much powder stuck to them.

- Update the computers once in a while.

C. Superplasticizer series

Mixture	Channel /Mean	Max. Infl. point (min)	1st Infl. point (min)	2nd Infl point (min)	1500 m/s thresh. (min)	2975 m/s thresh. (min)	2/3 of final vel. (min)	20% of max grad. (min)
S-000-F-100-A-0-R-0	A	234	234	617	264	543	496	756
	B	241	241	621	269	564	497	741
	C	251	251	693	293	613	554	810
	D	247	247	675	277	586	539	799
	E	234	234	605	261	513	486	700
	F	240	240	600	265	525	488	704
	Mean	**241**	**241**	**635**	**272**	**557**	**510**	**752**
	Standard dev.	**7**	**7**	**39**	**12**	**38**	**29**	**46**
S-50-F-072-A-0-R-0	A	404	404	689	394	637	623	804
	B	402	402	692	392	634	635	812
	C	400	400	684	386	624	635	858
	D	395	395	682	380	622	616	804
	E	425	425	744	412	674	675	884
	F	427	427	744	415	679	679	910
	Mean	**409**	**409**	**706**	**397**	**645**	**644**	**845**
	Standard dev.	**14**	**14**	**30**	**14**	**25**	**27**	**46**
S-75-F-072-A-0-R-0	A	532	532	856	500	773	764	1037
	B	516	516	859	490	766	739	1001
	C	521	521	841	480	751	720	963
	D	514	514	838	485	751	717	958
	E	511	511	834	484	751	738	1003
	F	504	504	834	470	747	734	975
	Mean	**516**	**516**	**844**	**485**	**757**	**735**	**990**
	Standard dev.	**10**	**10**	**11**	**10**	**10**	**17**	**30**
S-100-F-072-A-0-R-0	A	604	604	1019	538	890	908	1300
	B	612	612	1017	531	884	913	1270
	C	588	588	953	543	867	850	1081
	D	596	596	987	536	870	878	1176
	E	560	560	955	532	862	832	1137
	F	567	567	955	527	857	850	1171
	Mean	**588**	**588**	**981**	**535**	**872**	**872**	**1189**
	Standard dev.	**21**	**21**	**31**	**6**	**13**	**33**	**82**
S-125-F-072-A-0-R-0	A	987	541	987	512	888	875	1235
	B	987	523	987	499	883	887	1242
	C	1052	572	1052	539	943	959	1312
	D	1057	577	1057	531	941	941	1297
	E	1021	552	1021	534	912	908	1287
	F	1014	558	1014	529	908	902	1296
	Mean	**1020**	**554**	**1020**	**524**	**913**	**912**	**1278**
	Standard dev.	**30**	**20**	**30**	**15**	**25**	**32**	**32**
S-150-F-072-A-0-R-0	A	1109	640	1109	622	1015	1037	1371
	B	1115	627	1115	597	1016	1026	1350
	C	1068	604	1068	565	981	984	1340
	D	1067	600	1067	557	988	987	1356
	E	1125	576	1125	568	1026	1042	1417
	F	1129	592	1129	575	1022	1026	1383
	Mean	**1102**	**607**	**1102**	**581**	**1008**	**1017**	**1370**
	Standard dev.	**28**	**23**	**28**	**24**	**19**	**25**	**28**

Table C.1: *Detailed results of the p-wave transmission test for the SP series*

Mixture	Repetition /Mean	qmin+0.2*△q time (min)	qmin+1.5 J/gh time (min)	qmax time (min)
S-00-F-100-A-0-R-0	A	272	241	586
	B	289	253	578
	C	299	249	601
	Mean	**286**	**248**	**588**
	Standard dev.	**14**	**6**	**12**
S-50-F-072-A-0-R-0	A	469	330	745
	B	466	321	754
	C	470	329	756
	Mean	**468**	**327**	**751**
	Standard dev.	**2**	**5**	**6**
S-75-F-072-A-0-R-0	A	547	424	779
	B	548	425	779
	C	542	420	767
	Mean	**546**	**423**	**775**
	Standard dev.	**3**	**3**	**7**
S-100-F-072-A-0-R-0	A	683	545	909
	B	687	544	912
	C	692	552	920
	Mean	**687**	**547**	**914**
	Standard dev.	**4**	**5**	**6**
S-125-F-072-A-0-R-0	A	815	656	1041
	B	781	624	1004
	C	798	646	1021
	Mean	**798**	**642**	**1022**
	Standard dev.	**17**	**16**	**19**
S-150-F-072-A-0-R-0	A	902	614	1138
	B	934	660	1150
	C	939	661	1177
	Mean	**925**	**645**	**1155**
	Standard dev.	**20**	**27**	**20**

Table C.2: *Detailed results of the semi-adiabatic calorimetry test for the SP series*

Mixture		m	c	r	IST (min)
S-50-F-072-A-0-R-0	A	14.74	-37.56	0.978	400
	B	20.52	-52.47	0.972	395
	C	23.09	-59.19	0.979	395
	Mean				**397**
	Standard dev.				**3**
S-75-F-072-A-0-R-0	A	17.26	-46.62	0.972	560
	B	14.25	-38.43	0.978	565
	C	12.66	-33.93	0.983	555
	Mean				**560**
	Standard dev.				**5**
S-100-F-072-A-0-R-0	A	19.44	-52.52	0.977	550
	B	13.20	-35.22	0.999	535
	C	12.80	-34.41	0.953	560
	Mean				**548**
	Standard dev.				**13**
S-125-F-072-A-0-R-0	A	18.88	-51.79	0.990	610
	B	22.39	-61.17	0.986	585
	C	15.44	-42.16	0.938	605
	Mean				**600**
	Standard dev.				**13**

Table C.3: *Detailed results of the Vicat needle test for the SP series*

Mixture		m	c	r	IST (min)	FST (min)
S-50-F-072-A-0-R-0	A	5.64	-7.24	0.996	275	400
	B	5.74	-7.33	0.994	260	375
	C	5.67	-7.28	0.989	275	395
	Mean				**270**	**390**
	Standard dev.				**9**	**13**
S-75-F-072-A-0-R-0	A	8.67	-16.54	0.992	460	585
	B	8.68	-16.57	0.985	460	585
	C	9.42	-18.49	0.981	455	565
	Mean				**458**	**578**
	Standard dev.				**3**	**12**
S-100-F-072-A-0-R-0	A	8.81	-17.52	0.994	535	680
	B	8.80	-17.50	0.993	540	685
	C	8.80	-17.49	0.994	540	680
	Mean				**538**	**682**
	Standard dev.				**3**	**3**
S-125-F-072-A-0-R-0	A	7.50	-14.15	0.997	570	755
	B	7.10	-12.92	0.996	545	735
	C	7.19	-13.21	0.995	555	740
	Mean				**557**	**743**
	Standard dev.				**13**	**10**

Table C.4: *Detailed results of the penetration resistance test for the SP series*

D. Accelerator series

Mixture	Channel /Mean	Max. Infl. point (min)	1st Infl. point (min)	2nd Infl point (min)	1500 m/s thresh. (min)	2975 m/s thresh. (min)	2/3 of final vel. (min)	20% of max grad. (min)
S-100-F-072-A-0-R-0	A	604	604	1019	538	890	908	1300
	B	612	612	1017	531	884	913	1270
	C	588	588	953	543	867	850	1081
	D	596	596	987	536	870	878	1176
	E	560	560	955	532	862	832	1137
	F	567	567	955	527	857	850	1171
	Mean	**588**	**588**	**981**	**535**	**872**	**872**	**1189**
	Standard dev.	**21**	**21**	**31**	**6**	**13**	**33**	**82**
S-100-F-072-A-40-R-0	A	483	483	835	455	831	806	1196
	B	463	463	840	446	826	828	1230
	C	515	515	834	477	831	792	1160
	D	531	531	821	481	831	820	1188
	E	483	483	847	457	833	832	1219
	F	466	466	847	445	830	835	1251
	Mean	**490**	**490**	**837**	**460**	**830**	**819**	**1207**
	Standard dev.	**27**	**27**	**10**	**15**	**2**	**17**	**33**
S-100-F-072-A-100-R-0	A	248	248	680	309	703	715	1027
	B	274	274	685	311	702	705	1018
	C	249	249	629	281	653	635	910
	D	206	206	652	276	658	631	919
	E	255	255	631	293	669	663	927
	F	250	250	632	284	657	649	913
	Mean	**247**	**247**	**652**	**292**	**674**	**666**	**952**
	Standard dev.	**22**	**22**	**25**	**15**	**23**	**36**	**55**
S-100-F-072-A-200-R-0	A	175	175	467	216	580	566	581
	B	175	175	468	215	590	545	578
	C	174	174	466	217	599	575	584
	D	174	174	463	213	589	575	569
	E	171	171	493	205	584	518	560
	F	171	171	496	209	601	576	587
	Mean	**173**	**173**	**476**	**213**	**591**	**559**	**577**
	Standard dev.	**2**	**2**	**15**	**5**	**8**	**23**	**10**
S-100-F-072-A-300-R-0	A	138	138	390	173	688	561	252
	B	139	139	389	171	662	581	252
	C	136	136	395	166	727	637	245
	D	137	137	393	169	732	731	246
	E	142	142	397	175	754	740	249
	F	144	144	400	173	718	722	250
	Mean	**139**	**139**	**394**	**171**	**714**	**662**	**249**
	Standard dev.	**3**	**3**	**4**	**3**	**33**	**80**	**3**

Table D.1: *Detailed results of the p-wave transmission test for the AC series*

Mixture	Repetition /Mean	qmin+0.2*△q time (min)	qmin+1.5 J/gh time (min)	qmax time (min)
S-100-F-072-A-0-R-0	A	683	545	909
S-100-F-072-A-0-R-0	B	687	544	912
S-100-F-072-A-0-R-0	C	692	552	920
	Mean	**687**	**547**	**914**
	Standard dev.	**5**	**5**	**6**
S-100-F-072-A-40-R-0	A	567	485	803
S-100-F-072-A-40-R-0	B	568	482	805
S-100-F-072-A-40-R-0	C	566	485	807
	Mean	**567**	**484**	**805**
	Standard dev.	**1**	**2**	**2**
S-100-F-072-A-100-R-0	A	488	300	720
S-100-F-072-A-100-R-0	B	491	296	727
S-100-F-072-A-100-R-0	C	474	295	701
	Mean	**484**	**297**	**716**
	Standard dev.	**9**	**3**	**13**
S-100-F-072-A-200-R-0	A	(429)	(417)	622
S-100-F-072-A-200-R-0	B	(461)	(419)	640
S-100-F-072-A-200-R-0	C	(459)	(418)	624
	Mean	**450**	**418**	**629**
	Standard dev.	**18**	**1**	**10**
S-100-F-072-A-300-R-0	A	(355)	(200)	(468)
S-100-F-072-A-300-R-0	B	(350)	(488)	(462)
S-100-F-072-A-300-R-0	C	(362)	(440)	(464)
	Mean	**(356)**	**(464)**	**(465)**
	Standard dev.	**(6)**	**34**	**(3)**

Table D.2: *Detailed results of the semi-adiabatic calorimetry test for the AC series*

Mixture		m	c	R2	IST [min]
S-100-F-072-A-0-R-0	A	19.44	-52.52	0.977	550
	B	13.20	-35.22	0.999	535
	C	12.80	-34.41	0.953	560
	Mean				**548**
	Standard dev.				**13**
S-100-F-072-A-40-R-0	A	16.11	-42.82	0.958	510
	B	11.37	-29.88	0.977	495
	C	15.60	-41.09	0.977	480
	Mean				**495**
	Standard dev.				**15**
S-100-F-072-A-100-R-0	A	15.62	-38.68	0.937	335
	B	13.39	-32.96	0.942	330
	C	16.74	-41.63	0.974	340
	Mean				**335**
	Standard dev.				**5**
S-100-F-072-A-200-R-0	A	13.45	-31.52	0.971	250
	B	18.02	-43.18	0.992	275
	C	14.91	-35.35	0.994	265
	Mean				**263**
	Standard dev.				**13**
S-100-F-072-A-300-R-0	A	12.79	-29.03	0.987	215
	B	20.43	-46.80	0.982	215
	C	17.32	-39.20	0.986	205
	Mean				**212**
	Standard dev.				**6**

Table D.3: *Detailed results of the Vicat needle test for the AC series*

Mixture		m	c	R2	IST [min]	FST [min]
S-100-F-072-A-0-R-0	A	8.81	-18.52	0.994	535	680
	B	8.80	-18.50	0.993	540	685
	C	8.80	-18.49	0.994	540	680
	Mean				**538**	**682**
	Standard dev.				**3**	**3**
S-100-F-072-A-40-R-0	A	7.86	-15.43	0.999	465	605
	B	7.24	-13.79	0.999	465	620
	C	7.23	-13.71	0.994	460	610
	Mean				**463**	**612**
	Standard dev.				**3**	**8**
S-100-F-072-A-100-R-0	A	4.16	-4.63	0.996	275	455
	B	4.16	-4.62	0.992	280	460
	C	3.85	-3.83	0.996	270	460
	Mean				**275**	**458**
	Standard dev.				**5**	**3**
S-100-F-072-A-200-R-0	A	3.94	-3.74	0.998	230	385
	B	3.85	-3.58	0.998	235	405
	C	3.86	-3.60	0.997	235	400
	Mean				**233**	**397**
	Standard dev.				**3**	**10**
S-100-F-072-A-300-R-0	A	2.86	-1.13	0.982	215	440
	B	2.81	-0.97	0.990	205	430
	C	2.84	-1.02	0.993	205	425
	Mean				**208**	**432**
	Standard dev.				**6**	**8**

Table D.4: *Detailed results of the penetration resistance test for the AC series*

E. Analysis

E.1. Initial setting time

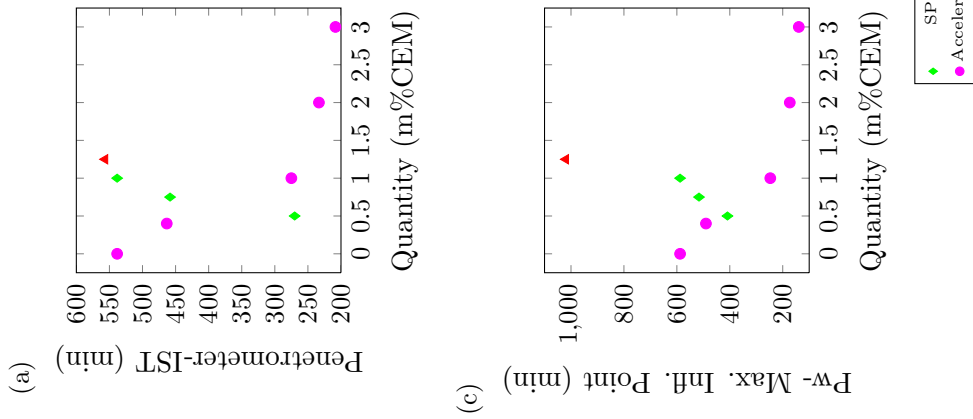### E.1.1. Penetration resistance test versus vicat needle test
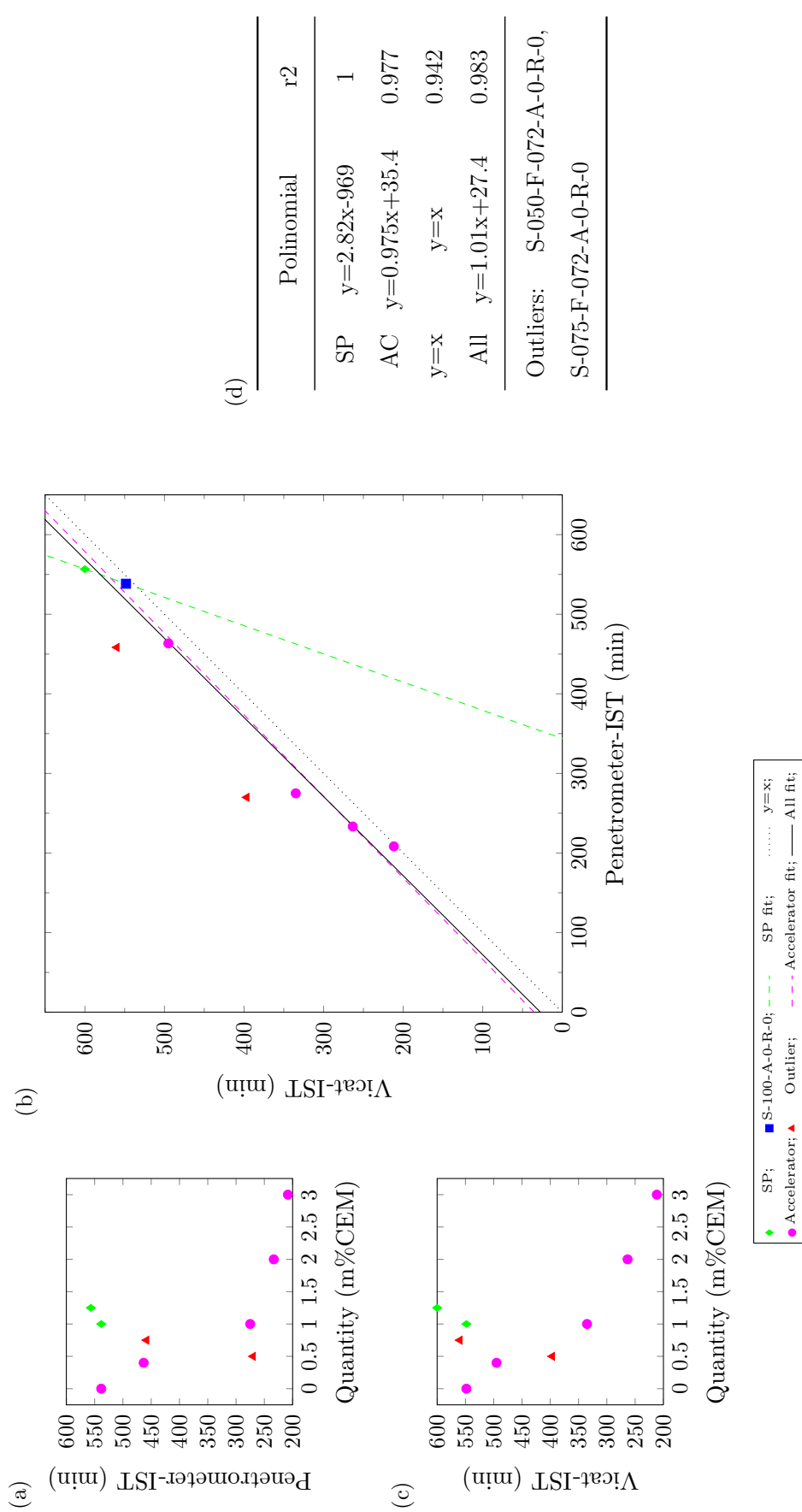
Figure E.1: *Penetrometer-IST vs Vicat-IST*

E.1.2. Penetration resistance test versus p-wave transmission test
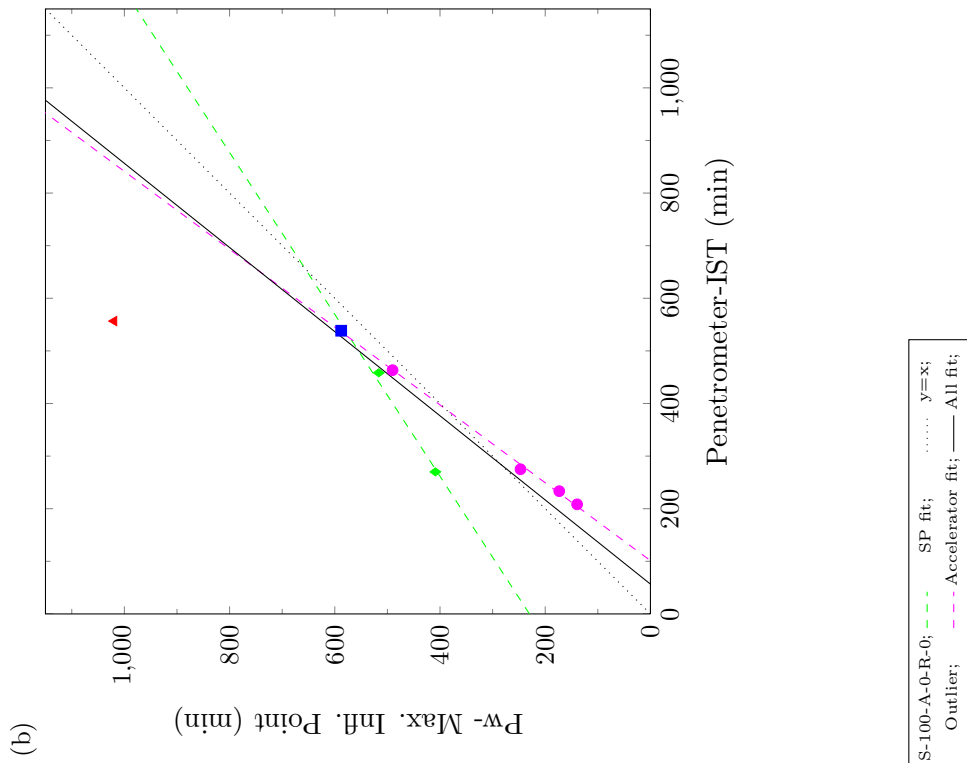
	Polinomial	r2
SP	y=0.65x+230	0.987
AC	y=1.35x-137	0.999
y=x	y=x	0.818
All	y=1.25x-70.9	0.862

Outliers: S-125-F-072-A-0-R-0

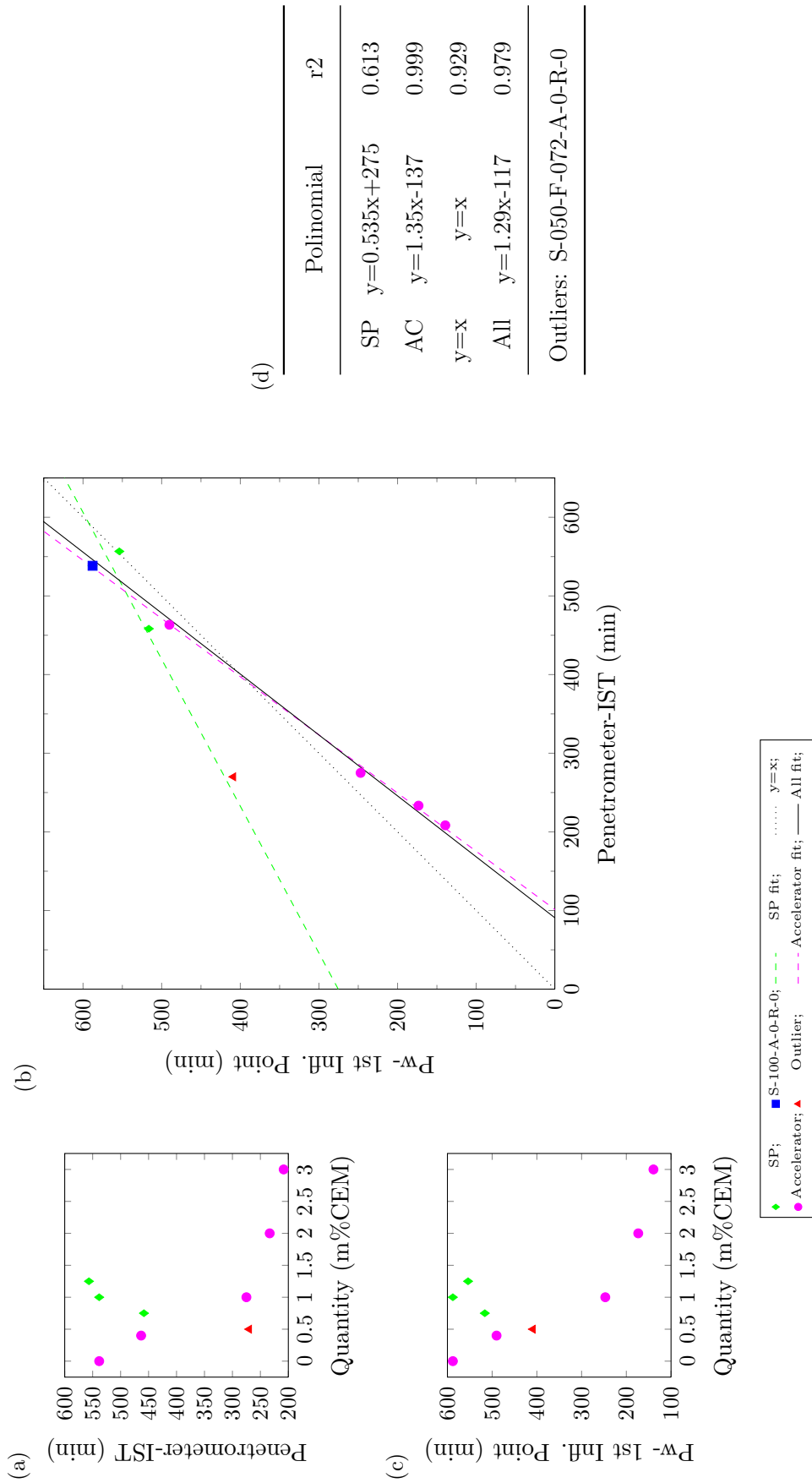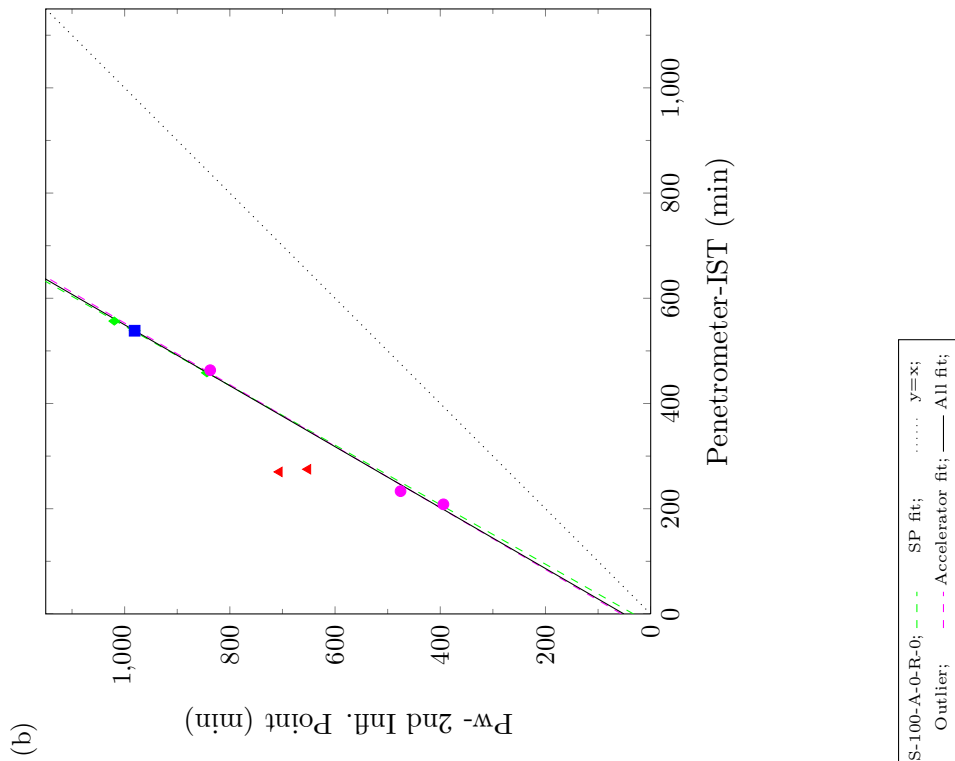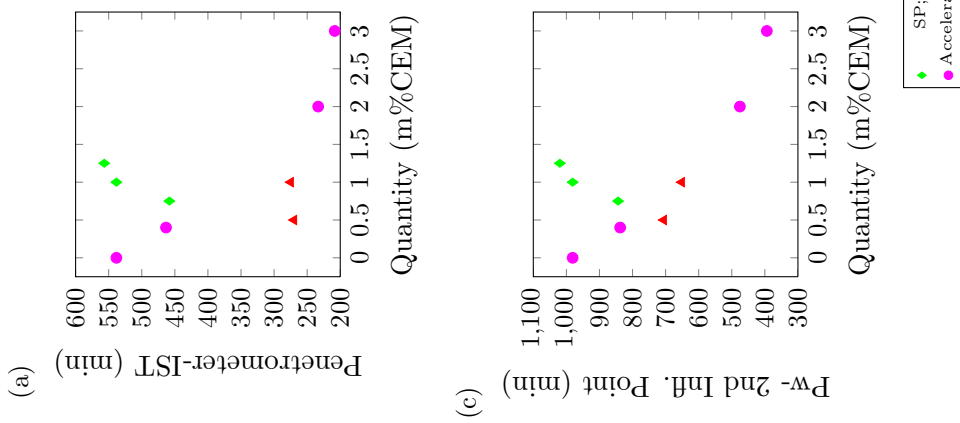**Figure E.2:** *Penetrometer-IST vs P-wave- Mortar Age at Maximum Inflection Point*

	Polinomial	r2
SP	y=0.535x+275	0.613
AC	y=1.35x-137	0.999
y=x	y=x	0.929
All	y=1.29x-117	0.979

Outliers: S-050-F-072-A-0-R-0

Figure E.3: *Penetrometer-IST vs P-wave- Mortar Age at 1st Inflection Point*

Figure E.4: *Penetrometer-IST vs P-wave- Mortar Age at 2nd Inflection Point*
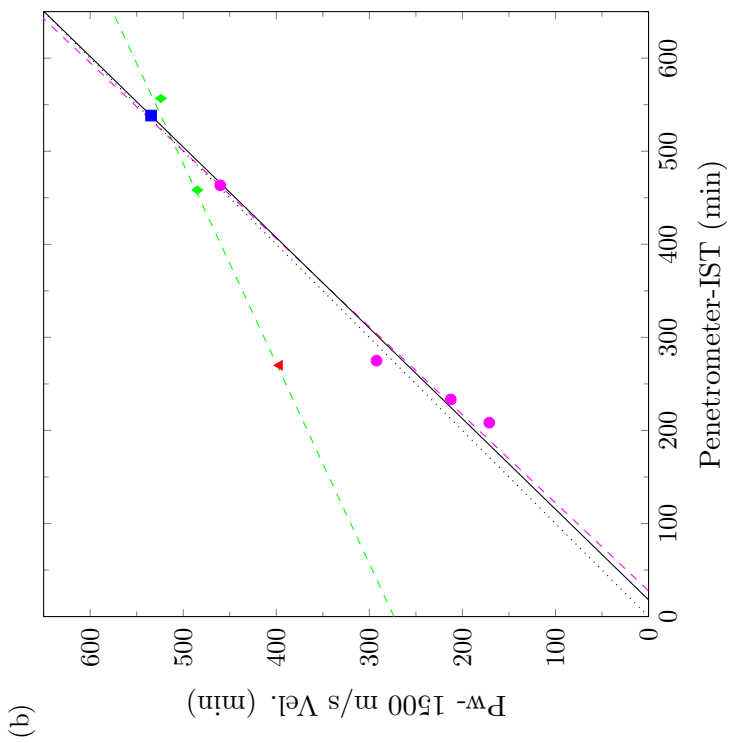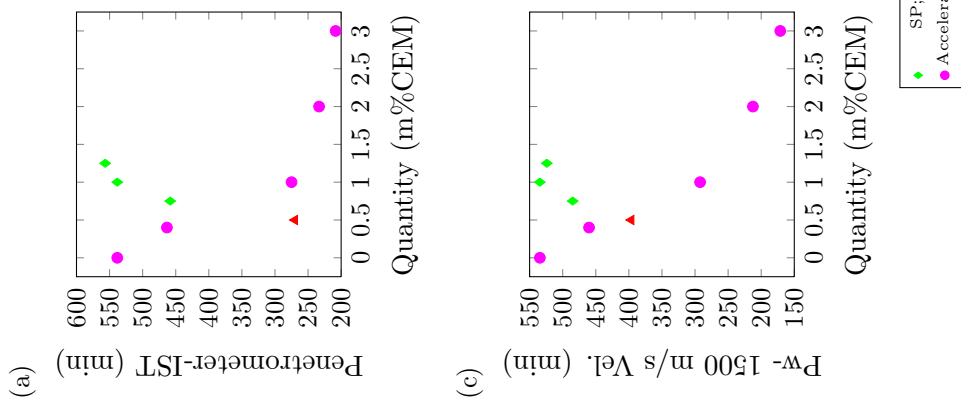
	Polinomial		r2
SP	y=1.77x+32.8		0.999
AC	y=1.71x+55.7		0.996
y=x	y=x		0
All	y=1.73x+50.9		0.997
Outliers:	S-050-F-072-A-0-R-0,		
	S-100-F-072-A-100-R-0		

	Polinomial	r2
SP	y=0.465x+274	0.864
AC	y=1.06x-29.2	0.986
y=x	y=x	0.972
All	y=1.03x-18.5	0.976
Outliers: S-050-F-072-A-0-R-0		

Figure E.5: *Penetrometer-IST vs P-wave- Mortar Age at 1500 m/s Velocity Threshold*

E.1.3. Vicat needle test test versus p-wave transmission test
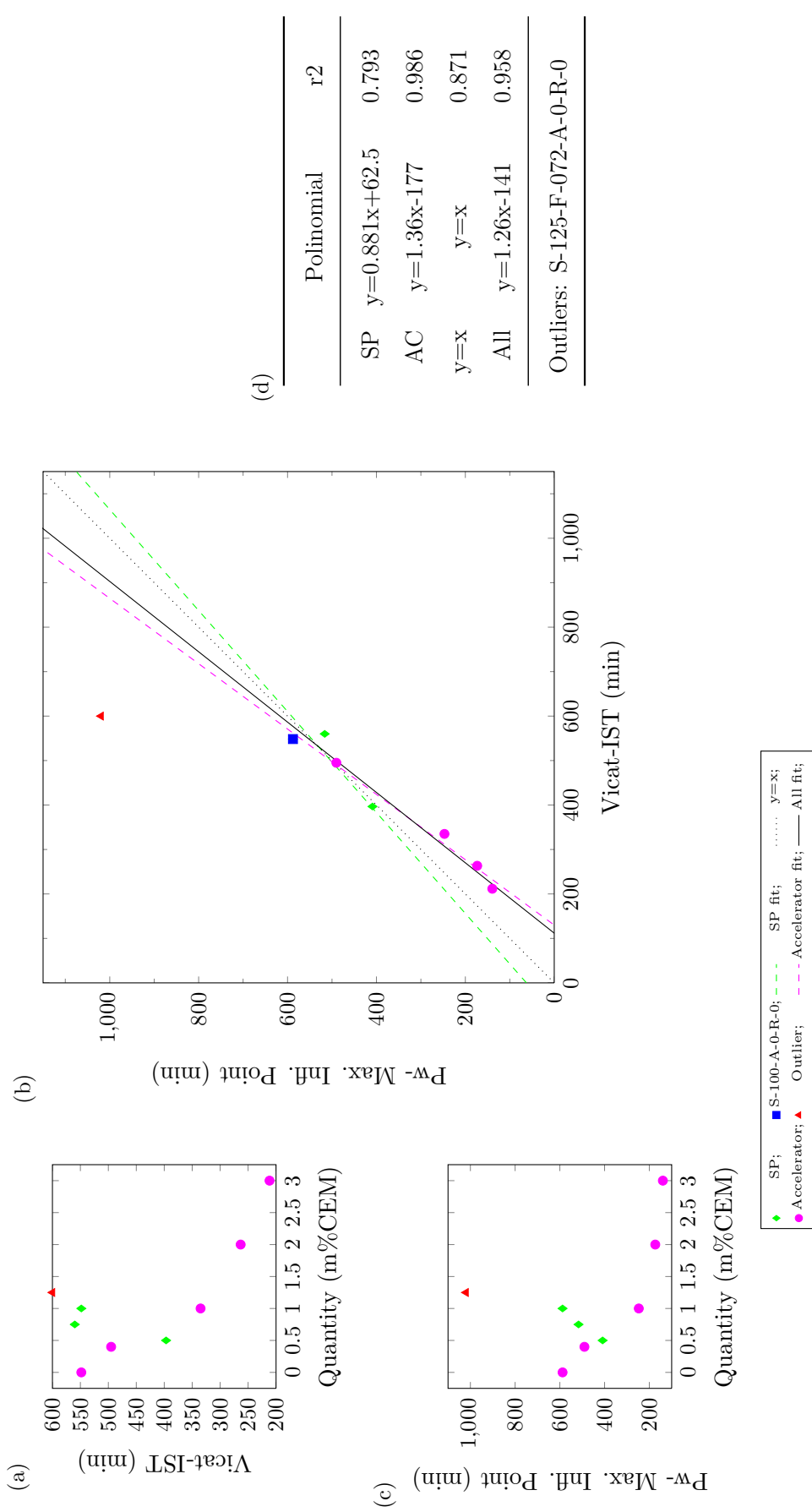
Figure E.6: *Vicat-IST vs P-wave- Mortar Age at Maximum Inflection Point*

	Polinomial	r2
SP	y=0.881x+62.5	0.793
AC	y=1.36x-177	0.986
y=x	y=x	0.871
All	y=1.26x-141	0.958

Outliers: S-125-F-072-A-0-R-0

	Polinomial	r²
SP	y=0.766x+114	0.774
AC	y=1.36x-177	0.986
	y=x	0.879
All	y=1.19x-118	0.952
Outliers:		

(d)
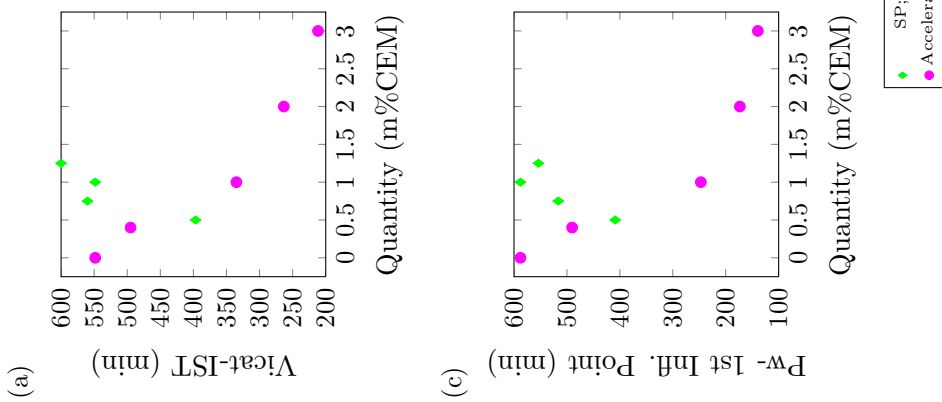
Figure E.7: *Vicat-IST vs P-wave- Mortar Age at 1st Inflection Point*
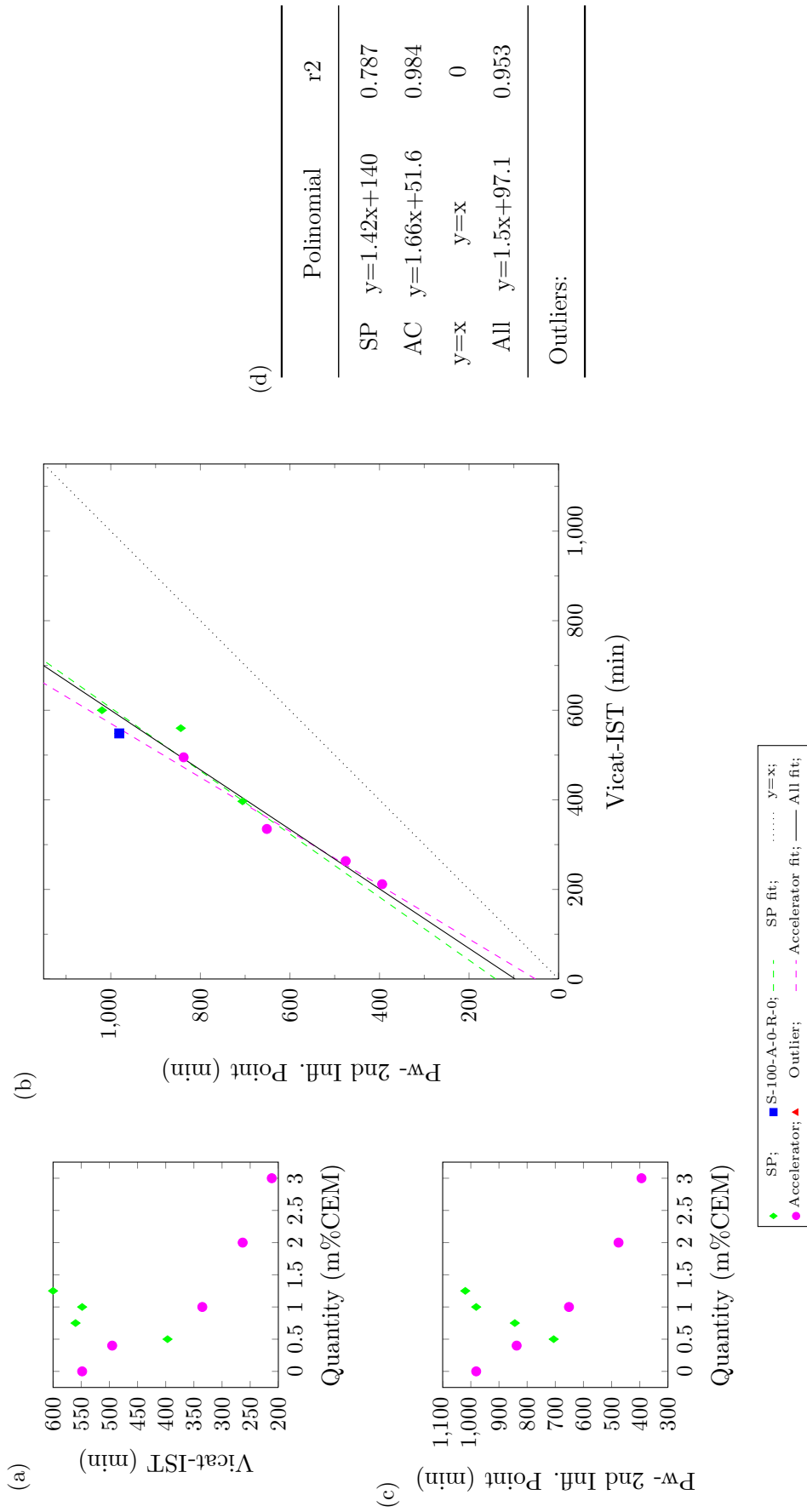
Figure E.8: *Vicat-IST vs P-wave- Mortar Age at 2nd Inflection Point*

(d)	Polinomial		r2
SP	y=1.42x+140		0.787
AC	y=1.66x+51.6		0.984
y=x	y=x		0
All	y=1.5x+97.1		0.953
Outliers:			
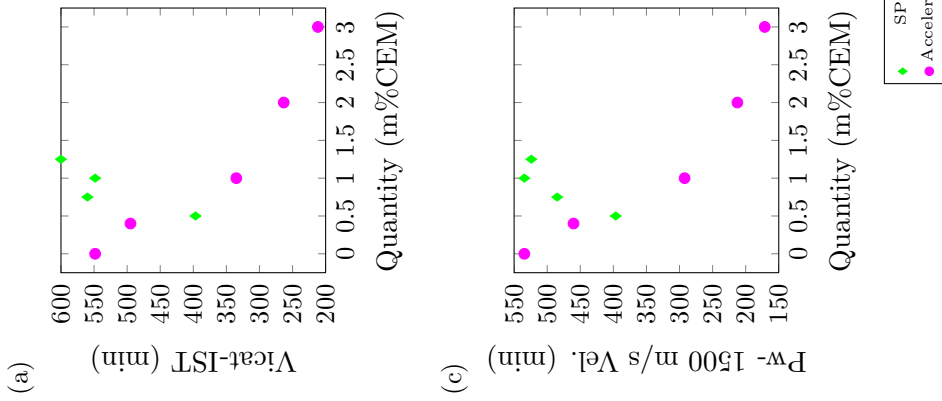
Figure E.9: *Vicat-IST vs P-wave- Mortar Age at 1500 m/s Velocity Threshold*

	Polinomial	r2
SP	y=0.647x+145	0.846
AC	y=1.08x-65.4	0.997
y=x	y=x	0.867
All	y=0.957x-23.3	0.967

Outliers:

E.1.4. Penetration resistance test versus semi-adiabatic calorimetry test
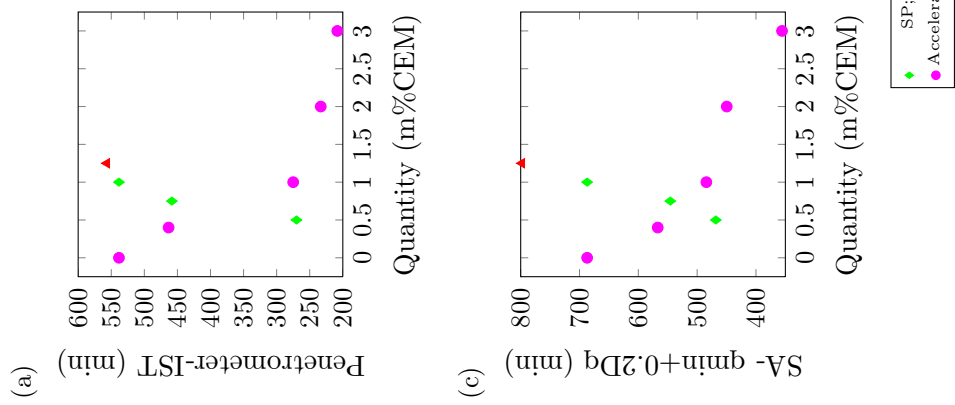
Figure E.10: *Penetrometer-IST vs Semi adiabatic- Mortar Age at qmin+0.2Dq*
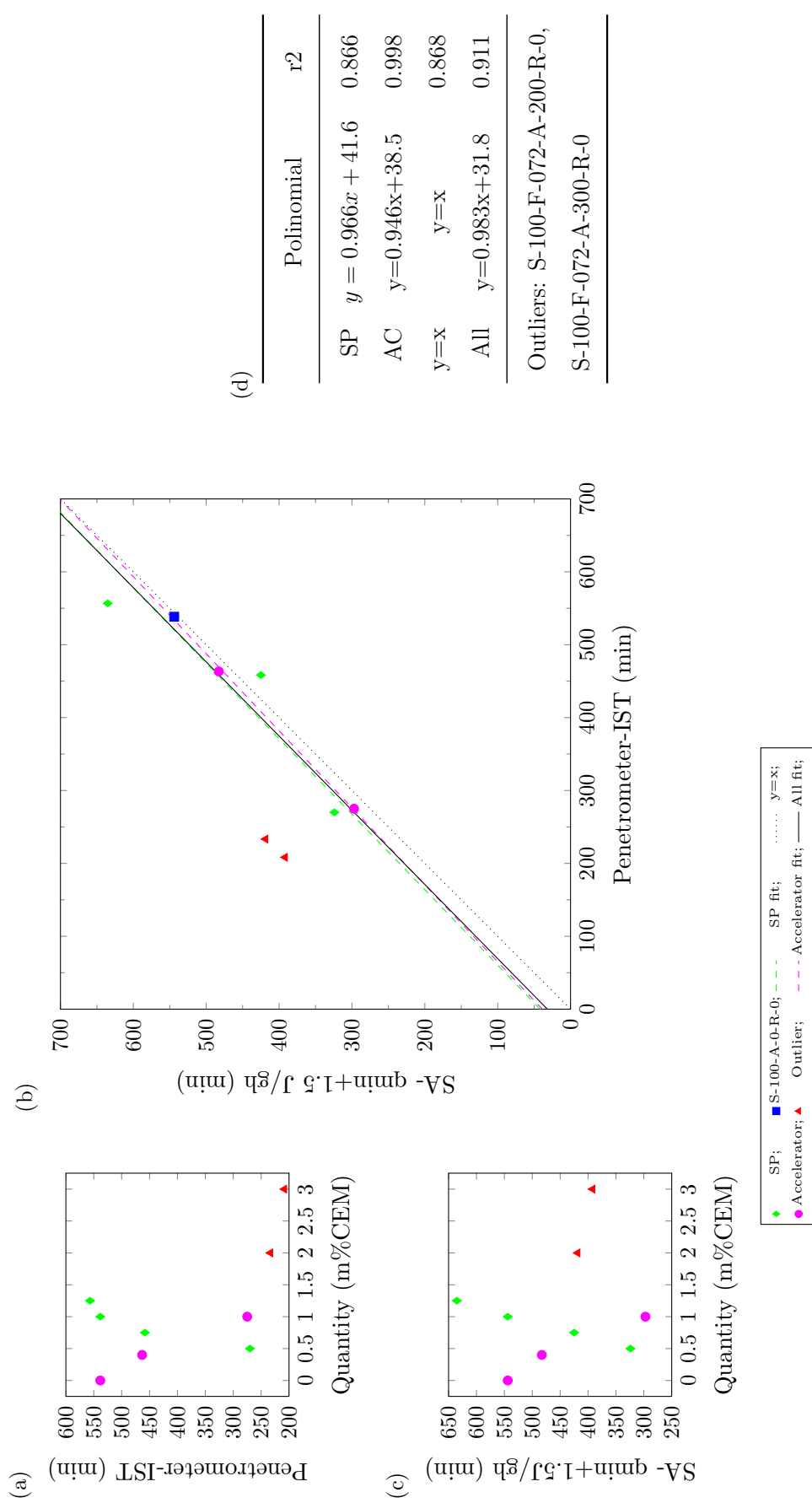
Figure E.11: *Penetrometer-IST vs Semi adiabatic- Mortar Age at qmin+1.5J/gh*

	Polinomial	r2
SP	$y = 0.966x + 41.6$	0.866
AC	y=0.946x+38.5	0.998
y=x	y=x	0.868
All	y=0.983x+31.8	0.911

Outliers: S-100-F-072-A-200-R-0,

S-100-F-072-A-300-R-0

E.1.5. Vicat needle resistance test versus semi-adiabatic calorimetry test
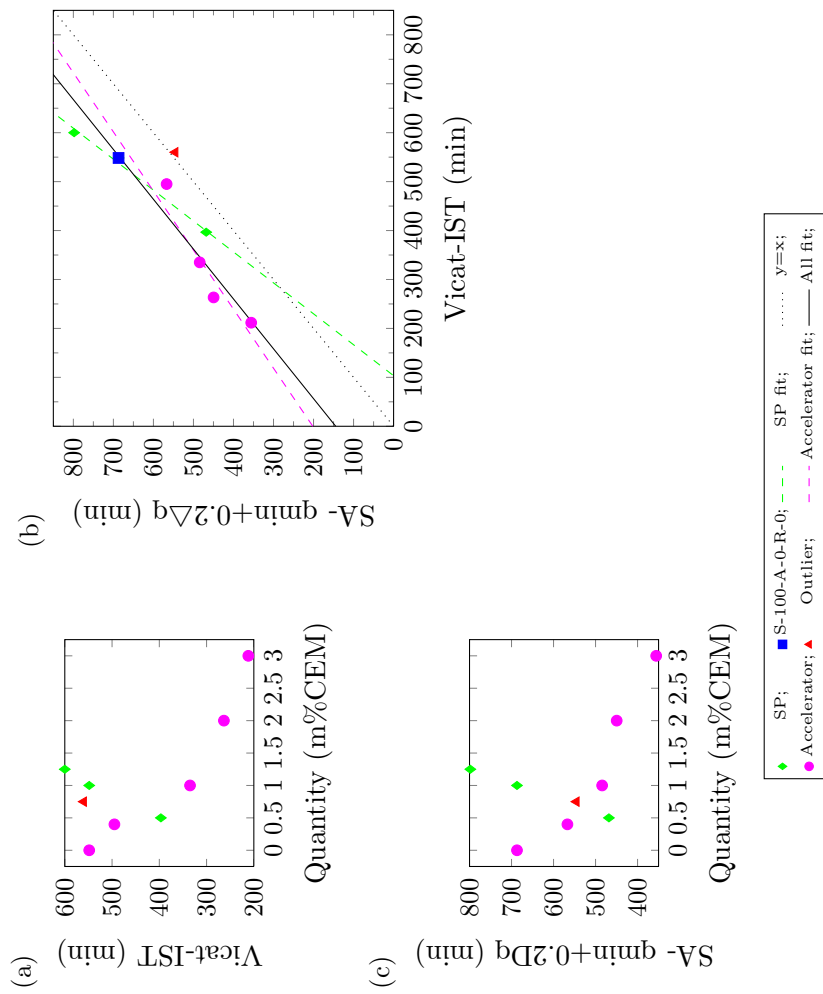
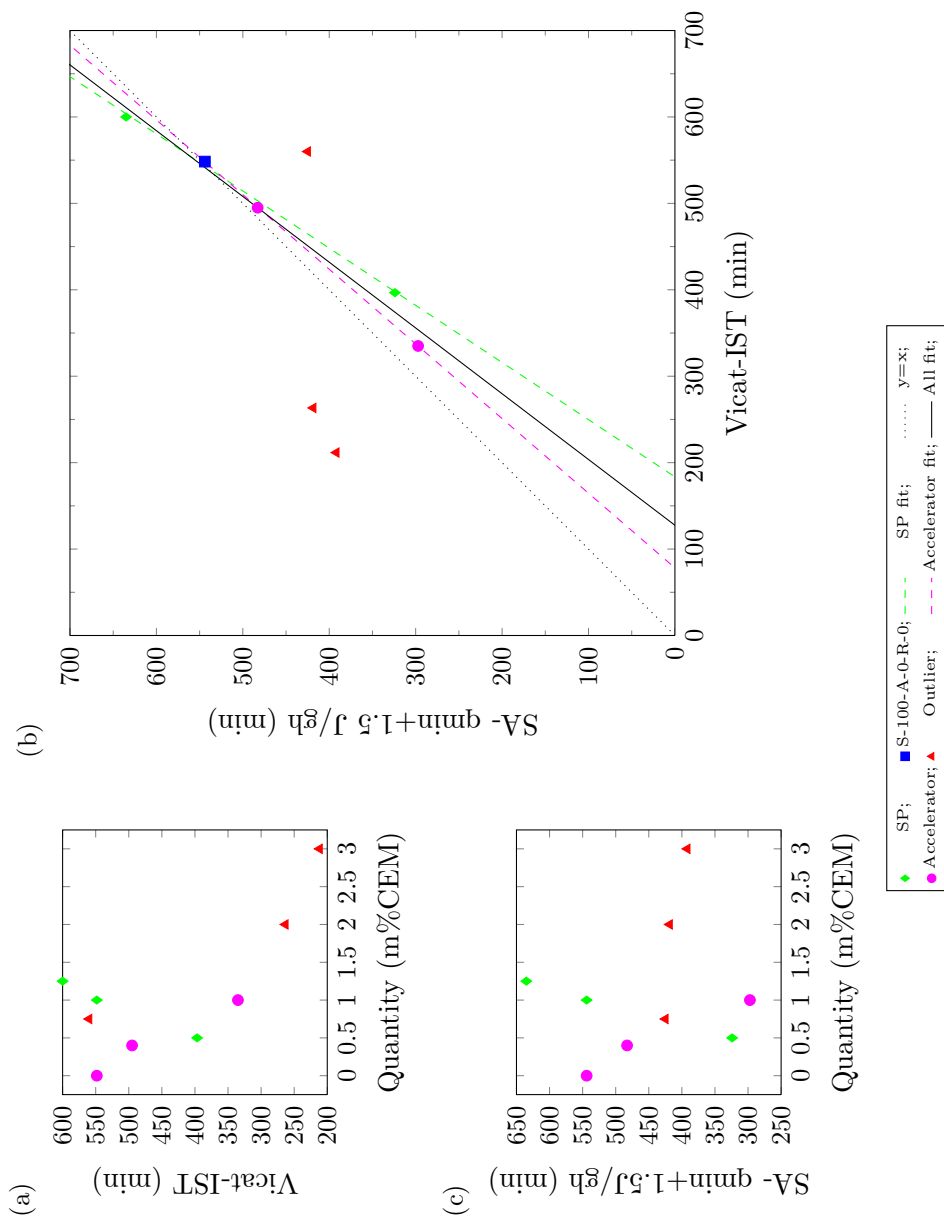**Figure E.12:** *Vicat-IST vs Semi adiabatic- Mortar Age at qmin+0.2Dq*

Figure E.13: *Vicat-IST vs Semi adiabatic- Mortar Age at qmin+1.5J/gh*

E.2. Final setting time

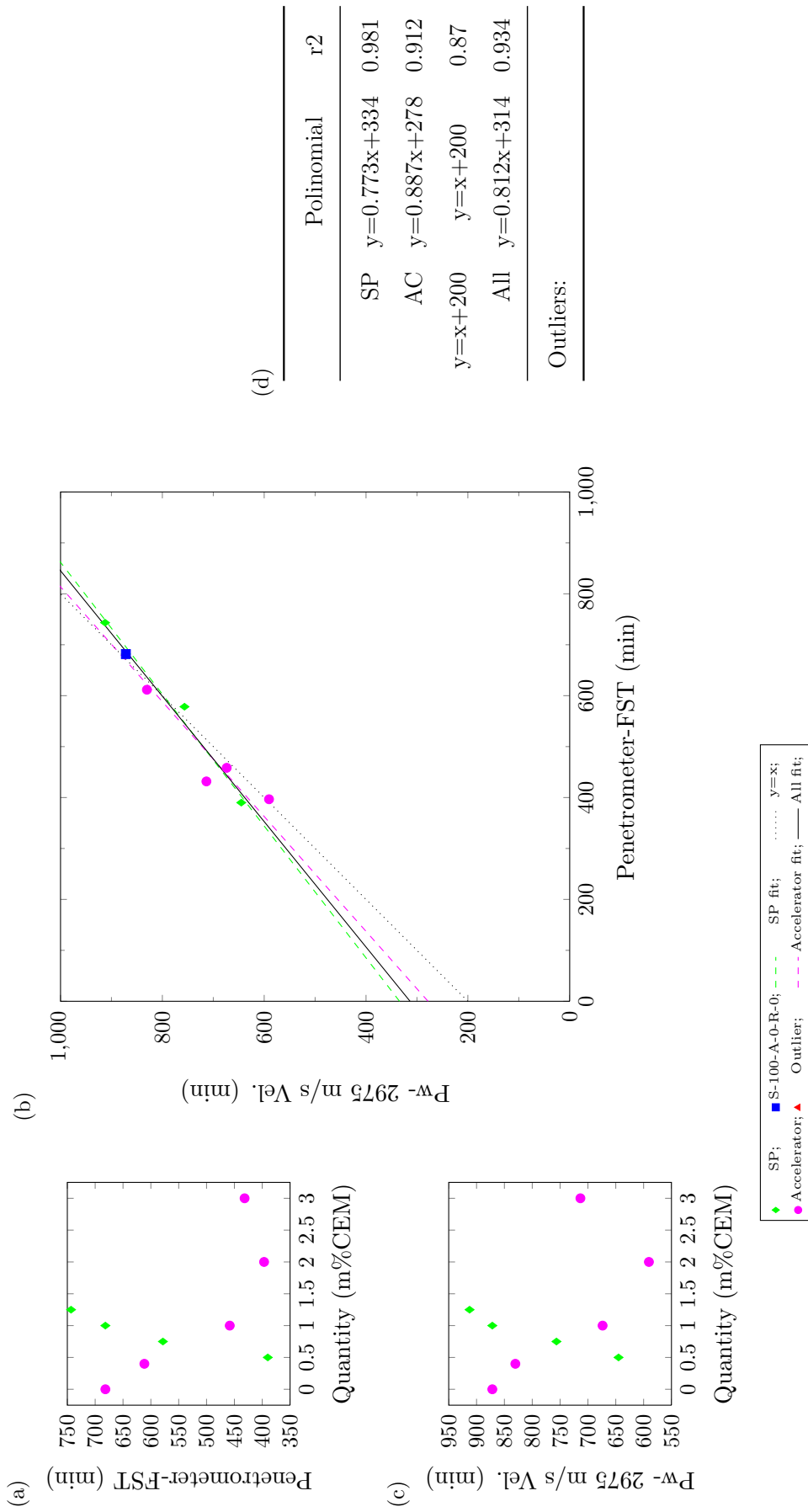### E.2.1. Penetration resistance test versus p-wave transmission test

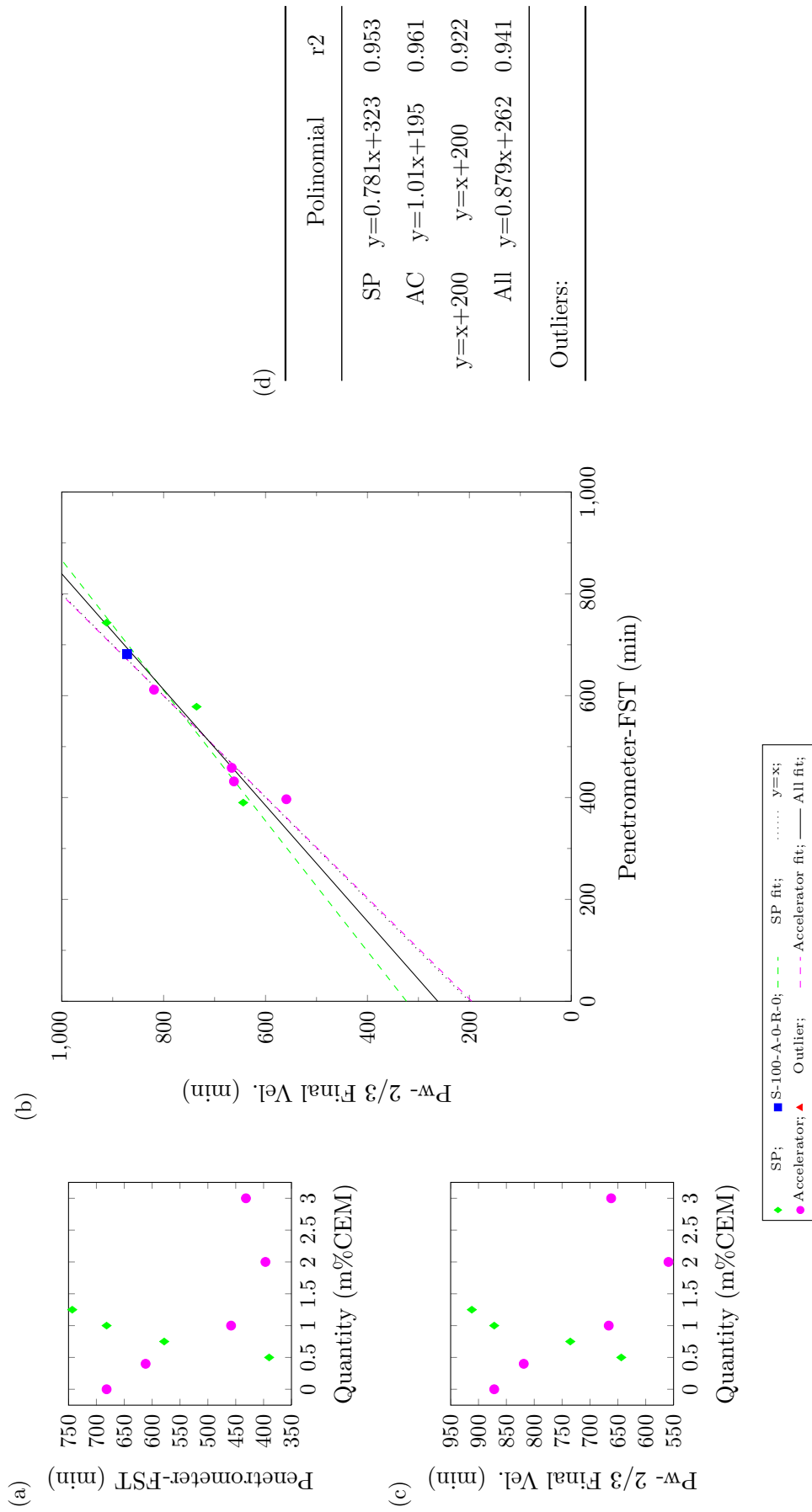**Figure E.14:** *Penetrometer-FST vs P-wave- Mortar Age at 2975 m/s Velocity Threshold*

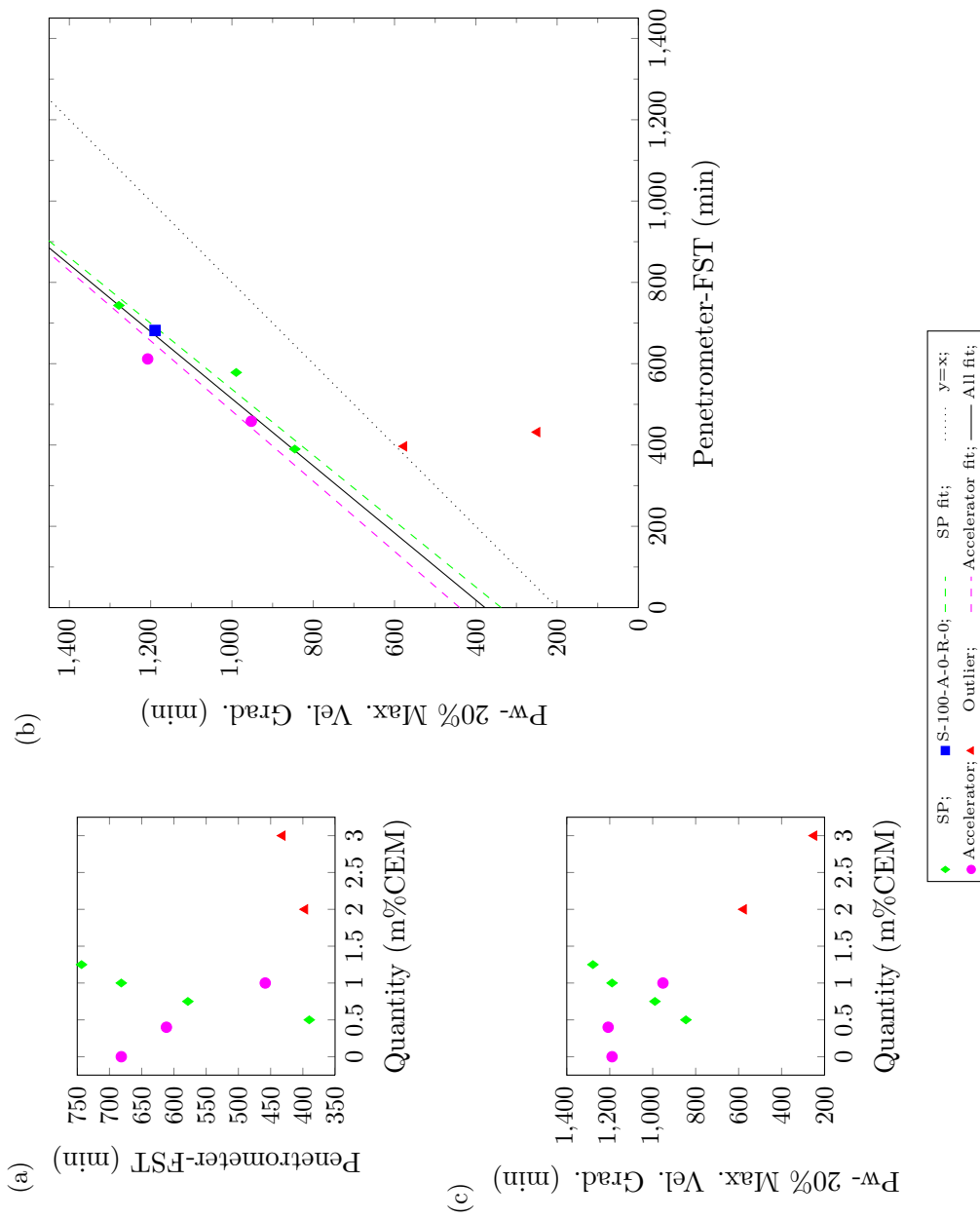**Figure E.15:** *Penetrometer-FST vs P-wave- Mortar Age at 2/3 of Final Velocity*

Figure E.16: *Penetrometer-FST vs P-wave- Mortar Age at 20% Maximum Velocity Gradient*
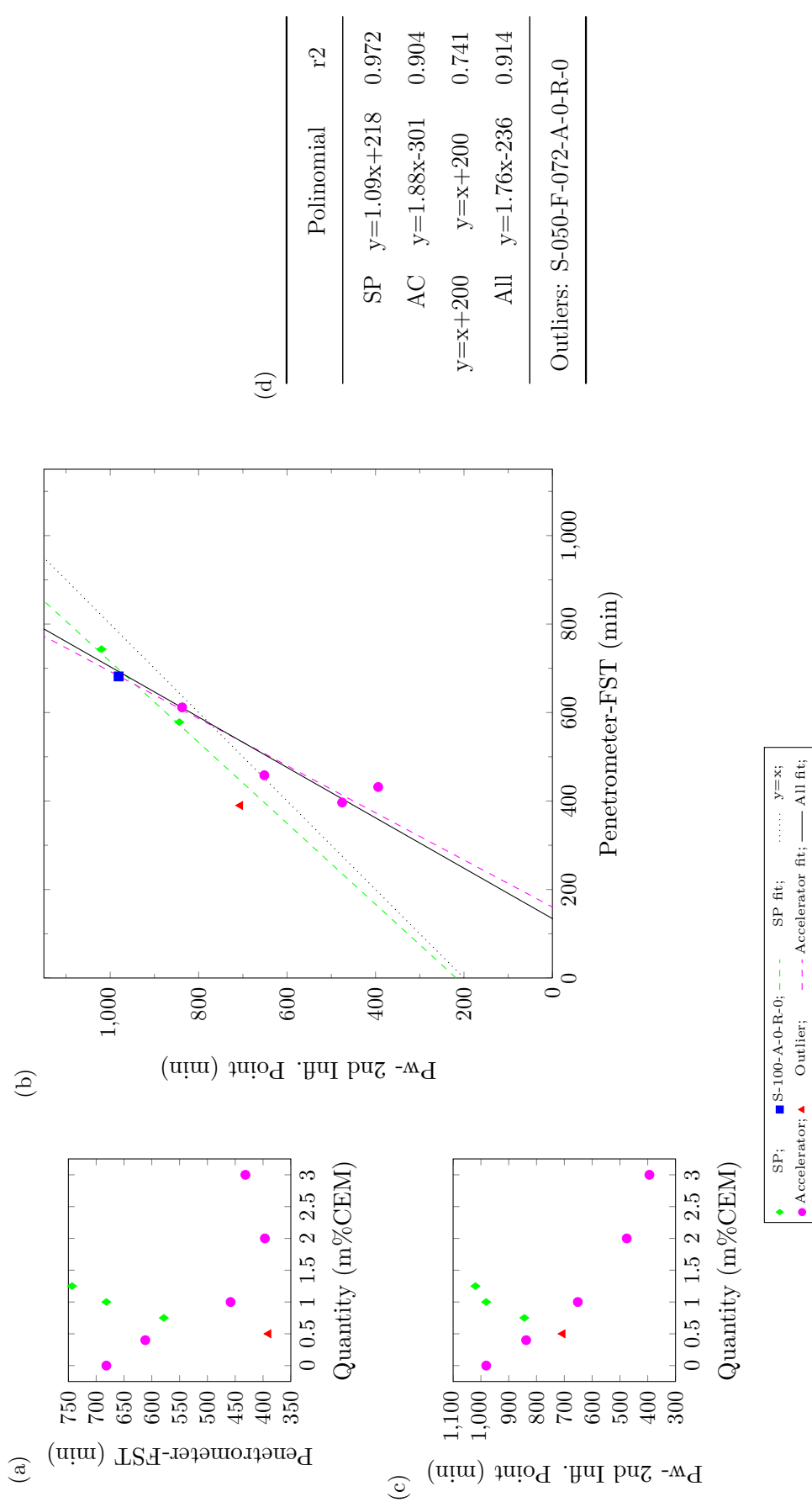
	Polinomial	r2
SP	y=1.23x+338	0.955
AC	y=1.16x+440	0.866
	y=x+200	0
All	y=1.21x+377	0.889

Outliers: S-100-F-072-A-200-R-0,

S-100-F-072-A-300-R-0

(d)

Figure E.17: *Penetrometer-FST vs P-wave- Mortar Age at 2nd Inflection Point*

	Polinomial	r2
SP	y=1.09x+218	0.972
AC	y=1.88x-301	0.904
y=x+200	y=x+200	0.741
All	y=1.76x-236	0.914

Outliers: S-050-F-072-A-0-R-0

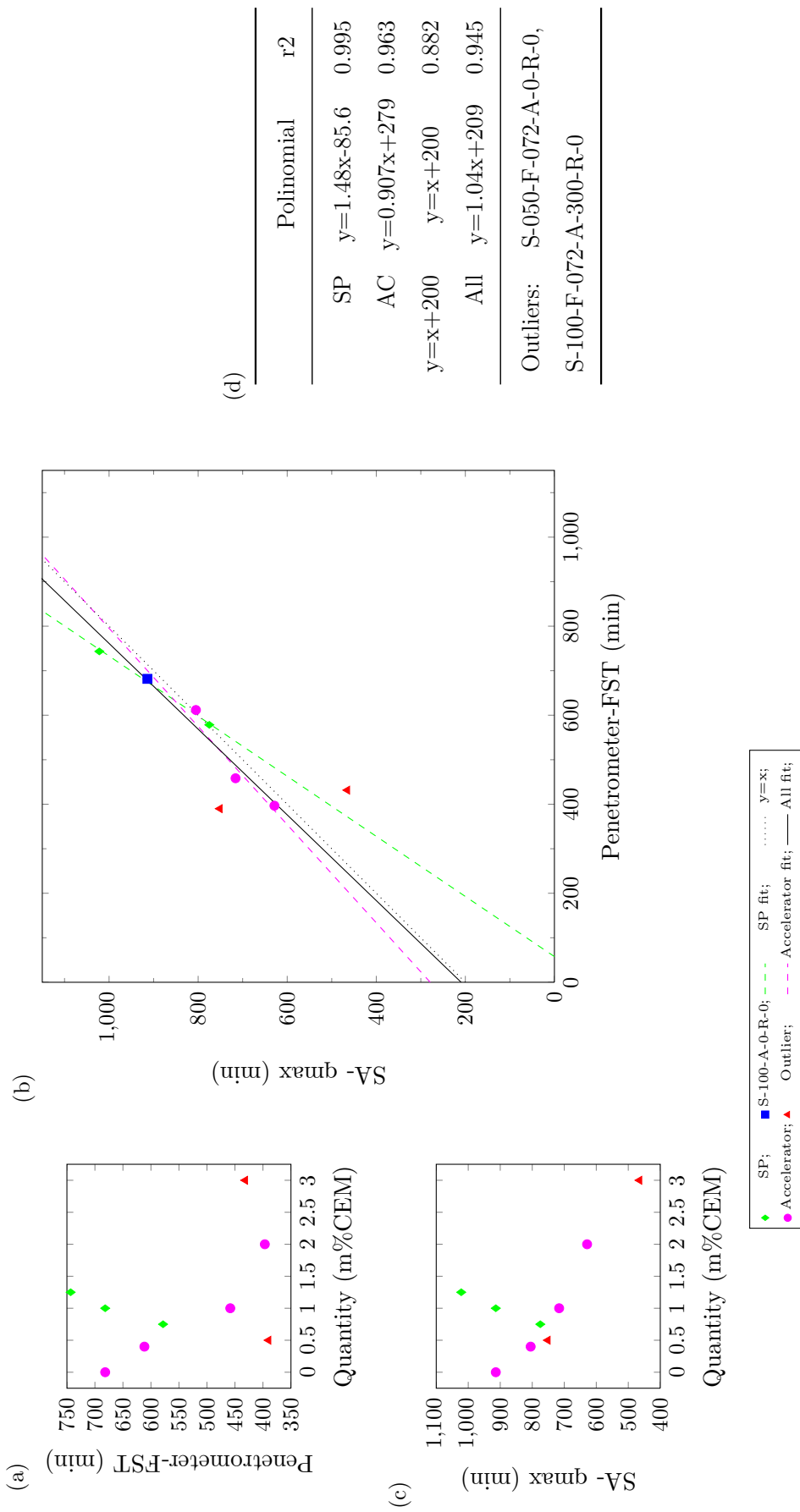## E.2.2. Penetration resistance test versus semi-adiabatic calori-metry test

Figure E.18: *Penetrometer-FST vs Semi adiabatic- Mortar Age at qmax*